SpringerBriefs in Applied Sciences and Technology

For further volumes:
http://www.springer.com/series/8884

N. S. Manjarekar · Ravi N. Banavar

# Nonlinear Control Synthesis for Electrical Power Systems Using Controllable Series Capacitors

Springer

N. S. Manjarekar (Doctoral Student)
Systems and Control Engineering
Indian Institute of Technology Bombay
Mumbai, India

Prof. Ravi N. Banavar
Systems and Control Engineering
Indian Institute of Technology Bombay
Mumbai, India

ISSN 2191-530X
ISBN 978-3-642-27530-2
DOI 10.1007/978-3-642-27531-9
Springer Heidelberg New York Dordrecht London

e-ISSN 2191-5318
e-ISBN 978-3-642-27531-9

Library of Congress Control Number: 2012930129



Printed on acid-free paper

Springer is part of Springer Science+Business Media (www.springer.com)

# Abstract

Electrical power system stabilization continues to be a challenging problem in the area of power system networks. Power electronic devices that are being increasingly used in the community to achieve better and faster responses offer an opportunity to relook at control algorithms. Much of the prevailing theory and control design however, relies on simplified models. In this monograph, we tackle the stabilization problem using more realistic models as well as actuator dynamics. Further, the single machine infinite bus (SMIB) system has been considered extensively in the literature of power system stabilization using field excitation so far, due to simplicity of the problem. Here we employ a controllable series capacitor (CSC)—a power electronic device–as the actuator. The synchronous generator is often described by one of the two nonlinear Reduced Network Models (RNMs)—the swing equation or the third order flux-decay model. Here, we have also used the Structure Preserving Model (SPM) which consists of differential algebraic equations (DAEs), to describe the power system. In general, control synthesis for DAEs is a hard problem. We employ the CSC as the power electronic device actuating the power system. This device is modeled in two different ways—(a) an injection model, (b) a first order model. The first order model is an attempt to account for the actuator dynamics. Two nonlinear control strategies developed in the recent years are employed to stabilize the power system: (1) Interconnection and Damping Assignment Passivity-based Control (IDAPBC) and (2) Immersion and Invariance (I&I) control. Both these control strategies offer certain advantages over conventional methods in terms of exploiting the structure of the system and the use of energy-based control. The IDA-PBC control strategy consists of two parts:

- changing the interconnection structure and damping structure of the closed-loop system, and
- shaping the energy of the closed-loop system.

We approach the SMIB stabilization via IDA-PBC. The SMIB is modeled by the two RNM models. The CSC is described by the two different models.

We achieve the control objectives of energy shaping and damping assignment for this system. Estimates of the domain of attraction for the closed-loop system are also presented. Further, we synthesize a stabilizing control law for a two machine infinite bus system.

In the I&I control technique we choose a suitable lower order target dynamics depending on the open loop dynamics and then immerse the target dynamics on a manifold in the original space by a suitable mapping. We design a control law to render the manifold invariant and to match the closed-loop trajectories to the immersed target dynamics asymptotically. Using this framework, we have successfully achieved the control objective of transient stabilization of the RNM as well as the SPM models. We have then used the I&I framework for the two-machine stabilization problem as well.

**Keywords** Power system stabilization · SMIB system · Multimachine system · RNM · SPM · CSC · Port-Hamiltonian systems · IDA-PBC · I&I

# Acknowledgments

This work was partially supported by an Indo-French research project (Project No. 3602-1) under the aegis of the Indo-French Centre for the Promotion of Advanced Research (IFCPAR). We are thankful to Dr. Romeo Ortega from LSS, Supélec, France for his ever-willing discussions, prompt and enthusiastic feedback on email, and constructive suggestions regarding this work. We are also thankful to Prof. A. M. Kulkarni from the Department of Electrical Engineering, IIT Bombay for providing helpful references and for sharing many insights into the engineering aspects of the problem.

# Contents

# Part I
# Interconnection and Damping Assignment-Based Control Synthesis

# Chapter 3
# Stabilization via Interconnection and Damping Assignment: Injection Model for the CSCs

## 3.1 Introduction

The method of Interconnection and Damping Assignment [1] is a passivity-based control synthesis technique. It is based on matching a closed-loop system with a desired behaviour, specified using a desired interconnection and damping structure and a desired energy function. Applications of this technique for synthesizing stabilizing control laws for excitation control of electrical power systems have been reported in the literature. In this chapter the IDA-PBC methodology is used to derive stabilizing control laws for electrical power systems using controllable series capacitors. The swing equation model is used to represent the generators. The CSC is modeled using the injection model. The control objective is to asymptotically stabilize a desired operating point and modify the transient response of the system. It is achieved by assigning a suitable energy function to the closed-loop system and modifying the interconnection and damping structures. Estimate of the domain of attraction of the operating point are also given.

The chapter is organized as follows: A short introduction to the IDA-PBC methodology is given in Sect. 3.2. In Sect. 3.3 the control technique is applied to the SMIB system with a CSC. The SMIB is modeled by the swing equation model and the CSC is modeled by the injection model. Simulation results are provided. In Sect. 3.4 a two machine infinite bus system is considered and a stabilizing control law is synthesized based on IDA-PBC. Simulation results are provided to assess the controller performance. Section 3.5 concludes the chapter.

## 3.2 Interconnection and Damping Assignment

The IDA-PBC control approach is based on treating the components of a (complex, nonlinear) dynamical system as energy-processing components and interconnecting them in a specific manner to get the complete dynamical system. Then, the objective

N. S. Manjarekar and R. N. Banavar, *Nonlinear Control Synthesis for Electrical Power Systems Using Controllable Series Capacitors*, SpringerBriefs in Applied Sciences and Technology, DOI: 10.1007/978-3-642-27531-9_3, © The Author(s) 2012

of the control law to be designed becomes- 'to shape the energy of the closed-loop system along with modifying the internal structures in a suitable way'. The classical control/performance objectives are thus achieved as by-products of the energy-shaping. The port-Hamiltonian formulation [2–4] of a dynamical system has been found to be suitable for this methodology, as it gives the important information about the physical structure of the system, internal structures, as well as energy of the system. We now present the main result in [1].

**Theorem 3.2.1** *Consider the state space model of the system*

$$\dot{x} = f(x) + g(x)u \tag{3.1}$$

*where $x \in \mathbb{R}^n$ is the state vector and $u \in \mathbb{R}^m$, $m < n$, is the control action. Let $x_\star$ be the stable equilibrium of the system. We assume that the closed system is of the form:*

$$\dot{x} = (J_d(x) - R_d(x)) \frac{\partial H_d(x)}{\partial x} \tag{3.2}$$

*where $J_d(x) = -J_d^T(x)$ is a desired interconnection structure matrix, $R_d(x) = R_d^T(x) \geq 0$ is a desired damping matrix, and $H_d(x)$ is a desired Hamiltonian function such that $x_\star = \arg\min H_d(x)$, and satisfying the following equations:*

$$g^\perp(x) \left( f(x) - (J_d(x) - R_d(x)) \frac{\partial H_d(x)}{\partial x} \right) = 0, \tag{3.3}$$

*where $g^\perp(x)$ is a full rank left annihilator of the input matrix $g(x)$. Then the closed-loop system (3.1) with a feedback control law given by*

$$u = \left( g^T(x) g(x) \right)^{-1} g^T(x) \left( (J_d(x) - R_d(x)) \frac{\partial H_d(x)}{\partial x} - f(x) \right) \tag{3.4}$$

*will be a port-controlled Hamiltonian (PCH) system with dissipation of the form (3.2) with $x_\star$ a stable equilibrium. Further, $x_\star$ will be asymptotically stable if the largest invariant set under the closed-loop system (3.2) contained in*

$$\left\{ x \in \mathbb{R}^n \;\middle|\; \left( \frac{\partial H_d(x)}{\partial x} \right)^T R_d(x) \frac{\partial H_d(x)}{\partial x} = 0 \right\} \tag{3.5}$$

*equals $\{x_\star\}$. An estimate of its domain of attraction is given by the largest bounded level set $\{x \in \mathbb{R}^n \mid H_d(x) \leq c\}$.*

## 3.3 Transient Stabilization of the SMIB System

In this section we synthesize a stabilizing control law based on IDA-PBC for the SMIB system.The SMIB system as shown in Fig. 3.1 consists of a synchronous

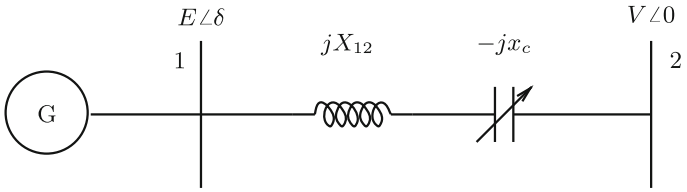


**Fig. 3.1** The SMIB system with a CSC

generator connected to the infinite bus or reference bus. The magnitude of the voltage and the frequency for the infinite bus is assumed to be constant. In Fig. 3.1 the generator bus is numbered as 1 and the infinite bus as 2. They are connected to each other through a series combination of the line reactance $X_{12}$ and a CSC denoted by $-jx_c$.

We use the following notation: $\delta$ is the rotor angle and $\omega$ is the rotor angular speed deviation with respect to a synchronously rotating reference for the generator. Let $D > 0$, $M > 0$ and $P > 0$ be the damping constant, moment of inertia constant and the mechanical power input to the generator, respectively. The dynamics of the synchronous generator is described by the swing equation model as,

$$\begin{pmatrix} \dot{x}_1 \\ \dot{x}_2 \end{pmatrix} = \begin{pmatrix} x_2 \\ \frac{1}{M}\left(P - b_1 \sin x_1 - Dx_2\right) \end{pmatrix} + \begin{pmatrix} 0 \\ -\frac{b_1}{M} \sin x_1 \end{pmatrix} u \tag{3.6}$$

where $x_1 = \delta$ and $x_2 = \omega$ and are the state variables, $u$ is the input to the CSC, $x_{l\star}$ is the open loop reactance between buses 1 and 2, and $b_1 = \frac{EV}{x_{l\star}}$. We assume that the domain of operation is

$$\mathcal{D} = \left\{(x_1, x_2) \in S^1 \times I\!R^1 \mid d_1 < x_1 < \frac{\pi}{2} - d_1, d_1 > 0\right\}. \tag{3.7}$$

The open loop equilibria of (3.6) are given by $\bar{x} = (\bar{x}_1, 0)$, where $\bar{x}_1 = \arcsin\left(\frac{P}{b_1}\right)$. We denote the operating equilibrium by $x_\star = (x_{1\star}, 0)$ where $x_{1\star} = \bar{x}_1|_{(0,\frac{\pi}{2})}$. With

$$H(x) = \frac{1}{2}Mx_2^2 - Px_1 - b_1 \cos x_1 \tag{3.8}$$

as the energy function we can rewrite (3.6) as the following port-Hamiltonian system,

$$\begin{aligned} \begin{pmatrix} \dot{x}_1 \\ \dot{x}_2 \end{pmatrix} &= (J(x) - R(x)) \frac{\partial H(x)}{\partial x} + g(x)u \\ &= \begin{pmatrix} 0 & \frac{1}{M} \\ -\frac{1}{M} & -\frac{D}{M^2} \end{pmatrix} \begin{pmatrix} -P + b_1 \sin x_1 \\ Mx_2 \end{pmatrix} + \begin{pmatrix} 0 \\ -\frac{b_1}{M} \sin x_1 \end{pmatrix} u. \end{aligned} \tag{3.9}$$

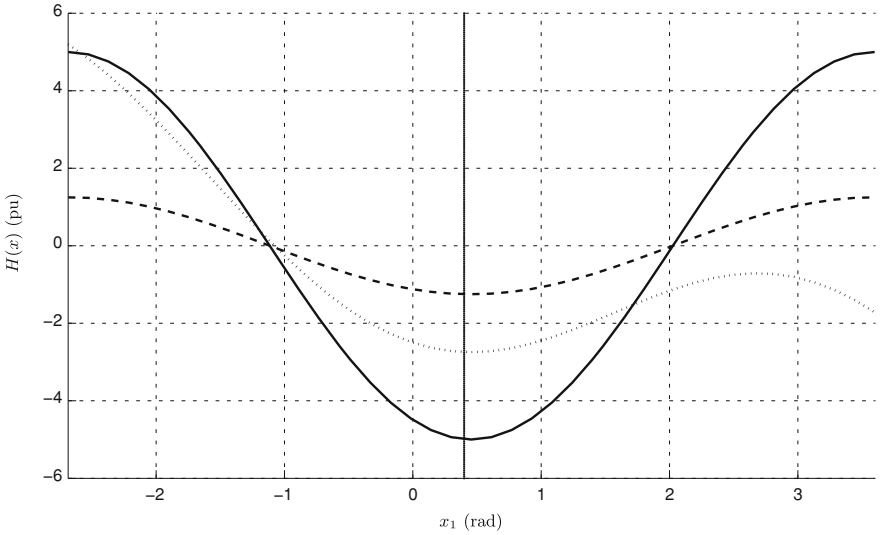


**Fig. 3.2** Variation of the energy function with respect to $x_1$: *Dotted* line (open loop energy function), *dashed* line (closed-loop energy function with $\beta = 0.5$), *solid* line (closed-loop energy function with $\beta = 2.0$)

Using (3.8) as a Lyapunov function, it can be shown that (3.9) is asymptotically stable at $x_\star$. The energy function $H(x)$ is quadratic in $x_2$, and hence has a minimum at the desired value, that is, at $x_2 = 0$. However, in the $x_1$ coordinate it is given by $-Px_1 - b_1 \cos x_1$ and is plotted in Fig. 3.2. Although it has a minimum at $x_1 = x_{1\star}$, due to its shape we get a restrictive estimate of the domain of attraction. As a part of the control objective we shape the closed-loop energy function in $x_1$ as follows:

$$H_d(x) = \frac{1}{2}Mx_2^2 - \beta \cos \tilde{x}_1 \tag{3.10}$$

where $\tilde{x}_1 := (x_1 - x_{1\star})$ and $\beta > 0$ to be chosen. Further, from (3.9) it is evident that there is a damping term in the $x_2$ coordinate, which is typically low. For efficient damping of power oscillations an additional damping $\gamma > 0$ can be assigned in the $x_2$ coordinate. The desired dynamics, then, can be written as

$$\begin{aligned} \begin{pmatrix} \dot{x}_1 \\ \dot{x}_2 \end{pmatrix} &= (J_d(x) - R_d(x)) \frac{\partial H_d(x)}{\partial x} \\ &= \begin{pmatrix} 0 & \frac{1}{M} \\ -\frac{1}{M} & -\left(\frac{D}{M^2} + \gamma\right) \end{pmatrix} \begin{pmatrix} \beta \sin \tilde{x}_1 \\ Mx_2 \end{pmatrix}. \end{aligned} \tag{3.11}$$

Through straightforward computations it can be shown that the open loop system (3.6) and the desired behaviour (3.11) satisfy the matching Eq. (3.3). Thus, from Theorem 3.2.1 we can compute the IDA-PBC control law (3.4) as

$$u = \frac{\beta \sin \tilde{x}_1 + \gamma M^2 x_2 + P - b_1 \sin x_1}{b_1 \sin x_1} \tag{3.12}$$

Here, note that due to presence of the term $\sin x_1$ in the denominator of $u$, the magnitude of the control (3.12) becomes unbounded at $x_1 = 0$. This can cause saturation in the actuator. However, in the domain of operation the control magnitude is bounded, especially for heavily loaded machines.

Further, it can be shown that the energy function $H_d(x)$ is strongly convex in $\mathcal{D}$, and hence entire $\mathcal{D}$ is an estimate of the domain of attraction for the closed-loop system at $x_\star$. We summarize the above discussion on control synthesis in the following proposition:

**Proposition 3.3.1** *The closed-loop system* (3.6) *with the control law* (3.12) *is asymptotically stable at* $x_\star \in \mathcal{D}$ *with the energy function* (3.10) *and the closed-loop Hamiltonian form* (3.11). *An estimate of the domain of attraction is given by* $\mathcal{D}$.

*Proof* Based on the arguments given above. □

### *3.3.1 Simulation Results*

We use the following system parameters for the SMIB system (3.6): $M = \frac{8}{100\pi}$, $D = \frac{0.4}{100\pi}$, $P = 1.1$pu, $b_1 = 1$pu, $x_{l\star} = 0.4$, $-\frac{1}{3} \leq u \leq 1$ and the operating equilibrium is $x_\star = (0.4556, 0)$. To assess the performance of the proposed control law we assume that a short circuit fault occurs at the far end of the transmission line at time $t = 1$ s for a duration of 0.1 s. The tuning parameters are $\beta$ and $\gamma$.

Figure 3.3 shows the responses of the system to the transient. The open loop response, represented by the dotted lines, shows heavy and sustained oscillations in $x_1$, $x_2$ and the generated power $P_G$. We examine the closed-loop response for three different sets of tuning parameters. It can be observed that an increase in the value of $\gamma$ damps the oscillations at a faster rate. This change is shown from the dash-dot lines to dashed lines. The response of the system to an increase in $\beta$ is shown by the solid line. An increase in the value of $\beta$ makes the shape of the closed-loop energy function deeper, see Fig. 3.4 , and hence improves the response of the system. The control magnitude $u$ is also shown in the plot. The saturation limits for the control magnitude is assumed to be $\left(-\frac{1}{3}, 1\right)$. The actuator doesn't saturate for the test fault. Another view of the response is shown in Fig. 3.5 in terms of the phase portrait, that is, the plot of $x_2$ against $x_1$.

#### Comparison of the Control Law

In [1] a nonlinear control law based on the concept of Control Lyapunov Function (CLF) is proposed. It is shown there that, the control law

$$u = k x_2 \sin x_1 \tag{3.13}$$

where $k > 0$ (to be chosen), assigns (3.8) as a CLF to the closed-loop system. Further, with the input (3.13), the time derivative of (3.8) along the trajectories of

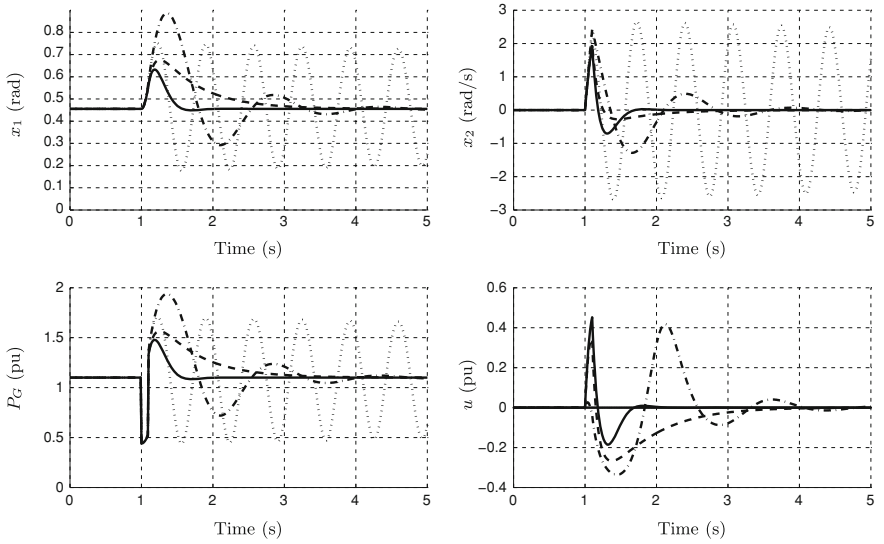


**Fig. 3.3** Response of the SMIB system (3.6) with the IDA-PBC control law (3.12): *Dotted* line (open loop response), *dash-dot* line (closed-loop response with $\beta = 0.5$ and $\gamma = 100$), *dashed* line (closed-loop response with $\beta = 0.5$ and $\gamma = 500$), *solid* line (closed-loop response with $\beta = 2$ and $\gamma = 500$)

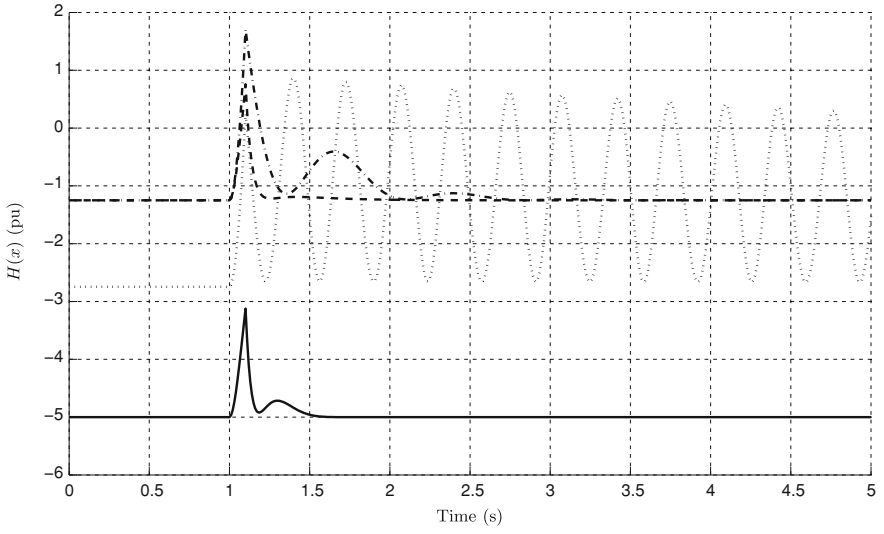


**Fig. 3.4** Variation of the energy function with respect to time: *Dotted* line (open loop response), *dash-dot* line (closed-loop response with $\beta = 0.5$ and $\gamma = 100$), *dashed* line (closed-loop response with $\beta = 0.5$ and $\gamma = 500$), *solid* line (closed-loop response with $\beta = 2$ and $\gamma = 500$)

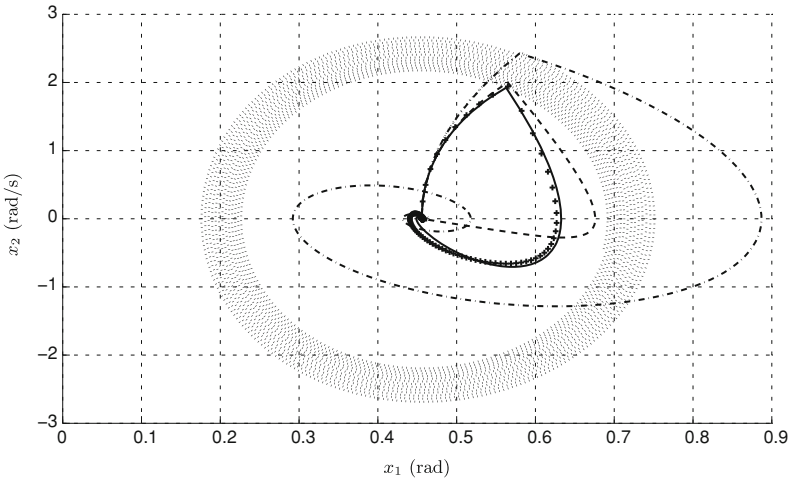


**Fig. 3.5** Phase plots for the SMIB system (3.6) with the IDA-PBC control law (3.12): *Dotted* line (open loop response), *dash-dot* line (closed-loop response with $\beta = 0.5$ and $\gamma = 100$), *dashed* line (closed-loop response with $\beta = 0.5$ and $\gamma = 500$), *solid* line (closed-loop response with $\beta = 2$ and $\gamma = 500$)

the closed-loop system is negative semi-definite, and hence the closed-loop system is stable.

In Fig. 3.6 we compare the the performance of the proposed control law with the control law in [5]. Both the performances match closely. However, it can be noted that the control law from [5] has a tuning parameter to decide the way the control law performance. The proposed control law, on the other hand, consists of two tuning parameters: one of them decides the shape of the energy function and the other one decides the rate at which the oscillations are damped. This gives more freedom on deciding the closed-loop response.

The other two plots show the variation of the energy function with respect to time and $x_1$ for different values of the tuning parameters.

## 3.4 Transient Stabilization of a Two Machine Infinite Bus System

In this section we synthesize a stabilizing control law for another system using IDA-PBC. The power system is as shown in Fig. 3.7. The two generators $G_1$ and $G_2$ are connected to bus 1 and bus 2, respectively and the infinite bus is denoted by bus 3. A CSC (not shown in the figure) is connected between buses 1 and 3, and another CSC (not shown in the figure) between buses 2 and 3. The synchronous

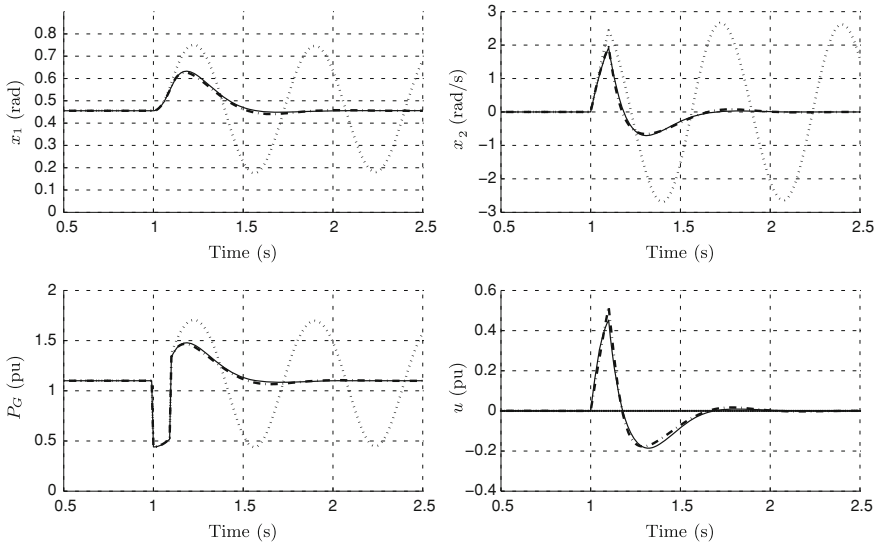


**Fig. 3.6** Comparison of the IDA-PBC control law (3.12) with a CLF-based control law (3.13): *Dotted* line (open loop response), *dash-dot* line (closed-loop response for the control law (3.13) with $k = 0.5$), *solid* line (closed-loop response for the control law (3.12) with $\beta = 2$ and $\gamma = 500$)

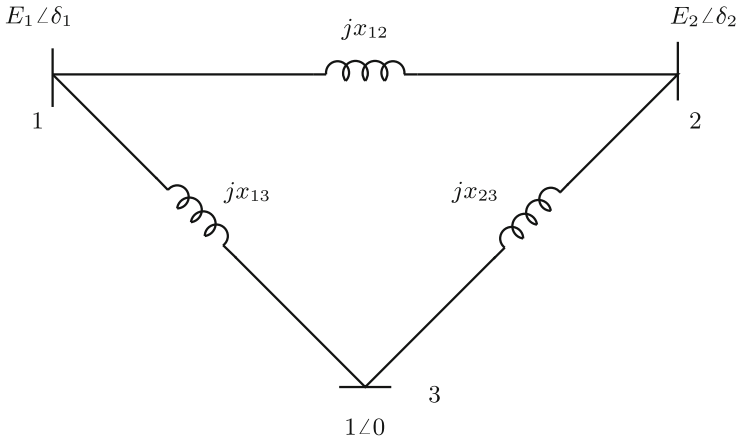


**Fig. 3.7** A two machine infinite bus system

generator dynamics are described by the swing equation for each generator, while the CSCs are modeled by the injection model. With $\delta_i$ as rotor angles, $\omega_i$ rotor angular velocities of the $i$-th generator for $i = 1, 2$ we can write the state space model for the system as

$$\begin{pmatrix} \dot{x}_1 \\ \dot{x}_2 \\ \dot{x}_3 \\ \dot{x}_4 \end{pmatrix} = \begin{pmatrix} x_3 \\ x_4 \\ \frac{1}{M_1}\left(P_1 - b_{12}\sin(x_1 - x_2) - b_1 \sin x_1 - D_1 x_3\right) \\ \frac{1}{M_2}\left(P_2 + b_{12}\sin(x_1 - x_2) - b_2 \sin x_2 - D_2 x_4\right) \end{pmatrix} + \begin{pmatrix} 0 & 0 \\ 0 & 0 \\ -\frac{b_1}{M_1}\sin x_1 & 0 \\ 0 & -\frac{b_2}{M_2}\sin x_2 \end{pmatrix} \begin{pmatrix} u_1 \\ u_2 \end{pmatrix} \tag{3.14}$$

where $x_1 = \delta_1$, $x_2 = \delta_2$, $x_3 = \omega_1$ and $x_4 = \omega_2$ are the state variables, $u_1$, $u_2$ are the inputs to the CSCs, and $D_i$, $M_i$, $b_i$ and $b_{12}$ are system constants for $i = 1, 2$. In [5] the following control law is proposed:

$$u_1 = k_1 x_3 \sin x_1 \tag{3.15a}$$

$$u_2 = k_2 x_4 \sin x_2 \tag{3.15b}$$

with tuning parameters $k_i > 0$, $i = 1, 2$. It is shown there that, (3.15) make

$$H(x) = \frac{1}{2}\left(M_1 x_3^2 + M_2 x_4^2\right) - P_1 x_1 - P_2 x_2 - b_1 \cos x_1 - b_2 \cos x_2 - b_{12}\cos(x_1 - x_2) \tag{3.16}$$

a Control Lyapunov Function for the system (3.14) and is a stabilizing control law. Further, it is shown that each CSC contributes to the negativeness of $\dot{H}(x)$, thus making the slope of $H(x)$ sharper. This amounts to better damping of the system.

We now propose an IDA-PBC control law for (3.14). Using (3.16) as an energy function we can obtain the following Hamiltonian representation for (3.14)

$$\begin{aligned} \begin{pmatrix} \dot{x}_1 \\ \dot{x}_2 \\ \dot{x}_3 \\ \dot{x}_4 \end{pmatrix} &= \left(J(x) - R(x)\right)\frac{\partial H(x)}{\partial x} + g(x)u \\ &= \begin{pmatrix} 0 & 0 & \frac{1}{M_1} & 0 \\ 0 & 0 & 0 & \frac{1}{M_2} \\ -\frac{1}{M_1} & 0 & -\frac{D_1}{M_1^2} & 0 \\ 0 & -\frac{1}{M_2} & 0 & -\frac{D_2}{M_2^2} \end{pmatrix} \begin{pmatrix} -P_1 + b_{12}\sin(x_1 - x_2) + b_1 \sin x_1 \\ -P_2 - b_{12}\sin(x_1 - x_2) + b_2 \sin x_2 \\ M_1 x_3 \\ M_2 x_4 \end{pmatrix} \\ &\quad + \begin{pmatrix} 0 & 0 \\ 0 & 0 \\ -\frac{b_1}{M_1}\sin x_1 & 0 \\ 0 & -\frac{b_2}{M_2}\sin x_2 \end{pmatrix} \begin{pmatrix} u_1 \\ u_2 \end{pmatrix}. \end{aligned} \tag{3.17}$$

From (3.17) we have that, the $x_3$ and $x_4$ coordinates have damping, however generally it is poor. Thus, as a control objective we introduce additional damping

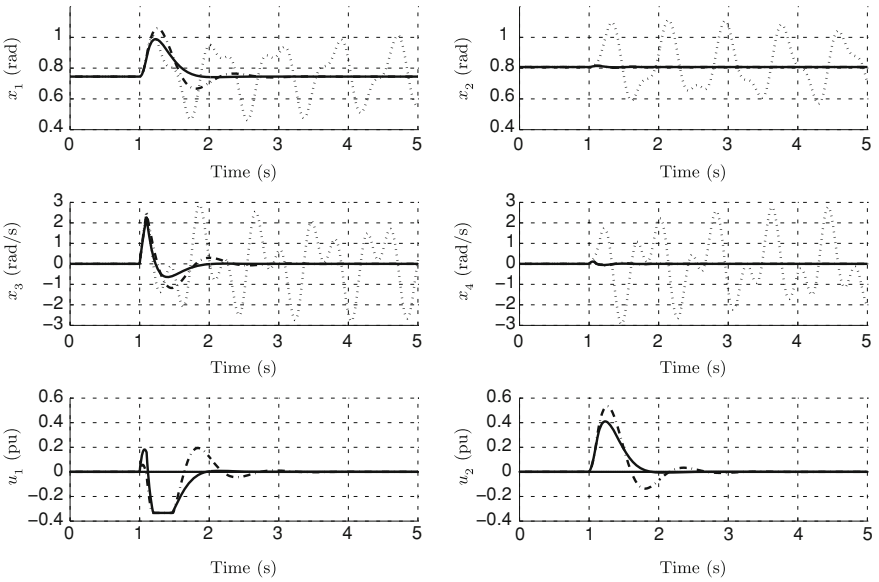


**Fig. 3.8** Response of the two machine infinite bus system (3.14) with the IDA-PBC control law (3.20): *Dotted* line (open loop response), *dash-dot* line (closed-loop response with $\beta_1 = 1$, $\beta_2 = 4$, $\gamma_1 = 5$ and $\gamma_2 = 5$), *solid* line (closed-loop response with $\beta_1 = 1$, $beta_2 = 4$, $\gamma_1 = 10$ and $\gamma_2 = 10$), $\alpha = 0$ for all plots

$\gamma_1 > 0$ and $\gamma_2 > 0$ in $x_3$ and $x_4$, respectively. In addition, we introduce an interconnection $\alpha > 0$ between $x_3$ and $x_4$. Further, we propose to use the following energy function as the desired Hamiltonian for the closed-loop system:

$$H_d(x) = \frac{1}{2}\left(M_1 x_3^2 + M_2 x_4^2\right) - \beta_1 \cos\tilde{x}_1 - \beta_2 \cos\tilde{x}_2 \tag{3.18}$$

where $\tilde{x}_i := (x_i - x_{i\star})$, $i = 1, 2$ and $x_\star = (x_{1\star}, x_{2\star}, 0, 0)$ denotes the open loop equilibrium of (3.14). It is clear that (3.18) has a strict local minimum at $x_\star$. Thus, the desired behaviour we have chosen can be written as

$$\begin{aligned}\begin{pmatrix}\dot{x}_1\\ \dot{x}_2\\ \dot{x}_3\\ \dot{x}_4\end{pmatrix} &= (J_d(x) - R_d(x))\,\frac{\partial H_d(x)}{\partial x}\\ &= \begin{pmatrix} 0 & 0 & \frac{1}{M_1} & 0\\ 0 & 0 & 0 & \frac{1}{M_2}\\ -\frac{1}{M_1} & 0 & -\left(\frac{D_1}{M_1^2} + \gamma_1\right) & \alpha\\ 0 & -\frac{1}{M_2} & -\alpha & -\left(\frac{D_2}{M_2^2} + \gamma_2\right)\end{pmatrix}\begin{pmatrix}\beta_1 \sin\tilde{x}_1\\ \beta_2 \sin\tilde{x}_2\\ M_1 x_3\\ M_2 x_4\end{pmatrix}.\end{aligned} \tag{3.19}$$

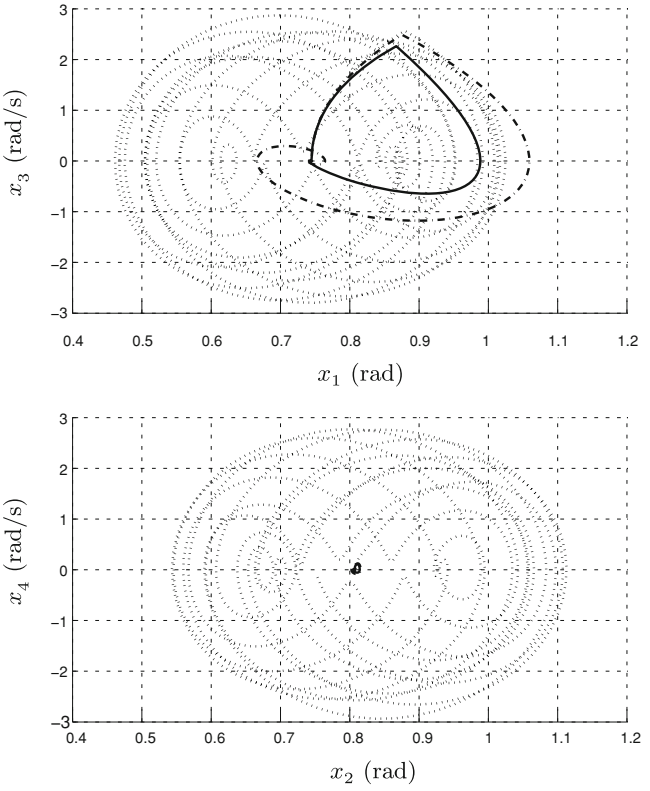


**Fig. 3.9** Phase plots for the two machine infinite bus system (3.14) with the IDA-PBC control law (3.20): *Dotted* line (open loop response), *dash-dot* line (closed-loop response with $\beta_1 = 1$, $\beta_2 = 4$, $\gamma_1 = 5$ and $\gamma_2 = 5$), *solid* line (closed-loop response with $\beta_1 = 1$, $\beta_2 = 4$, $\gamma_1 = 10$ and $\gamma_2 = 10$), $\alpha = 0$ for all plots

Through straightforward computations it can be shown that the open loop system (3.14) and the desired behaviour (3.19) satisfy the matching Eq. (3.3) and hence the IDA-PBC control law can be computed from (3.4) as

$$u_1 = \frac{\beta_1 \sin \tilde{x}_1 + \gamma_1 M_1^2 x_3 - \alpha M_2 x_4 + P_1 - b_{12} \sin(x_1 - x_2) - b_1 \sin x_1}{b_1 \sin x_1} \tag{3.20a}$$

$$u_2 = \frac{\beta_2 \sin \tilde{x}_2 - \gamma_2 M_2^2 x_4 + \alpha M_1 x_3 + P_2 + b_{12} \sin(x_1 - x_2) - b_2 \sin x_2}{b_2 \sin x_2}. \tag{3.20b}$$

It is to be noted here that the proposed control law, (3.20) grows unboundedly as $x_1$ and $x_2$ approach zero, which can cause saturation of the actuator. However, for heavily loaded machines the magnitude of the control law is well within bounds, and provides more flexibility in terms of additional damping, interconnection and

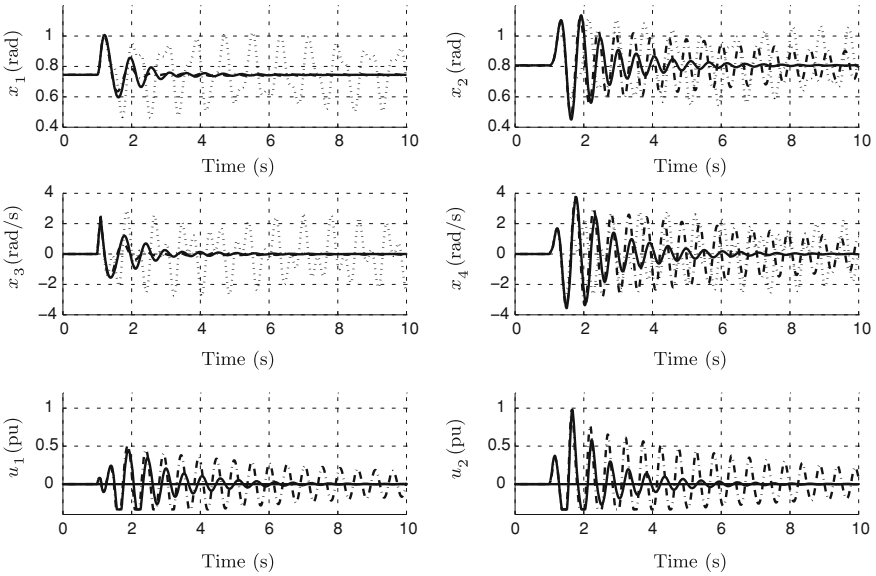


**Fig. 3.10** Response of the two machine infinite bus system (3.14) with the IDA-PBC control law (3.20): *Dotted* line (open loop response). Closed-loop response: $\beta_1 = 2, \gamma_1 = 5$, $u_2 = 0$ and, *dash-dot* line ($\alpha = 10$), *solid* line ($\alpha = 50$)

properly shaped energy function. Further, in a straightforward way it can be shown that the Hessian $\frac{\partial^2 H_d(x)}{\partial x^2}$ is strongly convex in the domain of operation

$$\mathcal{D} = \left\{(x_1, x_2, x_3, x_4) \in S^1 \mathbf{x} S^1 \mathbf{x} I\!R^2 \mid d_i < x_i < \frac{\pi}{2} - d_i, d_i > 0, i = 1, 2\right\}, \tag{3.21}$$

and hence $\mathcal{D}$ is an estimate of the domain of attraction for the closed-loop system. We summarize the above discussion on control synthesis in the following proposition:

**Proposition 3.4.1** *The closed-loop system* (3.14) *with the control law* (3.20) *is asymptotically stable at* $x_\star \in \mathcal{D}$ *with the energy function* (3.18) *and the Hamiltonian model* (3.19). *An estimate of the domain of attraction is given by* $\mathcal{D}$.

*Proof* Based on the arguments given above. □

### *3.4.1 Simulation Results*

We use the following system parameters for the SMIB system (3.14), as given in [5]: $M_1 = M_2 = \frac{8}{100\pi}$, $D_1 = D_2 = \frac{0.4}{100\pi}$, $b_1 = b_2 = 2$(p. u.), $b_{12} = 2.5$(p. u.), $x_{l_\star} = 0.4$, $P_1 = 1.2$(p.u.), $P_2 = 1.6$(p.u.), $-\frac{1}{3} \leq u \leq 1$ and and the operating

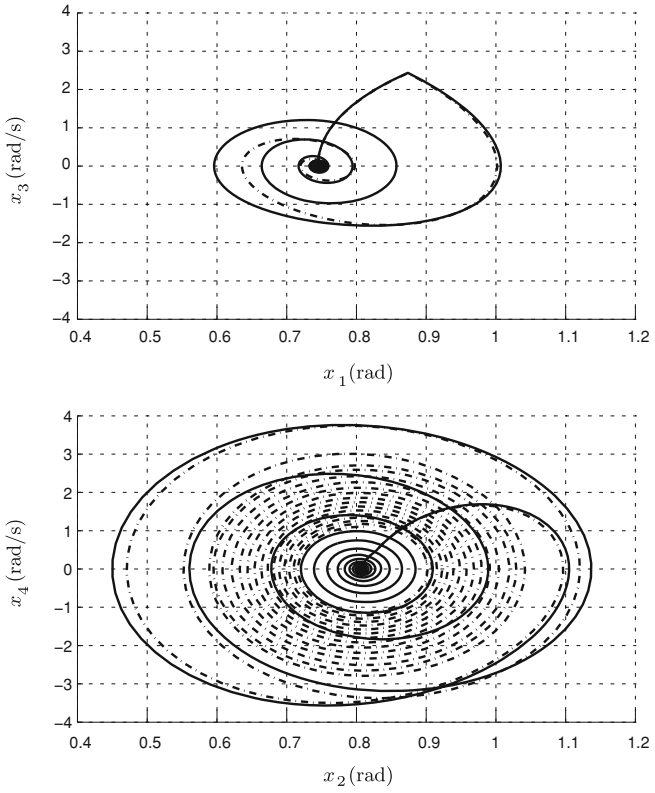


**Fig. 3.11** Phase plots for the two machine infinite bus system (3.14) with the IDA-PBC control law (3.20): *Dotted* line (open loop response). Closed-loop response: $\beta_1 = 2,\ \gamma_1 = 5,\ u_2 = 0$ and, *dash-dot* line ($\alpha = 10$), *solid* line ($\alpha = 50$)

equilibrium is $x_\star = (0.7447, 0.807, 0, 0)$. The tuning parameters are $\beta_1,\ \beta_2,\ \gamma_1$ and $\gamma_2$ . To assess the performance of the proposed control law we assume that a short circuit fault occurs at bus 1 at time $t = 1$ s for a duration of 0.1 s.

In Fig. 3.8 oscillatory nature of the open loop response in response to the disturbance is shown by dotted line. For the closed-loop response we consider two different cases. In the first case the effect of increasing the value of $\gamma_1$ is shown in the plot for $x_1$ from the dash-dot line to the solid line. In the second case the effect of $\beta_2 > \beta_1$ is shown. The oscillations $x_2$ are negligibly small as compared to those in $x_1$. The phase portraits of the open loop and the closed-loop responses are shown in Fig. 3.9 .

For the same transient we consider another case with only one CSC between buses 1 and 3, and $u_2 = 0$. In this case the role of the interconnection parameter $\alpha$ is shown in Figs. 3.10 and 3.11. An increase in the value of $\alpha$ improves the closed-loop response as indicated by the dash-dot line and the solid line plots.

## 3.5 Summary

In this chapter we presented IDA-PBC control laws for transient stabilization of electrical power systems. A power electronic device, a CSC, was used as the actuator. It was modeled by the injection model. We considered two systems- an SMIB system and a two machine system. For the SMIB system we achieved a two-fold control objective- damping injection and energy shaping. For the two machine case we achieved damping and interconnection assignment with energy shaping and proposed an IDA-PBC control law. Simulation results were provided to examine the controller performance.

## References

1. R. Ortega, A.J. van der Schaft, B.M. Maschke, G. Escobar, Interconnection and damping assignment passivity-based control: a survey. Eur. J. Control **10**(5), 432–450 (2004)
2. A.J. van der Schaft, Port-controlled Hamiltonian systems: towards a theory for control and design of nonlinear physical systems. J. Soc. Instrum. Control Eng. Jpn. (SICE) **39**, 91–98 (2000)
3. A.J. van der Schaft, Port-Hamiltonian systems: an approach to modeling and control of complex physical systems. in *Proceedings of the Sixteenth International Symposium on Mathematical Theory of Networks and Systems (MTNS2004)*, (Leuven, 2004)
4. A.J. van der Schaft, Port-Hamiltonian systems: network modeling and control of nonlinear physical systems. in *Advanced Dynamics and Control of Structures and Machines, CISM Courses and lectures*, (New York, 2004), pp. 127–168
5. M. Ghandhari, Control Lyapunov functions: a control strategy for damping of power oscillations in large power systems. PhD thesis, KTH, Bonn, Germany, (2000)

# Part II
# Immersion and Invariance-Based Control Synthesis

# Chapter 4
# Stabilization Via Interconnection and Damping Assignment: First Order Model of the CSC

## 4.1 Introduction

While studying the role of the CSCs for power system stabilization, the dynamics of the CSC can be accounted for by modeling it as a dynamical system. However, for stability studies it is not necessary to have a detailed model. It is adequate to assume that the desired value of the CSC reactance is achieved within a specified time interval. Hence, a first order model is sufficient for this purpose [1]. In this chapter we apply the IDA-PBC methodology to the SMIB system with a CSC, where the CSC is modeled by a first order model and synthesize stabilizing control laws. The SMIB system is modeled by the swing equation model and the classical flux-decay model. In the control synthesis process we assign (a) a suitable interconnection and damping structure and (b) a desired energy function, to the closed-loop system. In this way, we synthesize a control law to asymptotically stabilize the closed-loop system at a desirable equilibrium and to improve the transient damping in the system. Estimates of the domain of attraction of the operating point are also given.

The chapter is organized as: In Sect. 4.2 the SMIB is described by the swing equation. The IDA-PBC control strategy is used to synthesize a stabilizing control. An estimate of the domain of attraction for the closed-loop system is given. In Sect. 4.3 the SMIB system is described by the third order flux-decay model. The IDA-PBC control strategy is used to synthesize a stabilizing control and an estimate of the domain of attraction for the closed-loop system is given. In Sect. 4.4 a few simulation results are presented to assess the performance of the controller. Section 4.5 concludes the chapter.

## 4.2 IDA-PBC Control Synthesis for the Swing Equation

Consider the SMIB system with a CSC as shown in Fig. 3.1. Here the control system consists of two subsystems: one describing the SMIB system and the other describing the actuator (CSC) dynamics. We describe the SMIB system using the swing equation

N. S. Manjarekar and R. N. Banavar, *Nonlinear Control Synthesis for Electrical Power Systems Using Controllable Series Capacitors*, SpringerBriefs in Applied Sciences and Technology, DOI: 10.1007/978-3-642-27531-9_4, © The Author(s) 2012

model given by (2.2). The actuator dynamics is represented by (2.10). Here, we assume that the region of operation is

$$\mathcal{D} = \left\{ (\delta, \omega, E, x_l) \;\middle|\; d_1 < \delta < \frac{\pi}{2} - d_1, E > d_2, x_l > d_3 \right\},$$

where $d_1 > 0$, $d_2 > 0$ and $d_3 > 0$ are small numbers.

We define the state variables of the system as $x_1 = \delta$, $x_2 = \omega$, $x_3 = x_l$ and let $x = [x_1\ x_2\ x_3]^T$ be the state vector. The open loop system can then be written as

$$\dot{x}_1 = x_2 \tag{4.1a}$$

$$\dot{x}_2 = \frac{1}{M}\left(P - Dx_2 - \frac{EV\sin x_1}{x_3}\right) \tag{4.1b}$$

$$\dot{x}_3 = \frac{1}{T_{\text{CSC}}}\left(-x_3 + x_{3_\star} + u\right), \tag{4.1c}$$

where $x_{3_\star} = \frac{EV\sin x_{1_\star}}{P}$ for a given $x_{1_\star}$. Equivalently, we can rewrite (4.1) as

$$\begin{aligned} \dot{x} &= f(x) + g(x)u \\ &= \begin{bmatrix} x_2 \\ \frac{1}{M}\left(P - Dx_2 - \frac{EV\sin x_1}{x_3}\right) \\ \frac{1}{T_{\text{CSC}}}\left(-x_3 + x_{3_\star}\right) \end{bmatrix} + \begin{bmatrix} 0 \\ 0 \\ \frac{1}{T_{\text{CSC}}} \end{bmatrix} u. \end{aligned} \tag{4.2}$$

The open loop system is given by (4.2) with $x_3 \equiv x_{3_\star}$, $u \equiv 0$, and hence $\dot{x}_3 \equiv 0$. It takes the following form:

$$\dot{x}_1 = x_2 \tag{4.3a}$$

$$\dot{x}_2 = \frac{1}{M}\left(P - Dx_2 - \frac{EV\sin x_1}{x_{3_\star}}\right). \tag{4.3b}$$

For the swing equation model (4.3) of the SMIB system we take the following energy function,

$$H(x) = -Px_1 + \frac{Mx_2^2}{2} - \frac{EV\cos x_1}{x_{3_\star}}. \tag{4.4}$$

Using the theory of port-Hamiltonian systems [2], we can represent (4.3) in the port-Hamiltonian form as follows:

$$\dot{x} = (J(x) - R(x)) \frac{\partial H}{\partial x} \tag{4.5}$$

with

$$J(x) = \begin{bmatrix} 0 & \frac{1}{M} \\ -\frac{1}{M} & 0 \end{bmatrix} \tag{4.6a}$$

$$R(x) = \begin{bmatrix} 0 & 0 \\ 0 & \frac{D}{M^2} \end{bmatrix} \tag{4.6b}$$

where $J(x) = -J^T(x)$ is the interconnection structure matrix, $R(x) = R^T(x) \geq 0$ is the damping matrix, and $H(x)$ is as in (4.4).

The system given by (4.3) has one open loop equilibrium in $\mathcal{D}$, and using (4.4) as a Lyapunov function it can be shown the equilibrium is a stable equilibrium. It is the operating point of the open loop system (4.2) and is denoted by $x_\star = (x_{1_\star}, 0, x_{3_\star})$.

From (4.6) we get that, there is an interconnection between $x_1$ and $x_2$, and also there is a dissipation term given by $\frac{D}{M^2}$ in the $x_2$ coordinate of (4.3). Generally, this dissipation is negligibly small, and hence to improve the transient performance of the SMIB system we aim at introducing additional dissipation in the $x_2$ coordinate. This could be achieved by introducing additional damping in the actuator dynamics, and then assigning an interconnection term between $x_2$ and the actuator dynamics. At the same time we aim at assigning a suitable energy function to the closed-loop dynamics such that the closed-loop system is stable at $x_\star$.

### *4.2.1 Controller Synthesis*

Consider the swing equation model (4.2) of the SMIB with CSC. We propose the following energy function for the closed-loop dynamics:

$$H_d(x) = -Px_1 + \frac{Mx_2^2}{2} - \frac{EV\cos x_1}{x_{3_\star}} + \frac{1}{2}(x_3 - x_{3_\star})^2. \tag{4.7}$$

It is evident that $\frac{\partial H_d(x)}{\partial x}\Big|_{x=x_\star} = 0$ and $\frac{\partial^2 H_d(x)}{\partial x^2}\Big|_{x=x_\star} > 0$, that is, the energy function (4.7) has an isolated minimum at $x_\star \in \mathcal{D}$. Further, we choose the desired interconnection matrix $J_d(x)$ and damping matrix $R_d(x)$ as

$$J_d(x) = \begin{bmatrix} 0 & \frac{1}{M} & 0 \\ -\frac{1}{M} & 0 & J_{d23} \\ 0 & -J_{d23} & 0 \end{bmatrix} \tag{4.8a}$$

$$R_d(x) = \begin{bmatrix} 0 & 0 & 0 \\ 0 & \frac{D}{M^2} & 0 \\ 0 & 0 & \frac{1}{T_{\text{CSC}}} + \gamma_3 \end{bmatrix} \tag{4.8b}$$

where $J_{d23} = \frac{EV \sin x_1}{M x_3 x_{3_\star}}$. The matrix $J_d$ is chosen in order to have a coupling between the SMIB system and the CSC dynamics. The damping matrix is chosen such that it introduces additional damping $\gamma_3 \geq 0$ in the $x_3$ coordinate.

Through straightforward calculations we can show that the closed-loop system (3.2) with $H_d$, $J_d$ and $R_d$ given by (4.7), (4.8a) and (4.8b) respectively, and the open loop system (4.2) satisfy the matching Equation (3.3). Then, using (3.4) we compute the control law $u(x)$ as

$$u(x) = -T_{\text{CSC}} \left( \frac{EV x_2 \sin x_1}{x_3 x_{3_\star}} + \gamma_3 (x_3 - x_{3_\star}) \right). \tag{4.9}$$

The control law $u(x)$ consists of two components- energy shaping control $u_e(x)$ given by

$$u_e(x) = -\frac{T_{\text{CSC}} EV x_2 \sin x_1}{x_3 x_{3_\star}}, \tag{4.10}$$

and damping injection control $u_d(x)$ given by

$$u_d(x) = -T_{\text{CSC}}\, \gamma_3 (x_3 - x_{3_\star}), \tag{4.11}$$

that is, $u(x) = u_e(x) + u_d(x)$.

### 4.2.2 Asymptotic Stability

From Theorem 3.2.1 the closed-loop system (4.2) with the control (4.9) is stable. To show the asymptotic stability we use LaSalle's invariance principle. The time derivative of $H_d(x)$ along the trajectories of the closed-loop system is

$$\begin{aligned} \dot{H}_d(x) &= -\left( \frac{\partial H_d(x)}{\partial x} \right)^T R_d(x) \frac{\partial H_d(x)}{\partial x} \\ &= -D x_2^2 - \left( \frac{1}{T_{\text{CSC}}} + \gamma_3 \right) (x_3 - x_{3_\star})^2. \end{aligned} \tag{4.12}$$

Then, we have that, $\dot{H}_d(x) \equiv 0$ implies that $x_2 \equiv 0$ as well as $x_3 \equiv x_{3_\star}$. From (4.9) this further implies that $u \equiv 0$. From the closed-loop system (4.2) with $u \equiv 0$, $x_2 \equiv 0$, and $x_3 \equiv x_{3_\star}$ we get

$$0 \equiv \dot{x}_2 \;=\; P - \frac{EV \sin \hat{x}_1}{x_{3_\star}}$$

or

$$\hat{x}_1 = \arcsin\left(\frac{Px_{3_\star}}{EV}\right).$$

Further, we have that $\hat{x}_1\big|_{\mathcal{D}} = x_{1_\star}$. Thus, the closed-loop system (4.2) with the control (4.9) is asymptotically stable at $x_\star \in \mathcal{D}$.

### 4.2.3 Domain of Attraction

We now give an estimate of the domain of attraction for the closed-loop system. We follow the discussion in [3] and check the strong convexity property of the Hessian $\frac{\partial^2 H_d(x)}{\partial x^2}$ to give the estimate. We denote the sublevel sets of the Lyapunov function $H_d(x)$ by $\Omega_c := \left\{x \in S^1 \times \mathbb{R}^2 \;\middle|\; H_d(x) \leq c\right\}$.

**Proposition 4.2.1** *Fix a small number $d_1 > 0$. Estimates of the domain of attraction of the stable equilibrium $x_\star$ of the closed-loop system (4.2) with the control input given by (4.9) are the sublevel sets $\Omega_c$ that are contained in $\mathcal{S}_\epsilon \cap \mathcal{D}$ where*

$$\mathcal{S}_\epsilon := \left\{x \in S^1 \times \mathbb{R}^2 \;\middle|\; \frac{EV\cos x_1}{x_{3_\star}} > \epsilon, \quad \forall 0 < \epsilon < \min\left\{1, M, \frac{EV\sin d_1}{x_{3_\star}}\right\}\right\}.$$

*Proof* Based on the arguments given above. □

We summarize the above discussion on control synthesis in the following proposition:

**Proposition 4.2.2** *The closed-loop system (4.2) with the control law as in (4.9) is asymptotically stable at $x_\star \in \mathcal{D}$ with the energy function (4.7), interconnection structure matrix (4.8a) and damping matrix (4.8b). An estimate of the domain of attraction is given by Proposition* 4.2.1.

*Proof* Based on the arguments given above. □

## 4.3 The Flux-Decay Model

Consider the SMIB system with a CSC as shown in Fig. 3.1. Similar to the previous section, the control system here consists of two subsystems: one describing the SMIB system and the other describing the actuator (CSC) dynamics. We describe the SMIB system using the classical third order flux-decay model. This model includes the flux decay effect in addition to the rotor dynamics described by the second order swing equation. Once again the actuator dynamics is represented by (2.10).

We define the state variables of the system as $x_1 = \delta$, $x_2 = \omega$, $x_3 = E$ and $x_4 = x_l$, and $x = [x_1\ x_2\ x_3\ x_4]^T$ as the state vector. Further, we define the following variables:

$$\begin{aligned} X_d &= x_d + x_{\text{line}} - x_c \\ X'_d &= x'_d + x_{\text{line}} - x_c \\ X_q &= x_q + x_{\text{line}} - x_c. \end{aligned}$$

Normally, it is assumed that $X_q = X'_d$. The complete control system can then be written as

$$\dot{x}_1 = x_2 \tag{4.13a}$$

$$\dot{x}_2 = \frac{1}{M}\left(P - Dx_2 - \frac{Vx_3 \sin x_1}{x_4}\right) \tag{4.13b}$$

$$\dot{x}_3 = \frac{1}{T_{d0}}\left(E_{fd} - V\cos x_1 + \frac{x_d - x'_d + x_4}{x_4}(V\cos x_1 - x_3)\right) \tag{4.13c}$$

$$\dot{x}_4 = \frac{1}{T_{\text{CSC}}}\left(-x_4 + x_{4_\star} + u\right), \tag{4.13d}$$

where $x_{4_\star} = \frac{Vx_{3_\star}\sin x_{1_\star}}{P} = -\frac{(x_d - x'_d)(V\cos x_{1_\star} - x_{3_\star})}{E_{fd} - x_{3_\star}}$, for a given $x_{1_\star}$ and $x_{3_\star}$, is the effective line reactance at the operating equilibrium. We can rewrite (4.13) as

$$\begin{aligned} \dot{x} &= f(x) + g(x)u \\ &= \begin{bmatrix} x_2 \\ \frac{1}{M}\left(P - Dx_2 - \frac{Vx_3\sin x_1}{x_4}\right) \\ \frac{1}{T_{d0}}\left(E_{fd} - V\cos x_1 + \frac{x_d - x'_d + x_4}{x_4}(V\cos x_1 - x_3)\right) \\ \frac{1}{T_{\text{CSC}}}\left(-x_4 + x_{4_\star}\right) \end{bmatrix} + \begin{bmatrix} 0 \\ 0 \\ 0 \\ \frac{1}{T_{\text{CSC}}} \end{bmatrix} u. \end{aligned} \tag{4.14}$$

The open loop system given by (4.14) with $x_4 \equiv x_{4_\star}$, $u \equiv 0$, and hence $\dot{x}_4 \equiv 0$, takes the following form:

$$\dot{x}_1 = x_2 \tag{4.15a}$$

$$\dot{x}_2 = \frac{1}{M}\left(P - Dx_2 - \frac{Vx_3\sin x_1}{x_{4_\star}}\right) \tag{4.15b}$$

$$\dot{x}_3 = \frac{1}{T_{d0}}\left(E_{f_d} - V\cos x_1 + \frac{x_d - x'_d + x_{4_\star}}{x_{4_\star}}(V\cos x_1 - x_3)\right). \tag{4.15c}$$

Following the discussion in [3] it can be shown that there are two open loop equilibria in $\mathcal{D}$ denoted by $\bar{x} = (\bar{x}_1, 0, \bar{x}_3, x_{4_\star})$, where $\bar{x}_1$ and $\bar{x}_3$ are the solutions of the following set of equations:

$$P - \frac{V\bar{x}_3 \sin \bar{x}_1}{x_{4_\star}} = 0$$

$$E_{fd} - V\cos\bar{x}_1 + \frac{x_d - x'_d + x_{4_\star}}{x_{4_\star}}(V\cos\bar{x}_1 - \bar{x}_3) = 0.$$

One of the equilibria is stable and is denoted by $x_\star$, while the other is an unstable equilibrium which we denote by $x_u$. Further, (4.15) can be rewritten in the port-Hamiltonian form [2], using the energy function

$$H(x) = -Px_1 + \frac{Mx_2^2}{2} - \frac{Vx_3\cos x_1}{x_{4\star}} - \frac{E_{fd}x_3}{x_d - x'_d} + \frac{(x_d - x'_d + x_{4\star})x_3^2}{2x_{4\star}(x_d - x'_d)} \tag{4.16}$$

as follows:

$$\dot{x} = (J(x) - R(x))\frac{\partial H}{\partial x} \tag{4.17}$$

with

$$J(x) = \begin{bmatrix} 0 & \frac{1}{M} & 0 \\ -\frac{1}{M} & 0 & 0 \\ 0 & 0 & 0 \end{bmatrix} \tag{4.18a}$$

$$R(x) = \begin{bmatrix} 0 & 0 & 0 \\ 0 & \frac{D}{M^2} & 0 \\ 0 & 0 & \frac{x_d - x'_d}{T_{d0}} \end{bmatrix} \tag{4.18b}$$

where $J(x) = -J^T(x)$ is the interconnection structure matrix and $R(x) = R^T(x) \geq 0$ is the damping matrix. From the damping matrix it is clear that there is dissipation in the $x_2$ and $x_3$ coordinates given by $\frac{D}{M^2}$ and $\frac{x_d - x_{4_\star}}{T_{d0}}$, respectively. Generally, the dissipation in $x_2$ is negligibly small, and hence to improve the transient performance of the SMIB system we aim at introducing additional dissipation in the $x_2$ coordinate. This could be achieved by assigning additional damping in the actuator dynamics, and then assigning an interconnection term between $x_2$ and the actuator dynamics. At the same time we aim at assigning a suitable energy function to the closed-loop dynamics such that the closed-loop system is stable at $x_\star$.

### *4.3.1 Controller Synthesis*

In this section we consider the classical flux-decay model (4.14) of the SMIB with a CSC to design an asymptotically stabilizing control law. The control objective is to make $x_\star$ asymptotically stable and assign a desired damping and interconnection structure to the closed-loop system.

We propose the following energy function for the closed-loop dynamics:

$$H_d(x) = -Px_1 + \frac{Mx_2^2}{2} - \frac{Vx_3\cos x_1}{x_{4\star}} - \frac{E_{fd}x_3}{x_d - x_d'} + \frac{(x_d - x_d' + x_{4\star})x_3^2}{2x_{4\star}(x_d - x_d')} + \frac{(x_4 - x_{4_\star})^2}{2}. \tag{4.19}$$

This energy function has an isolated local minimum at $x_\star$. Further, it is positive definite in some neighbourhood of $x_\star$, for all $d_2 > \frac{V(x_d - x_{4_\star})}{x_d d_1}$ for a given $x_{4_\star}$ and $d_1$. Next, we choose the desired interconnection matrix $J_d(x)$ and damping matrix $R_d(x)$ as

$$J_d(x) = \begin{bmatrix} 0 & \frac{1}{M} & 0 & 0 \\ -\frac{1}{M} & 0 & 0 & J_{d24} \\ 0 & 0 & 0 & J_{d34} \\ 0 & -J_{d24} & -J_{d34} & 0 \end{bmatrix} \tag{4.20a}$$

$$R_d(x) = \begin{bmatrix} 0 & 0 & 0 & 0 \\ 0 & \frac{D}{M^2} & 0 & 0 \\ 0 & 0 & \frac{x_d - x_d'}{T_{d0}} & 0 \\ 0 & 0 & 0 & \frac{1}{T_{\mathrm{CSC}}} + \gamma_4 \end{bmatrix} \tag{4.20b}$$

where $J_{d24} = \frac{Vx_3\sin x_1}{Mx_4x_{4_\star}}$, and $J_{d34} = \frac{(x_d - x_d')(x_3 - V\cos x_1)}{T_{d0}x_4x_{4_\star}}$. The matrix $J_d$ is chosen in order to have a coupling between the SMIB system and the CSC dynamics. Similar to the swing equation model we introduce a damping term $\gamma_4 > 0$ in the $x_4$ coordinate.

Through straightforward calculations it can be shown that the closed-loop system (3.2) with $H_d$, $J_d$ and $R_d$ given by (4.19), (4.20a) and (4.20b) respectively, and the open loop system (4.14) satisfy the matching equation (3.3). Then, using (3.4) we can compute the control $u(x)$ as

$$\begin{aligned} u(x) = &- \frac{T_{\mathrm{CSC}}(x_d - x_d')(x_3 - V\cos x_1)\left((x_d - x_d' + x_{4_\star})x_3 - x_{4_\star}E_{fd} - (x_d - x_d')V\cos x_1\right)}{T_{d0}x_4x_{4_\star}^2(x_d - x_d')} \\ &- T_{\mathrm{CSC}}\left(\frac{Vx_3x_2\sin x_1}{x_4x_{4_\star}} + \gamma_4(x_4 - x_{4_\star})\right). \end{aligned} \tag{4.21}$$

The control law given by (4.21) consists of two components- energy shaping control, $u_e(x)$, given by

$$\begin{aligned} u_e(x) = &- \frac{T_{\mathrm{CSC}}(x_d - x_d')(x_3 - V\cos x_1)\left((x_d - x_d' + x_{4_\star})x_3 - x_{4_\star}E_{fd} - (x_d - x_d')V\cos x_1\right)}{T_{d0}x_4x_{4_\star}^2(x_d - x_d')} \\ &- \frac{T_{\mathrm{CSC}}Vx_3x_2\sin x_1}{x_4x_{4_\star}}, \end{aligned} \tag{4.22}$$

and damping injection control, $u_d(x)$, given by

$$u_d(x) = -T_{\mathrm{CSC}}\,\gamma_4(x_4 - x_{4_\star}), \tag{4.23}$$

or in other words, $u(x) = u_e(x) + u_d(x)$.

### 4.3.2 Asymptotic Stability and Domain of Attraction

Fix two numbers $d_1 > 0$ and $d_2 > 0$ such that $d_1 d_2 > \frac{V(x_d - x'_d)}{x_d - x'_d + x_{4_\star}}$ for a given $x_{4_\star}$. Let

$$\mathcal{S}_\epsilon := \left\{ x \in S^1 \times \mathbb{R}^3 \;\middle|\; \frac{V x_3 \sin x_1 (x_d - x'_d + x_{4\star}) - (x_d - x'_d)(V \sin x_1)^2}{x_{4_\star}\left(\left(x_d - x'_d\right) V x_3 \cos x_1 + x_d - x'_d + x_{4\star}\right)} > \epsilon, \right.$$
$$\left. \forall 0 < \epsilon < \min\left\{ 1, M, \frac{x_d - x'_d + x_{4_\star}}{x_{4_\star}(x_d - x'_d)}, \frac{V d_2 \cos d_1}{x_{4_\star}} \right\} \right\}.$$

The energy function (4.19) has an isolated local minimum at $x_\star$ and (4.19) is strongly convex in a neighbourhood $\mathcal{S}_\epsilon$ of $x_\star$. Hence, the closed-loop system (4.14) with the control law (4.21) is asymptotically stable at $x_\star$.

The region of operation $\mathcal{D}$ contains both $x_\star$ and $x_u$. Due to presence of the unstable equilibrium there is a restriction on the domain of attraction for the stable equilibrium $x_\star$. Next, we give an estimate of the domain of attraction for the closed-loop system around the operating equilibrium $x_\star$. Similar to the swing equation model case, here we check for the strong convexity property of the Hessian $\frac{\partial^2 H_d(x)}{\partial x^2}$ to give the estimate. We denote the sublevel sets of the Lyapunov function $H_d(x)$ by $\Omega_c := \left\{ x \in S^1 \times \mathbb{R}^3 \mid H_d(x) \leq c \right\}$.

**Proposition 4.3.1** *Estimates of the domain of attraction of the stable equilibrium $x_\star$ of the closed-loop system* (4.14) *with the control law* (4.21) *are the sublevel sets $\Omega_c$ that are contained in $\mathcal{S}_\epsilon \cap \mathcal{D}$.*

*Proof* Based on the arguments given above. □

We summarize the above discussion on control synthesis in the following proposition:

**Proposition 4.3.2** *The closed-loop system* (4.14) *with the control input* (4.21) *is asymptotically stable at $x_\star \in \mathcal{D}$ with energy function* (4.19)*, interconnection structure matrix* (4.20a) *and damping matrix* (4.20b)*. An estimate of the domain of attraction is given by Proposition* 4.3.1.

*Proof* Based on the arguments given above. □

## 4.4 Simulation Results

We assume the following simulation parameters: $M = \frac{8}{100\pi}$, $D = \frac{0.4}{100\pi}$, $P = 1.1$ pu, $V = 1$ pu, $T_{\text{CSC}} = 0.02$ s, To assess the performance of the proposed control law we assume that a short circuit fault occurs at the far end of the transmission line at time $t = 1$ s for a duration of 0.1 s.

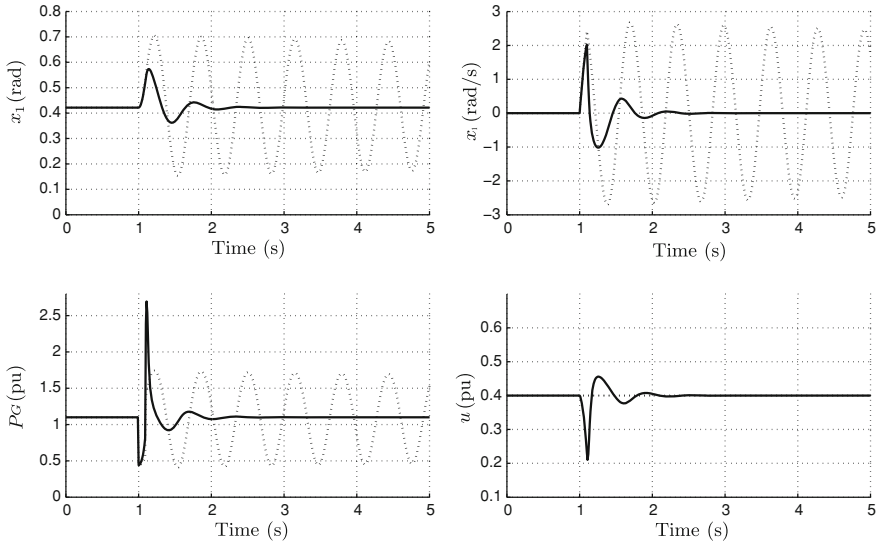


**Fig. 4.1** Response of the SMIB system (4.2) with the IDA-PBC control law (4.9): *Dotted line* (open loop response), *solid line* (closed-loop response with $\gamma_3 = 0$)

### *4.4.1 The Swing Equation Model*

For the swing equation model we assume $E = 1.075$ pu, $0.2 \leq x_3 \leq 0.6$ and the operating equilibrium is $x_\star = (0.4217, 0, 0.4)$. The tuning parameter is $\gamma_3$. The transient response of the swing equation model is shown in Fig 4.1. The open loop response is oscillatory as shown by dotted lines. The closed-loop response with $\gamma_3 = 0$ is shown by the solid lines. The oscillations decay in about 1 s. As the time constant, $T_{\text{CSC}}$, of a CSC is sufficiently small, there is inherent damping, given by $\frac{1}{T_{\text{CSC}}}$, in the dynamics of the CSC. Hence there is no need of any external damping $\gamma_3$. The inherent damping in the CSC dynamics, then, propagates in the SMIB dynamics through the interconnection term. Notice that the input doesn't cross the saturation limits. Figure 4.2 shows phase portraits of the responses.

### *4.4.2 The Flux Decay Model*

For the flux-decay model we assume that $0.6 \leq x_4 \leq 1.0 x_d = 0.95$, $E_{fd} = 1.5$ pu, $T_{d0} = 10$ s. and the operating equilibrium is $x_\star = (0.7179, 0, 1.4214, 0.85)$. The tuning parameter is $\gamma_4$. The transient response of the swing equation model is shown in Fig. 4.3 . The open loop response, represented by the dotted lines, shows heavy oscillations in $x_1$ and $x_2$ due to poor mechanical damping. On the other hand, the generator voltage shows a sluggish response due to comparatively large time constant.

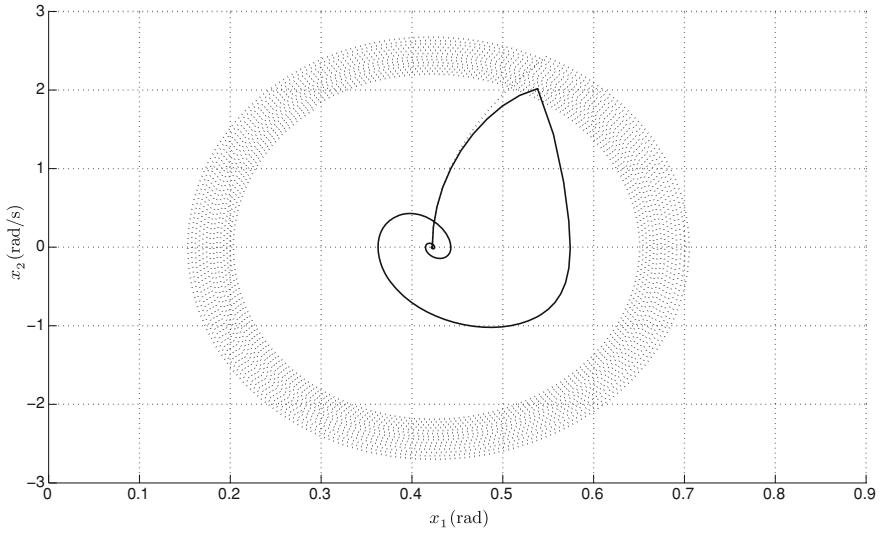


**Fig. 4.2** Phase plots for the SMIB system (4.2) with the IDA-PBC control law (4.9): *Dotted line* (open loop response), *solid line* (closed-loop response with $\gamma_3 = 0$)

The closed-loop response with $\gamma_4 = 0$ is shown by the solid lines. The oscillations in $x_1$ and $x_2$ decay in about 2 s. The response of $x_3$ also improves. As the time constant, $T_{\text{CSC}}$, of a CSC is sufficiently small, there is inherent damping, given by $\frac{1}{T_{\text{CSC}}}$, in the dynamics of the CSC. Hence there is no need of any external damping $\gamma_4$. The inherent damping in the CSC dynamics, then, propagates in the SMIB dynamics through the interconnection term. Further, the actuator doesn't cross the saturation limits. Figure 4.4 shows phase portraits of the responses.

## 4.5 Summary

Transient stabilization of the SMIB system using a CSC via IDA-PBC was investigated. In an attempt to take into account the actuator dynamics, the CSC was modeled by a first order system. We assigned a desired interconnection and damping structure, and a desired energy function to the closed-loop system for the swing equation as well as the flux-decay model. The closed-loop systems were shown to be asymptotically stable at the operating point. Also, estimates of the domain of attraction for the closed-loop systems were given in both the cases. Simulation results were provided to examine the performance of the control laws.

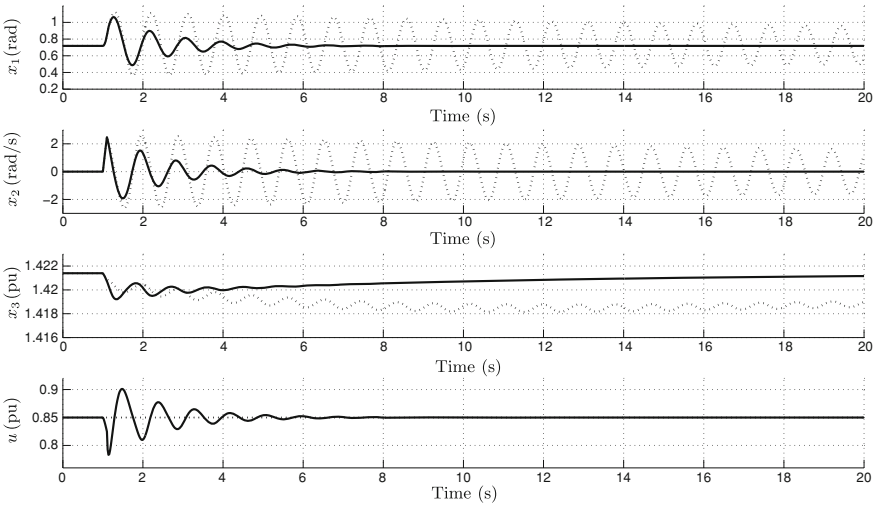


**Fig. 4.3** Response of the SMIB system (4.14) with the IDA-PBC control law (4.21): *Dotted line* (open loop response), *solid line* (closed-loop response with $\gamma_4 = 0$)

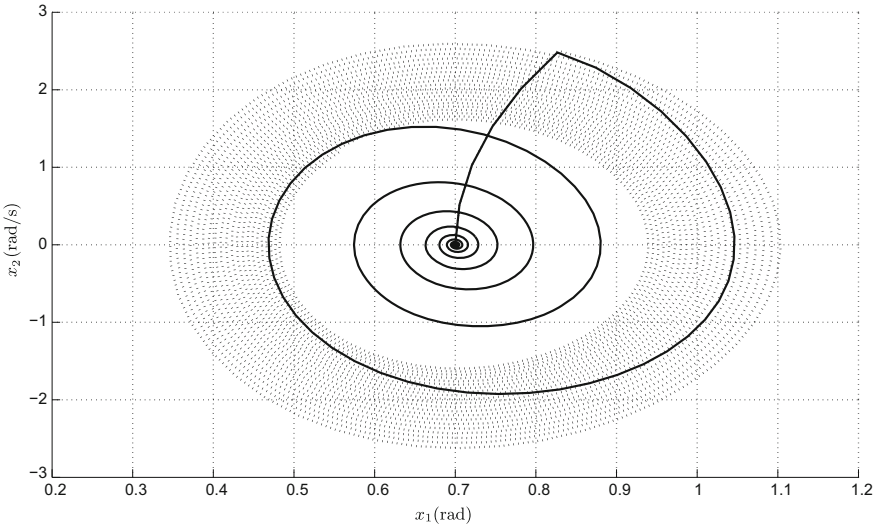


**Fig. 4.4** Phase plots for the SMIB system (4.14) with the IDA-PBC control law (4.21): *Dotted line* (open loop response), *solid line* (closed-loop response with $\gamma_4 = 0$)

## References

1. M.A. Pai, D.P.S. Gupta, K.R. Padiyar, *Small Signal Analysis of Power Systems* (Narosa Publishing House, New Delhi, 2004)

2. A.J. van der Schaft, *$L_2$-Gain and Passivity Techniques in Nonlinear Control* (Springer, London, 1996)
3. M. Galaz, R. Ortega, A.S. Bazanella, A.M. Stankovic, An energy-shaping approach to the design of excitation control of synchronous generators. Automatica **39**, 111–119 (2003)

# Chapter 5
# Stabilization via Immersion and Invariance with the First Order Model of the CSC

## 5.1 Introduction

The IDA-PBC methodology relies on the concept of exact model matching of the closed-loop system with a certain desired behaviour. Immersion and Invariance [1], on the other hand, is based on (a) immersing a lower order desired target dynamics onto a manifold in the original space, and (b) matching the closed-loop system with the immersed system asymptotically. The control objective is to make the immersed manifold attractive and invariant. This methodology, as it is based on the concept of asymptotic model matching, offers more flexibility over IDA-PBC. In this chapter we apply I&I to synthesize stabilizing control laws for the SMIB system using a CSC. The SMIB is expressed using the RNM model. The CSC is modeled by a first order model.

The chapter is organized as follows: In Sect. 5.2 a brief introduction to the I&I control synthesis is given. In Sect. 5.3 we propose a control law for the SMIB system with a CSC using the I&I strategy. The simulation results are provided in Sect. 5.4. In Sect. 5.5 we propose a target dynamics with additional damping and synthesize a control law using this target dynamics. Simulation plots are provided to assess the performance. Finally Sect. 5.6 concludes the chapter.

## 5.2 Immersion and Invariance

The method of I&I for stabilization of nonlinear systems is proposed in [1]. We now state the stability result of I&I.

**Theorem 5.2.1** *Consider the state space model of the system*

$$\dot{x} = f(x) + g(x)u \tag{5.1}$$

N. S. Manjarekar and R. N. Banavar, *Nonlinear Control Synthesis for Electrical Power Systems Using Controllable Series Capacitors*, SpringerBriefs in Applied Sciences and Technology, DOI: 10.1007/978-3-642-27531-9_5, © The Author(s) 2012

*where $f(x)$ and $g(x)$ are smooth functions, with state $x \in \mathbb{R}^n$ and control $u \in \mathbb{R}^m$, with an equilibrium point $x_\star \in \mathbb{R}^n$ to be stabilized. Let $p < n$ and assume we can find mappings*

$$\alpha : \mathbb{R}^p \to \mathbb{R}^p, \Pi : \mathbb{R}^p \to \mathbb{R}^n, c : im\, \Pi \to \mathbb{R}^m, \phi : \mathbb{R}^n \to \mathbb{R}^p, \psi : \mathbb{R}^n \times \mathbb{R}^{n-p} \to \mathbb{R}^m,$$

*such that the following hold.*

1. (*H*1) (*Target system*) *The system*

$$\dot{\xi} = \alpha(\xi) \tag{5.2}$$

*with state $\xi \in \mathbb{R}^p$ has an asymptotically stable equilibrium at $\xi_\star \in \mathbb{R}^p$ and $x_\star = \Pi(\xi_\star)$.*

2. (*H*2) (*Immersion condition*) *For all $\xi \in \mathbb{R}^p$*

$$f(\Pi(\xi)) + g(\Pi(\xi))c(\Pi(\xi)) = \frac{\partial \Pi}{\partial \xi}\alpha(\xi). \tag{5.3}$$

3. *(H3) (Implicit manifold) The following set identity holds*

$$\left\{x \in \mathbb{R}^n \mid \phi(x) = 0\right\} = \left\{x \in \mathbb{R}^n \mid x = \Pi(\xi) \text{ for some } \xi \in \mathbb{R}^p\right\}. \tag{5.4}$$

4. (*H*4) (*Manifold attractivity and trajectory boundedness*) *All trajectories of the system*

$$\dot{z} = \frac{\partial \phi}{\partial x}\left[f(x) + g(x)\psi(x, z)\right] \tag{5.5}$$

$$\dot{x} = f(x) + g(x)\psi(x, z) \tag{5.6}$$

*are bounded and satisfy*

$$\lim_{t\to\infty} z(t) = 0. \tag{5.7}$$

*Then $x_\star$ is an asymptotically stable equilibrium of the closed-loop system*

$$\dot{x} = f(x) + g(x)\psi(x, \phi(x)).$$

The I&I philosophy can be can be interpreted with the help of Fig. 5.1 as: Given the system (5.1) and the target dynamical system (5.2), find if possible, a manifold $\mathcal{M}$ such that

1. Restriction of the closed-loop system to $\mathcal{M}$ is the target dynamics.
2. $\mathcal{M}$ can be rendered invariant and attractive.

The left hand side of (5.4) gives an implicit description of $\mathcal{M}$ while the right hand side is a parametrized description. The control law $u = c(\Pi(\xi))$ renders $\mathcal{M}$ invariant. A measure of the distance of the system trajectories to $\mathcal{M}$ is given by it z, called as off-the-manifold coordinate. Our aim is to design a control law $u = \psi(x, z)$ that keeps the system trajectories bounded and drives the coordinate it z to zero.

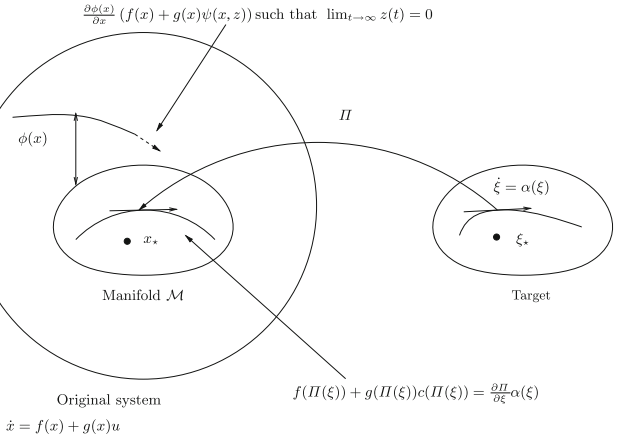


**Fig. 5.1** Immersion & invariance strategy

## 5.3 I&I-Based Control Synthesis for Transient Stabilization of the SMIB System

Consider the SMIB system with a CSC as shown in Fig 5.1. The SMIB system is described using the swing equation model, and the actuator dynamics using the first order system (2.10). The SMIB system with a CSC is then described by (4.2) which is reproduced here for convenience, as

$$\begin{aligned}\dot{x} &= f(x)+g(x)u \\ &= \begin{pmatrix} x_2 \\ \frac{1}{M}\left[P - Dx_2 - EV\frac{\sin x_1}{x_3}\right] \\ \frac{1}{T_{\text{CSC}}}\left[-x_3 + x_{3_\star}\right]\end{pmatrix} + \begin{pmatrix} 0 \\ 0 \\ \frac{1}{T_{\text{CSC}}}\end{pmatrix} u\end{aligned} \tag{5.8}$$

where $x_{3_\star} = \frac{EV\sin x_{1_\star}}{P}$ for a given $x_{1_\star}$. The open loop operating equilibrium is denoted by $x_\star = (x_{1_\star}, 0, x_{3_\star})$. We assume that,

**Assumption 5.3.1** The region of operation is

$$\mathcal{D} = \left\{ x \in S^1 \times I\!R^2 \mid d_1 < x_1 < \frac{\pi}{2} - d_1, \underline{d_3} < x_3 < \overline{d_3} \right\},$$

where $d_1 > 0$ and $0 < \underline{d_3} < \overline{d_3}$ are small numbers.

### *5.3.1 Control Objective*

As mentioned earlier, $x_\star$ denotes the operating stable equilibrium in $\mathcal{D}$. We assume that $x_\star$ is known to us and state the control objective as "to synthesize a control law

$u$ in order to make the system (5.8) asymptotically stable at $x_\star$, and to improve the transient response of the closed-loop system."

### 5.3.2 Controller Synthesis

Next, we synthesize a stabilizing controller for the SMIB system with a CSC. The control system is given by (5.8) and it consists of two subsystems- one is the second order swing equation, a slow system, and the other is the CSC which is the fast dynamics as compared to the swing dynamics.

We use the Immersion and Invariance methodology described earlier to synthesize the controller.

#### Target system

In general, selection of the target dynamics is a nontrivial task. As discussed in [1] we make a natural choice for the target system as the mechanical subsystem. As a first step in the control synthesis we define a two dimensional dynamical system as follows: Let $\xi = [\xi_1, \xi_2]^T \in S^1 \times I\!R$ be the state of the dynamical system.

$$\dot{\xi}_1 = \xi_2 \tag{5.9a}$$

$$\dot{\xi}_2 = -\frac{\partial V(\xi_1)}{\partial \xi_1} - R(\xi)\xi_2 \tag{5.9b}$$

where $V(\xi_1)$ denotes the potential energy of the system which is to be chosen, and $R(\xi_1, \xi_2)$ is a (possibly nonlinear) damping function which is to be chosen. The target system (5.9) is a simple pendulum system with a stable equilibrium $\xi_\star = (\xi_{1_\star}, 0)$ and with the energy function

$$H(\xi_1, \xi_2) = \frac{1}{2}\xi_2^2 + V(\xi_1). \tag{5.10}$$

To ensure the stability at the equilibrium we assume that

**Assumption 5.3.2**

1. The potential energy function $V(\xi_1)$ satisfies

$$\begin{cases} \left.\frac{\partial V(\xi_1)}{\partial \xi_1}\right|_{\xi_1=\xi_{1_\star}} = 0 \\ \left.\frac{\partial^2 V(\xi_1)}{\partial \xi_1^2}\right|_{\xi_1=\xi_{1_\star}} > 0 \end{cases}$$

2. The damping function satisfies $R(\xi_\star) \geq 0$.

**Immersion condition**

Once we define a desired target dynamics, we define a mapping $\Pi : S^1 \times I\!R \rightarrow S^1 \times I\!R^2$ as follows:

$$\Pi(\xi) := \begin{bmatrix} \xi_1 \\ \xi_2 \\ \Pi_3(\xi) \end{bmatrix} \tag{5.11}$$

where $\Pi_3(\xi)$ is to be chosen. Then with this choice of $\Pi(\xi)$ and the target dynamics (5.2), Eq. 5.3 becomes

$$\begin{aligned} &\begin{bmatrix} \xi_2 \\ \frac{1}{M}\left[P - D\xi_2 - EV\frac{\sin\xi_1}{\Pi_3(\xi)}\right] \\ \frac{1}{T_{\text{CSC}}}\left[-\Pi_3(\xi) + x_{3_\star}\right] \end{bmatrix} + \begin{bmatrix} 0 \\ 0 \\ \frac{1}{T_{\text{CSC}}} \end{bmatrix} c(\Pi(\xi)) \\ &= \begin{bmatrix} 1 & 0 \\ 0 & 1 \\ \frac{\partial \Pi_3(\xi)}{\partial \xi_1} & \frac{\partial \Pi_3(\xi)}{\partial \xi_2} \end{bmatrix} \begin{bmatrix} \xi_2 \\ -\frac{\partial V(\xi_1)}{\partial \xi_1} - R(\xi)\xi_2 \end{bmatrix}. \end{aligned} \tag{5.12}$$

Next we choose $\Pi_3(\xi)$ and $c(\Pi(\xi))$ to satisfy the above equation as follows: The first row of (5.12) is already satisfied. From the second row we have

$$\frac{1}{M}\left[P - D\xi_2 - EV\frac{\sin\xi_1}{\Pi_3(\xi)}\right] = -\frac{\partial V(\xi_1)}{\partial \xi_1} - R(\xi)\xi_2.$$

We choose $R(\xi) = \frac{D}{M}$ and $V(\xi_1) = -\beta\cos\tilde{\xi}_1$ for some $\beta > 0$ (to be chosen). We use $\tilde{\xi}_1$ to denote $\xi_1 - \xi_{1_\star}$. Then the above equation becomes

$$\frac{1}{M}\left[P - EV\frac{\sin\xi_1}{\Pi_3(\xi)}\right] = -\beta\sin\tilde{\xi}_1$$

from which we get

$$\Pi_3(\xi) = \frac{EV\sin\xi_1}{P + M\beta\sin\tilde{\xi}_1}.$$

Notice that $\Pi_3$ is a function of $\xi_1$ only. Here we make the following assumption:

**Assumption 5.3.3** $\beta < \frac{P}{M}$.

This assumption makes $\Pi_3(\xi_1)$ bounded for all $\xi_1$. From the third row we have

$$\frac{1}{T_{\text{CSC}}}\left[-\Pi_3(\xi_1) + x_{3_\star}\right] + \frac{1}{T_{\text{CSC}}}c(\Pi(\xi)) = \frac{\partial \Pi_3(\xi_1)}{\partial \xi_1}\xi_2.$$

By substituting for $\Pi_3(\xi_1)$ and $V(\xi_1)$ in the above equation we get

$$c(\Pi(\xi)) = T_{\text{CSC}} EV\xi_2 \left[ \frac{\cos\xi_1}{P + M\beta \sin\tilde{\xi}_1} - \frac{M\beta \sin\xi_1 \cos\tilde{\xi}_1}{\left[P + M\beta \sin\tilde{\xi}_1\right]^2} \right] + \frac{EV \sin\xi_1}{\left[P + M\beta \sin\tilde{\xi}_1\right]} - x_{3_\star}.$$

Thus we get $\Pi(\xi)$ and $c(\Pi(\xi))$.

**Implicit manifold**

The manifold $\mathcal{M}$ is implicitly described by

$$\mathcal{M} = \left\{ x \in S^1 \times I\!R^2 | \phi(x) = 0 \right\}$$

with

$$\begin{aligned} \phi(x) &= x_3 - \Pi_3(x_1) \\ &= x_3 - \frac{EV \sin x_1}{P + M\beta \sin\tilde{x}_1} \end{aligned}$$

where $\tilde{x}_1$ denotes $x_1 - x_{1_\star}$.

**Manifold attractivity and trajectory boundedness**

Here the off-the-manifold coordinate is $z = \phi(x)$ and we have that

$$\begin{aligned} \dot{z} &= \dot{x}_3 - \dot{\Pi}_3(x_1) \\ &= \dot{x}_3 - \frac{\partial \Pi_3(x_1)}{\partial x_1}\dot{x}_1 \\ &= \frac{1}{T_{\text{CSC}}}\left[-x_3 + x_{3_\star} + \psi(x,z)\right] - \frac{\partial \Pi_3(x_1)}{\partial x_1} x_2 \\ &= \frac{\psi(x,z)}{T_{\text{CSC}}} + \left[ \frac{-x_3 + x_{3_\star}}{T_{\text{CSC}}} - \frac{\partial \Pi_3(x_1)}{\partial x_1} x_2 \right]. \end{aligned}$$

To ensure the boundedness of the trajectories of the off-the-manifold coordinate it z and also that $\lim_{t\to\infty} z(t) = 0$ we take

$$\dot{z} = -\gamma z, \quad \gamma > 0 \tag{5.13}$$

and then we have

$$\psi(x,z) = T_{\text{CSC}} \left[ -\gamma z + \frac{x_3 - x_{3_\star}}{T_{\text{CSC}}} + \frac{\partial \Pi_3(x_1)}{\partial x_1} x_2 \right].$$

**The control law**

Next we calculate the control law as

$$\begin{aligned} u =& \psi(x, \phi(x)) \\ =& T_{\mathrm{CSC}} \left[ -\gamma \phi(x) + \frac{x_3 - x_{3_\star}}{T_{\mathrm{CSC}}} + \frac{\partial \Pi_3(x_1)}{\partial x_1} x_2 \right] \\ =& (x_3 - x_{3_\star}) - T_{\mathrm{CSC}} \gamma \left[ x_3 - \frac{EV \sin x_1}{P + M\beta \sin \tilde{x}_1} \right] - \left[ \frac{T_{\mathrm{CSC}} EV x_2 M\beta \sin x_1 \cos \tilde{x}_1}{\left[P + M\beta \sin \tilde{x}_1\right]^2} \right] \\ &+ \left[ \frac{T_{\mathrm{CSC}} EV x_2 \cos x_1}{P + M\beta \sin \tilde{x}_1} \right]. \end{aligned} \tag{5.14}$$

Finally, we establish boundedness of the trajectories of the closed-loop system (5.8) with the control law (5.14) and the off-the-manifold coordinate $z$

$$\dot{x}_1 = x_2 \tag{5.15a}$$

$$\dot{x}_2 = \frac{1}{M} \left[ P - Dx_2 - EV \frac{\sin x_1}{x_3} \right] \tag{5.15b}$$

$$\dot{x}_3 = \frac{1}{T_{\mathrm{CSC}}} \left[ -x_3 + x_{3_\star} + u \right], \tag{5.15c}$$

$$\dot{z} = -\gamma z. \tag{5.15d}$$

Here $x \in S^1 \times I\!R^2$ and $z \in I\!R$. This implies $x_1 \in \mathcal{L}_\infty$ where $\mathcal{L}_\infty$ denotes the space of bounded functions. Now,

$$\begin{aligned} \dot{x}_2 &= \frac{1}{M} \left[ P - Dx_2 - EV \frac{\sin x_1}{x_3} \right] \\ &= -\frac{D}{M} x_2 + \Delta(x_1, x_3) \end{aligned} \tag{5.16}$$

where $\Delta(x_1, x_3) = \frac{1}{M} \left[ P - EV \frac{\sin x_1}{x_3} \right]$. From Assumption 5.3.1 we have $x_3 \geq d_2 > 0$ and also $x_1$ is bounded as stated earlier. This implies $\delta(x_1, x_3)$ is bounded. As we have $D > 0$ and $M > 0$, (5.16) is an asymptotically stable linear system in $x_2$ with a bounded driving function $\Delta(x_1, x_3)$. This implies $x_2 \in \mathcal{L}_\infty$.

Next, we have $x_3 = z + \Pi_3(x_1)$. We have from (5.13) that it z is bounded. Also, from Assumption 5.3.3 we have that $\Pi_3(x_1)$ is bounded for all $x_1$, and hence we can conclude boundedness of $x_3$.

The above discussion on the control synthesis can be summarized in the following proposition which is the main result of this chapter.

**Proposition 5.3.1** *The closed-loop system* (5.8) *with the control law* (5.14) *is locally asymptotically stable at* $x_\star$.

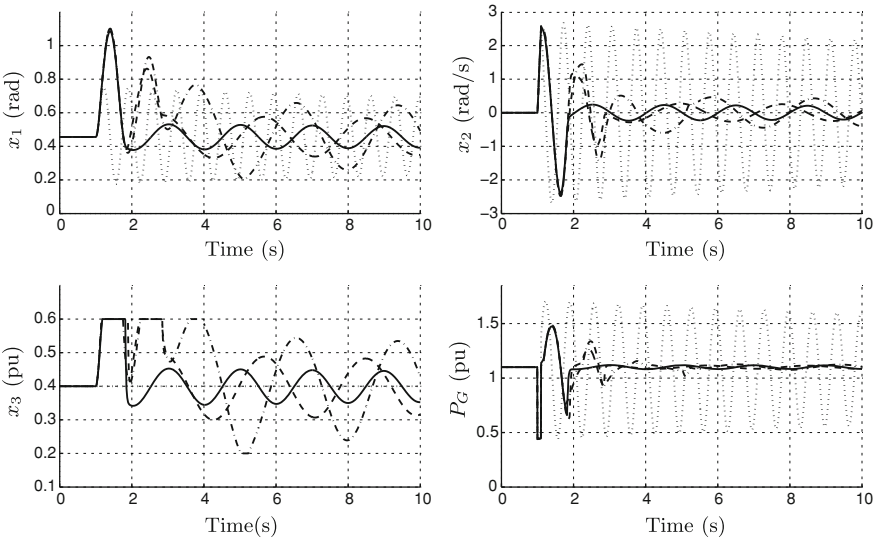


**Fig. 5.2** Response of the SMIB system (5.8) with the I&I control law (5.14): *Dotted line* (open loop response), *dash-dot line* (closed-loop response with $\beta = 5$ and $\gamma = 5$), *dashed line* (closed-loop response with $\beta = 5$ and $\gamma = 50$), *solid line* (closed-loop response with $\beta = 10$ and $\gamma = 50$)

***Proof*** Based on the arguments given above. □

## 5.4 Simulation Results

We assume the following simulation parameters: $M = \frac{8}{100\pi}$, $D = \frac{0.4}{100\pi}$, $P = 1.1\text{pu}$, $E = V = 1\text{pu}$, $T_{\text{CSC}} = 0.02\,\text{s}$, $0.2 \leq x_3 \leq 0.6$ and the operating equilibrium is $x_\star = (0.4556, 0, 0.4)$. The tuning parameters are $\beta$ and $\gamma$. From Assumption 5.3.3 an upper bound on the tuning parameter $\beta$ is 43.19. To assess the performance of the proposed control law we assume that a short circuit fault occurs at the far end of the transmission line at time $t = 1\text{s}$ for a duration of 0.1 s.

The open loop system exhibits heavy and sustained oscillations in $x_1$, $x_2$ and $P_G$ in response to the applied transient as shown by dotted lines in Fig. 5.2. The closed-loop response is plotted for three different sets of tuning parameters. An increase in the value of $\beta$ results in making the energy function of the target dynamics deeper, and hence improves the closed-loop response. By increasing the value of $\gamma$ makes the closed-loop system to match with the trajectories of the desired dynamics at a faster rate. The change in the response for increased value of $\gamma$ is shown from the dash-dot line to the solid line. Note that in this case the oscillations in $P_G$ die out quickly, in about 1 s. The phase portraits of the system are shown in Fig. 5.3. Further, the plot of $\phi(x)$ is presented in Fig. 5.4. Notice that, as discussed earlier the manifold $\mathcal{M}$ is implicitly described by $\phi(x) = 0$.

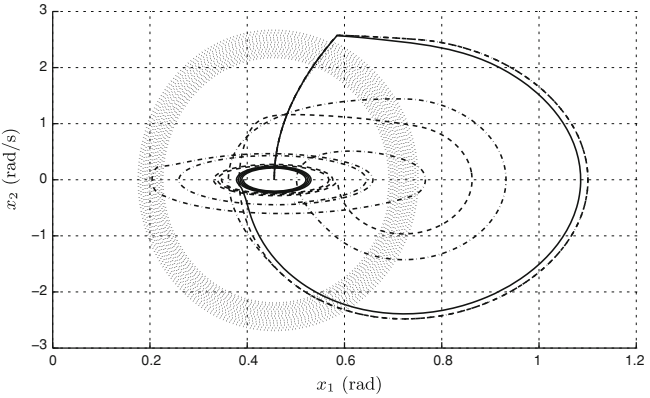


**Fig. 5.3** Phase plots for the SMIB system (5.8) with the I&I control law (5.14): *Dotted line* (open loop response), *dash-dot line* (closed-loop response with $\beta = 5$ and $\gamma = 5$), *dashed line* (closed-loop response with $\beta = 5$ and $\gamma = 50$), *solid line* (closed-loop response with $\beta = 10$ and $\gamma = 50$)

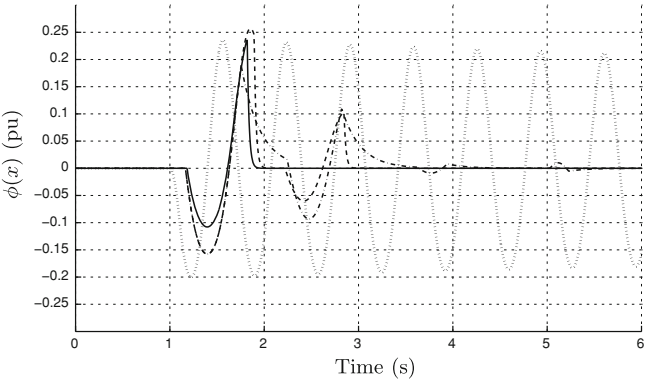


**Fig. 5.4** Plots of $\phi(x)$ for the SMIB system (5.8) with the I&I control law (5.14): *Dotted line* (open loop response), *dash-dot line* (closed-loop response with $\beta = 5$ and $\gamma = 5$), *dashed line* (closed-loop response with $\beta = 5$ and $\gamma = 50$), *solid line* (closed-loop response with $\beta = 10$ and $\gamma = 50$)

## 5.5 Damping Assignment for the SMIB System

In the previous section we proposed a stabilizing control law for the SMIB system using I&I. There we chose the target dynamics based on the open loop system by properly choosing an energy function, but keeping the damping term unchanged. In this manner, as evident from the simulation plots, the stability property can be improved by properly choosing the shape of the energy function. However, the open loop system is poorly damping, in general, the transient response is not satisfactory.

In this section. we modify the target dynamics (5.9) by introducing an additional damping term as follows:

$$\dot{\xi}_1 = \xi_2 \tag{5.17a}$$

$$\dot{\xi}_2 = -\frac{\partial V(\xi_1)}{\partial \xi_1} - R(\xi)\xi_2 \tag{5.17b}$$

with $V(\xi_1) = -\beta \cos \tilde{\xi}_1)$ and $R(\xi) = \frac{D}{M} + \gamma_d$ where $\gamma_d > 0$ is the additional damping. Then, the immersion condition (5.12) modifies to

$$\begin{bmatrix} \xi_2 \\ \frac{1}{M}\left[P - D\xi_2 - EV\frac{\sin\xi_1}{\Pi_3(\xi)}\right] \\ \frac{1}{T_{CSC}}\left[-\Pi_3(\xi) + x_{3_\star}\right] \end{bmatrix} + \begin{bmatrix} 0 \\ 0 \\ \frac{1}{T_{CSC}} \end{bmatrix} c(\Pi(\xi)) \\ = \begin{bmatrix} 1 & 0 \\ 0 & 1 \\ \frac{\partial \Pi_3(\xi)}{\partial \xi_1} & \frac{\partial \Pi_3(\xi)}{\partial \xi_2} \end{bmatrix} \begin{bmatrix} \xi_2 \\ -\beta \sin \tilde{\xi}_1 - \left(\frac{D}{M} + \gamma_d\right)\xi_2 \end{bmatrix}. \tag{5.18}$$

In this case $\Pi_3(\xi)$ modifies to

$$\Pi_3(\xi) = \frac{EV \sin \xi_1}{P + M(\gamma_d \xi_2 + \beta \sin \tilde{\xi}_1)}.$$

Here note that $\Pi_3$ is a function of both $\xi_1$ and $\xi_2$. To make $\Pi_3(\xi_1)$ bounded in a domain of operation we make the following assumptions: we assume that the domain of operation is

**Assumption 5.5.1**

$$\mathcal{D} = \left\{ x \in S^1 \times I\!R^2 |\ d_1 < x_1 < \frac{\pi}{2} - d_1, |x_2| < d_2, \underline{d_3} < x_3 < \overline{d_3} \right\},$$

where $d_1 > 0,\ d_2 > 0$ and $0 < \underline{d_3} < \overline{d_3}$ are small numbers.

Further, we make the following assumption:

**Assumption 5.5.2** $\beta < \frac{P}{M} - \gamma_d d_2$.
This assumption makes $\Pi_3(\xi_1)$ bounded for all $\xi_1$. Then, from the third row of (5.18) we have

$$c(\Pi(\xi)) = T_{CSC} EV \xi_2 \left[ \frac{\cos \xi_1}{P + M(\gamma_d \xi_2 + \beta \sin \tilde{\xi}_1)} - \frac{M\beta \sin \xi_1 \cos \tilde{\xi}_1}{\left[P + M(\gamma_d \xi_2 + \beta \sin \tilde{\xi}_1)\right]^2} \right] \\ + \frac{EVM\gamma_d \sin \xi_1 \left(\beta \sin \tilde{\xi}_1 + \left(\frac{D}{M} + \gamma_d\right)\xi_2\right)}{\left[P + M(\gamma_d \xi_2 + \beta \sin \tilde{\xi}_1)\right]^2} + \frac{EV \sin \xi_1}{\left[P + M(\gamma_d \xi_2 + \beta \sin \tilde{\xi}_1)\right]} - x_{3_\star}.$$

Thus we get $\Pi(\xi)$ and $c(\Pi(\xi))$.

**Implicit manifold**

The manifold $\mathcal{M}$ is implicitly described by

$$\mathcal{M} = \left\{ x \in S^1 \times I\!R^2 | \phi(x) = 0 \right\}$$

with

$$\begin{aligned} \phi(x) &= x_3 - \Pi_3(x_1) \\ &= x_3 - \frac{EV \sin x_1}{P + M(\gamma_d x_2 + \beta \sin \tilde{x}_1)} \end{aligned}$$

where $\tilde{x}_1$ denotes $x_1 - x_{1_\star}$.

**Manifold attractivity and trajectory boundedness**

Here the off-the-manifold coordinate is $z = \phi(x)$ and we have that

$$\begin{aligned} \dot{z} &= \dot{x}_3 - \dot{\Pi}_3(x_1, x_2) \\ &= \dot{x}_3 - \frac{\partial \Pi_3(x_1, x_2)}{\partial x_1}\dot{x}_1 - \frac{\partial \Pi_3(x_1, x_2)}{\partial x_2}\dot{x}_2 \\ &= \frac{1}{T_{\text{CSC}}}\left[-x_3 + x_{3_\star} + \psi(x, z)\right] - \frac{\partial \Pi_3(x_1, x_2)}{\partial x_1}x_2 - \frac{\partial \Pi_3(x_1, x_2)}{\partial x_2}\dot{x}_2 \\ &= \frac{\psi(x, z)}{T_{\text{CSC}}} + \left[\frac{-x_3 + x_{3_\star}}{T_{\text{CSC}}} - \frac{\partial \Pi_3(x_1, x_2)}{\partial x_1}x_2 - \frac{\partial \Pi_3(x_1, x_2)}{\partial x_2}\dot{x}_2\right]. \end{aligned}$$

To ensure the boundedness of the trajectories of the off-the-manifold coordinate $z$ and also that $\lim_{t\to\infty} z(t) = 0$ we choose the dynamics of the it z coordinate as in (5.13) and then we have

$$\psi(x, z) = T_{\text{CSC}}\left[-\gamma z + \frac{x_3 - x_{3_\star}}{T_{\text{CSC}}} + \frac{\partial \Pi_3(x_1, x_2)}{\partial x_1}x_2 + \frac{\partial \Pi_3(x_1, x_2)}{\partial x_2}\dot{x}_2\right].$$

**The control law**

Next we calculate the control law as

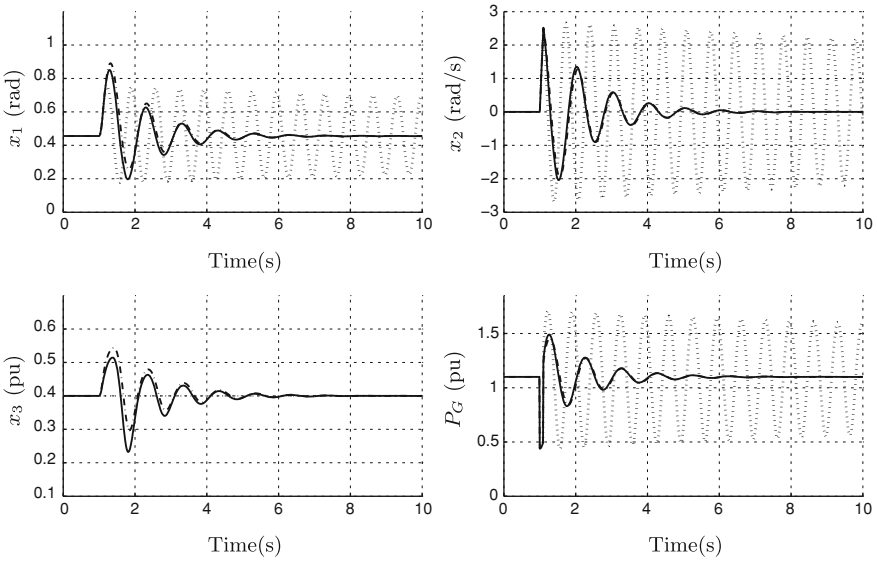


**Fig. 5.5** Response of the SMIB system (5.8) with the I&I control law (5.19): *Dotted line* (open loop response), *dash-dot line* (closed-loop response with $\beta = 38,\ \gamma = 1$ and $\gamma_d = \frac{5}{\pi}$), *solid line* (closed-loop response with $\beta = 38,\ \gamma = 10$ and $\gamma_d = \frac{5}{\pi}$)

$$
\begin{aligned}
u =& \psi(x, \phi(x)) \\
=& T_{\mathrm{CSC}} \left[ -\gamma \phi(x) + \frac{x_3 - x_{3_\star}}{T_{\mathrm{CSC}}} + \frac{\partial \Pi_3(x_1, x_2)}{\partial x_1} x_2 + \frac{\partial \Pi_3(x_1, x_2)}{\partial x_2} \dot{x}_2 \right] \\
=& (x_3 - x_{3_\star}) - T_{\mathrm{CSC}}\, \gamma \left[ x_3 - \frac{EV \sin x_1}{P + M(\gamma_d x_2 + \beta \sin \tilde{x}_1)} \right] - \left[ \frac{T_{\mathrm{CSC}} EV x_2 M \beta \sin x_1 \cos \tilde{x}_1}{\left[P + M(\gamma_d x_2 + \beta \sin \tilde{x}_1)\right]^2} \right] \\
& - \left[ \frac{T_{\mathrm{CSC}} EV \sin x_1 \left( \frac{1}{M} \left[ P - Dx_2 - EV \frac{\sin x_1}{x_3} \right] \right)}{\left[P + M(\gamma_d x_2 + \beta \sin \tilde{x}_1)\right]^2} \right] + \left[ \frac{T_{\mathrm{CSC}} EV x_2 \cos x_1}{P + M(\gamma_d x_2 + \beta \sin \tilde{x}_1)} \right].
\end{aligned}
\tag{5.19}
$$

Finally, we can establish boundedness of the trajectories of the closed-loop system (5.8) with the control law (5.19) and the off-the-manifold coordinate it z as in the previous section. However, note that we have $x_3 = z + \Pi_3(x_1, x_2)$. We have from (5.13) that it z is bounded. Also, from Assumption 5.3.3 we have that $\Pi_3(x_1, x_2)$, and hence $x_3$ is bounded in $\mathcal{D}_{\delta_2}$.

The above discussion on the control synthesis can be summarized in the following proposition which is the main result of this chapter.

**Proposition 5.5.1** *The closed-loop system* (5.8) *with the control law* (5.19) *is locally asymptotically stable at* $x_\star$.

***Proof*** Based on the arguments given above. □

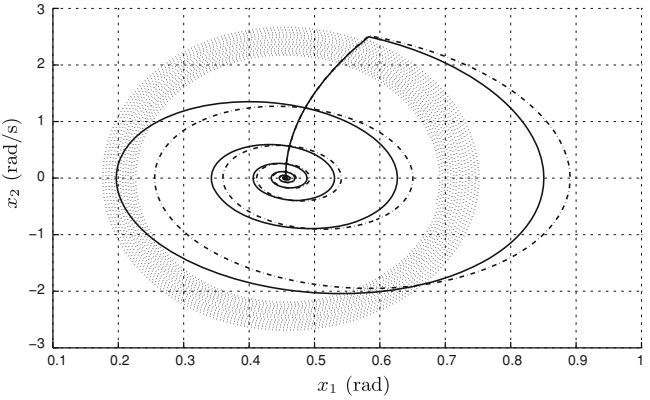


**Fig. 5.6** Phase plots the SMIB system (5.8) with the I&I control law (5.19): *Dotted line* (open loop response), *dash-dot line* (closed-loop response with $\beta = 38,\ \gamma = 1$ and $\gamma_d = \frac{5}{\pi}$), *solid line* (closed-loop response with $\beta = 38,\ \gamma = 10$ and $\gamma_d = \frac{5}{\pi}$)

## 5.6 Simulation Results

We assume the following simulation parameters $M = \frac{8}{100\pi}$, $D = \frac{0.4}{100\pi}$, $P = 1.1\,\text{pu}$, $E = V = 1\,\text{pu}$, $T_{\text{CSC}} = 0.02\,\text{s}$, $0.2 \leq x_3 \leq 0.6$ and the operating equilibrium is $x_\star = (0.4556, 0, 0.4)$. The tuning parameters are $\beta$, $\gamma_d$ and $\gamma$. We choose $\gamma_d = \frac{5}{\pi}$ and assume $d_2 = 2.5 rad/s$ and then from Assumption 5.5.2 an upper bound on the tuning parameter $\beta$ is 39.2. To assess the performance of the proposed control law we assume that a short circuit fault occurs at the far end of the transmission line at time $t = 1\text{s}$ for a duration of 0.1 s. As plotted in Figs. 5.5 and 5.6 the additional damping term in the target dynamics improves the transient response. Figure 5.7 gives an idea about the way the closed-loop system approaches the manifold $\mathcal{M}$.

## 5.7 Summary

In this chapter we presented a control law based on the I&I methodology to stabilize the SMIB system at an equilibrium. The SMIB was described by the swing equation model and the actuator by a first order model. A simple pendulum system with a suitable energy function was chosen as the target dynamics. We chose a manifold such that the closed-loop system restricted to the manifold is the target dynamics. The control law was synthesized in order to render the manifold invariant and attractive. Simulation results were provided to demonstrate the controller performance. Another

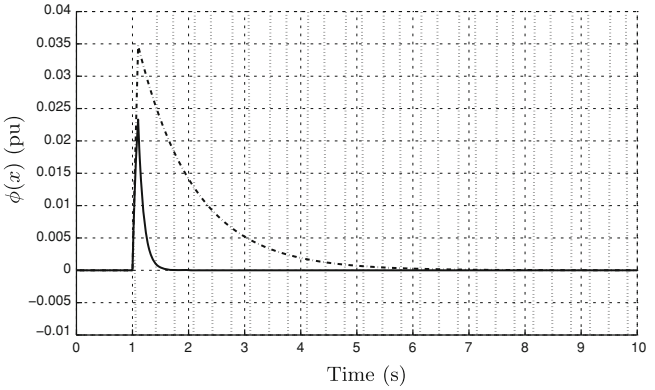


**Fig. 5.7** Plots of $\phi(x)$ for the SMIB system (5.8) with the I&I control law (5.19): *Dotted line* (open loop response), *dash-dot line* (closed-loop response with $\beta = 38,\ \gamma = 1$ and $\gamma_d = \frac{5}{\pi}$), *solid line* (closed-loop response with $\beta = 38,\ \gamma = 10$ and $\gamma_d = \frac{5}{\pi}$)

control law was synthesized to introduce additional damping in the target dynamics and the performance was assessed through the simulations.

## Reference

1. A. Astolfi, R. Ortega, Immersion and invariance: a new tool for stabilization and adaptive control of nonlinear systems. IEEE Trans. Autom. Control **48**(4), 590–606 (2003) April

# Chapter 6
# An Application of Immersion and Invariance to a Class of Differential Algebraic Systems

## 6.1 Introduction

Electrical power systems are naturally described by nonlinear differential-algebraic equations (DAEs). The dynamics of the dynamical components in the system such as the synchronous generators are given by the set of differential equations, while various network constraints such as power balance equations at different nodes are expressed by a set of algebraic equations. In this chapter we extend the I&I methodology to a class of differential algebraic systems, without the need for solving for the nonlinear algebraic equations explicitly. This class of systems is defined by the condition that, the Jacobian of the algebraic constraints with respect to the algebraic variables is full rank in a region of interest. We apply the control synthesis methodology to an SMIB system with a load bus, and then to a system of two machines with two load buses. The SPM model is used for the power systems and the actuator, the CSC, is modeled by a first order system.

The chapter is organized as follows: In Sect. 6.2 we propose an I&I-based stability result for a class of dynamical systems with algebraic constraints. In Sect. 6.3 we state a model of the SMIB system with the CSC and state the control objective. We use the result derived in Sect. 6.2 to synthesize a stabilizing control law for the SMIB system and provide a few simulation results. In Sect. 6.4 we consider a two machine system with a CSC and synthesize a stabilizing control law. Simulation results are given to assess the controller performance. Finally Sect. 6.5 concludes the chapter.

Next we extend the stability result from [1] to a class of nonlinear dynamical systems with algebraic constraints.

N. S. Manjarekar and R. N. Banavar, *Nonlinear Control Synthesis for Electrical Power Systems Using Controllable Series Capacitors*, SpringerBriefs in Applied Sciences and Technology, DOI: 10.1007/978-3-642-27531-9_6, © The Author(s) 2012

## 6.2 Immersion and Invariance for a Differential Algebraic System (IIDAS)

Consider a smooth dynamical system of the form

$$\dot{x} = f(x, y) + g(x, y)u \tag{6.1a}$$

$$h(x, y) = 0 \tag{6.1b}$$

on a smooth manifold $\mathcal{X}$ of dimension $n + q$. Locally, $f : \mathbb{R}^n \times \mathbb{R}^q \to \mathbb{R}^n$, $g : \mathbb{R}^n \times \mathbb{R}^q \to \mathbb{R}^{n\times m}$ and $h : \mathbb{R}^n \times \mathbb{R}^q \to \mathbb{R}^q$ are smooth functions in $U \subset \mathcal{X}$ and input $u \in \mathbb{R}^m$. Further, the function $h$ satisfies

$$\text{Rank} \begin{bmatrix} \text{grad}h_1 \\ \vdots \\ \text{grad}h_q \end{bmatrix} = q \qquad \forall (x, y) \in U.$$

We wish to propose a constructive procedure for asymptotically stabilizing the system to an equilibrium $(x_*, y_*)$ in a region $U \subset \mathcal{X}$. □

The rank condition on the gradient ensures that the system evolves on an *immersed submanifold* $\mathcal{S}$ of dimension $n$. $\mathcal{S}$ is described by the coordinate slice

$$\mathcal{S} = \left\{(x, y) \in \mathbb{R}^n \times \mathbb{R}^q \mid h(x, y) = 0\right\}.$$

**Philosophy of immersion and invariance:** The objective of the control philosophy based on the Immersion and Invariance technique is to asymptotically stabilize the system to $(x_\star, y_\star)$ in a region $U \subset \mathcal{X}$ in the following way.

1. Construct an immersed submanifold $\mathcal{M}$ of $\mathcal{S} \subset \mathcal{X}$ of dimension $p < n$ and containing $(x_\star, y_\star)$. Synthesize a feedback control law $u_i$ to make $\mathcal{M}$ invariant and to make the closed-loop system restricted to $\mathcal{M}$ asymptotically stable at $(x_\star, y_\star)$. This implies all trajectories originating in $\mathcal{M}$ stay in $\mathcal{M}$ for all time (backward and forward) and asymptotically converge to $(x_\star, y_\star)$.
2. Make the manifold $\mathcal{M}$ attractive in $U \bigcap \mathcal{S}$. This implies that trajectories of the closed-loop system (6.1) with a feedback control law $u_{\text{off}}$ (where the subscript $off$ denotes being "off" the manifold $\mathcal{M}$) originating anywhere in $U \bigcap \mathcal{S}$ would be attracted towards $\mathcal{M}$. Further, we make this attraction "asymptotic."

□

*Remark 6.1* Since $\mathcal{M}$ is an immersed submanifold of $\mathcal{X}$ sitting in $\mathcal{S}$ ($\mathcal{M} \subset \mathcal{S} \subset \mathcal{X}$), $\mathcal{M}$ could be described once again as a coordinate slice as

$$\mathcal{M} = \{(x, y) \in U : \phi_1(x, y) = 0, \ldots, \phi_{n-p}(x, y) = 0, h_1(x, y) = 0, \ldots, h_q(x, y) = 0\} \tag{6.2}$$

where $\phi_1, \ldots, \phi_{n-p}$ are smooth functions from $U$ to $\mathbb{R}$, with the assumption

**Assumption 6.2.1**

$$Rank \begin{bmatrix} grad\phi_1 \\ \vdots \\ grad\phi_{n-p} \end{bmatrix} = n - p \qquad \forall (x, y) \in U \subset \mathcal{X}$$

□

An alternate characterization of the manifold $\mathcal{M}$ in terms of $p$ parameters $\xi := (\xi_1, \ldots, \xi_p) \in \mathbb{R}^p$ and a smooth mapping $\Pi := (\Pi_x, \Pi_y) = (\Pi_{x_1}, \ldots, \Pi_{x_n}, \Pi_{y_1}, \ldots, \Pi_{y_q}) : \mathbb{R}^p \to \mathbb{R}^n \times \mathbb{R}^q$ is

$$\begin{aligned} \mathcal{M} := \Big\{ & (\Pi_x(\xi), \Pi_y(\xi)) \mid \xi \in \mathbb{R}^p,\ h(\Pi_x(\xi), \Pi_y(\xi)) = 0, \\ & \text{rank} \left( \frac{\partial \Pi_x}{\partial \xi}(\xi) \right) = p,\ \forall \xi \in \mathbb{R}^p \Big\}. \end{aligned} \tag{6.3}$$

The rank condition on the mapping $\Pi$ ensures that the manifold $\mathcal{M}$ is an *immersed submanifold* of dimension $p$.

For objective 1, we select the dynamics of the system in $\mathcal{M}$ to satisfy the invariance condition as well as asymptotic convergence. Through the parametrization (6.3), given

$$(x, y) = (\Pi_x(\xi), \Pi_y(\xi)) \in \mathcal{M}$$

the dynamics on the manifold $\mathcal{M}$ is described by

$$\dot{x}|_{(x,y)\in\mathcal{M}} = f(x, y) + g(x, y)u_i = f(\Pi_x(\xi), \Pi_y(\xi)) + g(\Pi_x(\xi), \Pi_y(\xi))u_i = \frac{\partial \Pi_x}{\partial \xi}(\xi)\dot{\xi} \tag{6.4}$$

with the equilibrium defined as

$$(x_\star, y_\star) := (\Pi_x(\xi_\star), \Pi_y(\xi_\star)).$$

Objective 1 involves

1. Choosing a vector field $\alpha(\xi)$ that renders the evolution of $\xi$ given by

$$\frac{d\xi}{dt} = \alpha(\xi) \tag{6.5}$$

to be Lyapunov stable and further, satisfies

$$\lim_{t\to\infty} \xi(t) = \xi_\star \ \ \forall \ \ \xi(0) \in \mathbb{R}^p \qquad \text{Asymptotic stability.}$$

2. The selection of the functions $\Pi_x(\xi)$, $\Pi_y(\xi)$ and a feedback control $u_i(\Pi_x(\xi), \Pi_y(\xi))$ to satisfy

$$f(\Pi_x(\xi), \Pi_y(\xi)) + g(\Pi_x(\xi), \Pi_y(\xi))u_i(\Pi_x(\xi), \Pi_y(\xi)) = \frac{\partial \Pi_x(\xi)}{\partial \xi}\alpha(\xi) \quad (6.6)$$

which ensures

$$(x(0), y(0)) \in \mathcal{M} \Rightarrow (x(s), y(s)) \in \mathcal{M} \quad \forall \quad s \in (-\infty, \infty) \quad \text{Invariance,}$$

and at the same time,

$$h(\Pi_x(\xi), \Pi_y(\xi)) = 0. \quad (6.7)$$

For objective 2, *any initial condition* $x_0 \in U \setminus \mathcal{M}$ *must move towards* $\mathcal{M}$. This involves choosing a feedback control $u_{\text{off}}(x, y)$ that renders the dynamics of the $\phi_i$s such that

$$\lim_{t\to\infty} \phi_i(x(t), y(t)) = 0 \quad \forall \quad i = 1, \ldots, n-p \quad (6.8)$$

The dynamics of $\phi := (\phi_1, \ldots, \phi_{n-p})^T$ could be written as

$$\frac{d\phi(x, y)}{dt} = \frac{\partial \phi}{\partial x}\dot{x} + \frac{\partial \phi}{\partial y}\dot{y} = \beta(\phi(x, y))$$

where $\beta(\cdot)$ ensures the previous condition (6.8). However, to synthesize the control law, an explicit expression for $\dot{y}$ would be required.

*Remark 6.2* Please note that so far the assumption is only on the rank condition on the gradient of $h$. In many applications, $y$ could be expressed as an implicit function of $x$ and hence the functions $\phi_i$s could be modified as $\tilde{\phi}_i$s that are functions of $x$ alone. In this case, we have an alternate description for $\mathcal{M}$ in terms of a smooth function $\phi : \mathbb{R}^n \to \mathbb{R}^{n-p}$ as

$$\mathcal{M} := \left\{(x, y) \in \mathbb{R}^n \times \mathbb{R}^q \mid \tilde{\phi}(x) = 0\right\}. \quad (6.9)$$

So we wish to make the dynamics of $\tilde{\phi}(x)$ along the trajectories of (6.1) with input $u_{\text{off}}$ such that

$$\lim_{t\to\infty} \tilde{\phi}(x(t)) = 0. \quad (6.10)$$

Then, we have

$$\frac{\partial \tilde{\phi}}{\partial x}\dot{x} = \beta(\tilde{\phi}(x))$$

□

Substituting for the dynamics of $x$, we have

$$\frac{\partial \tilde{\phi}}{\partial x}(f(x,y)+g(x,y)u_{\text{off}}(x,y)) = \beta(\tilde{\phi}(x))$$

In other words, if there exists a control $u_{\text{off}}(x,y)$ such that the trajectories of the system

$$\dot{\tilde{\phi}}(x) = \frac{\partial \tilde{\phi}}{\partial x}(x)\,[f(x,y)+g(x,y)u_{\text{off}}(x,y)] \tag{6.11}$$

$$\dot{x} = f(x,y)+g(x,y)u_{\text{off}}(x,y) \tag{6.12}$$

$$h(x,y) = 0; \tag{6.13}$$

are bounded and satisfy (6.10) then, the manifold $\mathcal{M}$ is attractive for (6.1) with input $u_{\text{off}}(x,y)$. Further, $(x_\star, y_\star)$ is an asymptotically stable equilibrium of (6.1) with input $u_{\text{off}}(x,y)$.

*Remark 6.3* Please note that on the manifold $\mathcal{M}$, $u_{\text{off}} = u_i$. □

*Remark 6.4* When the conditions of Remark 2 do not apply, we impose a stronger condition that

$$[\frac{\partial h(x,y)}{\partial y}]_{q\times q}$$

is invertible in the region $U$. This would ensure an explicit form of the dynamics of $y$ as

$$\dot{y} = -[\frac{\partial h(x,y)}{\partial y}]^{-1}[\frac{\partial h(x,y)}{\partial x}][f(x,y)+g(x,y)u]$$

□

The above theorem can be interpreted with the help of Fig. 6.1 as: Given the system (6.1) and the target dynamical system (6.5), find if possible, a submanifold $\mathcal{M} \subset \mathcal{S}$ such that

1. restriction of the closed-loop system to $\mathcal{M}$ is the target dynamics
2. $\mathcal{M}$ can be rendered invariant and attractive.

An implicit description of $\mathcal{M}$ is given by (6.2), while (6.3) gives a parametrized description. The control law $u = u_i(\Pi_x(\xi), \Pi_y(\xi))$ renders $\mathcal{M}$ invariant. A measure of the distance of the system trajectories to $\mathcal{M}$ is given by $z = \tilde{\phi}(x)$, called as off-the-manifold coordinate. Our aim is to design a control law $u = u_{\text{off}}(x,y,z)$ that keeps the system trajectories bounded and drives the coordinate $z$ to zero.

An important class of systems to which the above result proves very helpful in control synthesis is electrical power systems with load buses, expressed in the structure preserving model (SPM) form. We now demonstrate the application of the IIDAS to a two power systems.

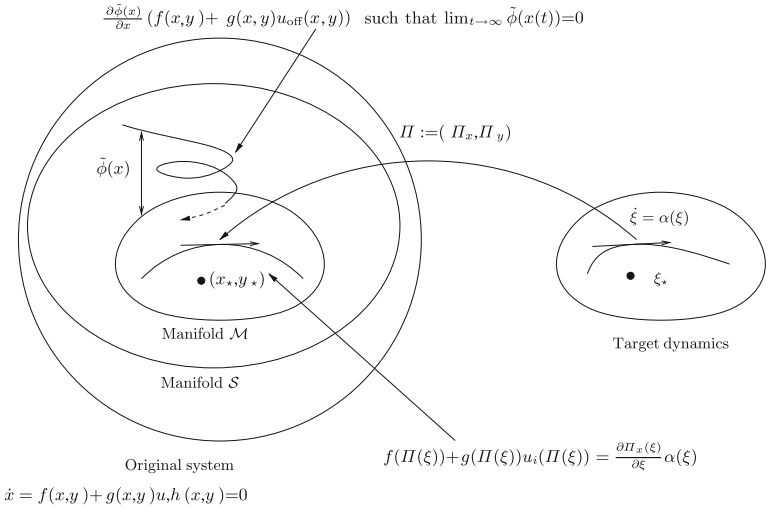


**Fig. 6.1** Immersion and invariance for constrained systems

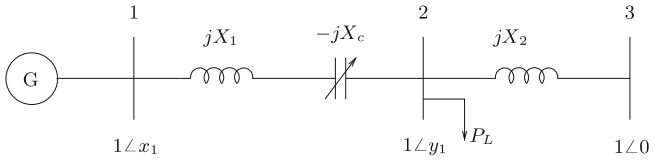


**Fig. 6.2** SMIB system with CSC

## 6.3 The SMIB with a CSC

In [2] the nonlinear swing equation model of the SMIB system has been stabilized using a CSC where the control law is synthesized using the I&I strategy. Here we synthesize a stabilizing control law for the SMIB system with a load modeled by differential algebraic equations. We model the CSC as a first order system to take into account the actuator dynamics.

Consider the SMIB system with a CSC as shown in Fig. 6.2. The generator bus 1 is connected to bus 2 through the reactance $jX_1$. A CSC is connected in between bus 1 and bus 2, and is represented by the variable capacitor $-jX_c$. The terminal bus is connected to the infinite bus through a reactance $jX_2$. The voltages at the infinite bus and the generator terminal bus are $1\angle 0$ and $1\angle y_1$, respectively. We use the following notation: $x_1$ is the rotor angle and $x_2$ is the rotor angular speed deviation with respect to a synchronously rotating reference for the generator. Let $D > 0,\ M > 0,\ P,\ P_L$ be the damping constant, moment of inertia constant, the mechanical power input, and load power at bus 2, respectively. Next we assume that the rotor is round rotor type,

and hence neglect the effect of the saliency of the rotor. Let the effective reactance between bus 1 and 2 be denoted by $x_3$.

### 6.3.1 Modeling

The generator rotor dynamics is modeled by the second order swing equation model and the CSC dynamics is by a first order system. The state vector is denoted by $x = [x_1\ x_2\ x_3]^T \in S^1 \times I\!R^2$ and let $y = y_1 \in S^1$ be the algebraic variable. We use $[x\ y]^T = [x_1\ x_2\ x_3\ y_1]^T$.

The open loop dynamics is then given by

$$\dot{x}_1 = x_2 \tag{6.14a}$$

$$\dot{x}_2 = \frac{1}{M}\left(P - Dx_2 - \frac{\sin(x_1 - y_1)}{x_3}\right) \tag{6.14b}$$

$$\dot{x}_3 = \frac{1}{T_{\text{CSC}}}\left(-x_3 + x_{3_\star} + u\right) \tag{6.14c}$$

and

$$\frac{\sin(x_1 - y_1)}{x_3} - b\sin y_1 - P_L = 0 \tag{6.14d}$$

where $b = \frac{1}{X_2}$, $T_{\text{CSC}}$ is the time constant of the actuator dynamics, $x_{3_\star}$ is the steady state value of $x_3$ at a given operating equilibrium and $u$ is the input to the actuator. Equation (6.14d) is the power balance equation at node 2, and is an algebraic constraint on the system dynamics. Thus, the system given by (6.14) can be considered as a dynamical system moving on a manifold $\mathcal{S} \subset S^1 \times I\!R^2 \times S^1$ defined by the algebraic constraint (6.14d) as

$$\mathcal{S} := \left\{(x, y) \in S^1 \times I\!R^2 \times S^1 \,\middle|\, \frac{\sin(x_1 - y_1)}{x_3} - b\sin y_1 - P_L = 0\right\}. \tag{6.15}$$

We assume,

**Assumption 6.3.1** The region of operation is

$$\mathcal{D} = \Big\{(x, y) \in S^1 \times I\!R^2 \times S^1 \mid -\frac{\pi}{2} + d_1 < x_1 - y_1 < \frac{\pi}{2} - d_1, x_3 \geq d_2,$$
$$-\frac{\pi}{2} + d_1 < y_1 < \frac{\pi}{2} - d_1\Big\},$$

where $d_1 > 0$ and $d_2 > 0$ are small numbers.

Note that the system (6.14) doesn't have singularities in $U := \mathcal{D} \cap \mathcal{S}$ and hence the result of IIDAS can be used for control synthesis locally on this region. Further, this is

a conservative estimate of such a neighbourhood of $(x_\star, y_\star)$ and actual neighbourhood can be larger than $U$.

For the nonlinear system given by (6.14) we can determine the open loop equilibria as follows: $\dot{x}_1 = 0 \Rightarrow x_2 = 0$, while $\dot{x}_3 = 0$ with $u \equiv 0$ together implies $x_3 = x_{3_\star}$. By substituting $x_2 = 0$ and $x_3 = x_{3_\star}$ and equating $\dot{x}_2$ to zero, we get from (6.14b), $\frac{\sin(\bar{x}_1 - \bar{y}_1)}{x_{3_\star}} = P$, where $\bar{x}_1$ and $\bar{y}_1$ denote the values of $x_1$ and $y_1$ at an equilibrium. Substituting $\frac{\sin(\bar{x}_1 - \bar{y}_1)}{x_{3_\star}} = P$ in (6.14d), we get $\bar{y}_1 = \arcsin\left(\frac{P - P_L}{b}\right)$. Substituting $\bar{y}_1$ in $\frac{\sin(\bar{x}_1 - \bar{y}_1)}{x_{3_\star}} = P$ we get $\bar{x}_1 = \arcsin(P x_{3_\star}) + \arcsin\left(\frac{P - P_L}{b}\right)$. Next, we denote $y_{1_\star} = \bar{y}_1|_{(-\frac{\pi}{2}, \frac{\pi}{2})}$ and $x_{1_\star} = \bar{x}_1|_{(y_{1_\star}, y_{1_\star} + \frac{\pi}{2})}$. We denote the open loop operating equilibrium by $(x_\star, y_\star) = (x_{1_\star}, 0, x_{3_\star}, y_{1_\star})$.

### 6.3.2 Control objective

As mentioned earlier, $(x_\star, y_\star)$ denotes the operating stable equilibrium in $\mathcal{D}$. We assume that $(x_\star, y_\star)$ is known to us and state the control objective as "to synthesize a control law $u$ in order to make the system given by (6.14) asymptotically stable at $(x_\star, y_\star)$ and to improve the stability properties of the system using an appropriate energy function."

### 6.3.3 Controller Synthesis Using IIDAS

In this section we synthesize a stabilizing controller for (6.14). The open loop system consists of two subsystems- one is the second order swing equation (a slow system), and the other is the CSC which is a fast dynamics as compared to the swing dynamics.

We use the stability result derived in Sect. 6.2 to synthesize a controller. As discussed in [1] we make a natural choice for the target system as the mechanical subsystem. We choose the lower order target dynamics as follows: Let $\xi = [\xi_1\ \xi_2]^T \in S^1 \times I\!R$ be the state vector of the target dynamics. Then the target dynamics is chosen as

$$\dot{\xi}_1 = \xi_2 \tag{6.16a}$$

$$\dot{\xi}_2 = -R(\xi)\xi_2 - V'(\xi_1) \tag{6.16b}$$

where $V(\xi_1)$ denotes the potential energy of the target dynamics and is to be chosen, and $R(\xi_1, \xi_2)$ is a (possibly nonlinear) damping function which is to be chosen. The target system (6.16) is a simple pendulum system with a stable equilibrium $\xi_\star = (\xi_{1_\star}, 0)$ with the energy function

$$H(\xi) = \frac{1}{2}\xi_2^2 + V(\xi_1). \tag{6.17}$$

To ensure the stability at the equilibrium $\xi_\star$ we assume the following

**Assumption 6.3.2**

1. The potential energy function $V(\xi_1)$ satisfies

$$\begin{cases} V'(\xi_1)\big|_{\xi_1=\xi_{1_\star}} = 0 \\ V''(\xi_1)\big|_{\xi_1=\xi_{1_\star}} > 0. \end{cases}$$

2. The damping function satisfies $R(\xi_\star) \geq 0$.

Consider the mapping $\Pi : S^1 \times I\!R \longrightarrow \mathcal{S}$ defined as

$$\Pi(\xi_1, \xi_2) := (\xi_1, \xi_2, \Pi_3(\xi), \Pi_4(\xi)) \tag{6.18}$$

where $\Pi_3(\xi)$ and $\Pi_4(\xi)$ are to be chosen such that (6.7) is satisfied, that is,

$$\frac{\sin(\xi_1 - \Pi_4(\xi))}{\Pi_3(\xi)} - b \sin \Pi_4(\xi) - P_L = 0. \tag{6.19}$$

Further, consider the submanifold $\mathcal{M} \subset \mathcal{S}$ defined as

$$\mathcal{M} := \left\{ (x, y) \in \mathcal{S} \mid \exists \xi \in S^1 \times I\!R \text{ such that} (x, y) = \Pi(\xi) \right\}. \tag{6.20}$$

We have to choose the mapping $\Pi$ and the target dynamics (6.16) such that the immersion condition (6.6) is satisfied on $\mathcal{M}$, that is,

$$\begin{aligned} &\begin{bmatrix} \xi_2 \\ \frac{1}{M}\left(P - D\xi_2 - \frac{\sin(\xi_1 - \Pi_4(\xi))}{\Pi_3(\xi)}\right) \\ \frac{1}{T_{\text{CSC}}}\left(-\Pi_3(\xi) + x_{3_\star}\right) \end{bmatrix} + \begin{bmatrix} 0 \\ 0 \\ \frac{1}{T_{\text{CSC}}} \end{bmatrix} c(\Pi(\xi)) \\ &= \begin{bmatrix} 1 & 0 \\ 0 & 1 \\ \frac{\partial \Pi_3}{\partial \xi_1} & \frac{\partial \Pi_3}{\partial \xi_2} \end{bmatrix} \begin{bmatrix} \xi_2 \\ -R(\xi)\xi_2 - V'(\xi_1) \end{bmatrix} \end{aligned} \tag{6.21}$$

with the constraint (6.19).

Each row of (6.21) gives a condition on the choice of the mapping $\Pi(\xi)$ and the target dynamics. The first row is satisfied for the mapping (6.18) and the target dynamics (6.16). We choose $R(\xi) = \frac{D}{M}$, $V(\xi_1) = -\beta \cos \tilde{\xi}_1$ for some $\beta > 0$ (to be chosen) and $\tilde{\xi}_1 = \xi_1 - \xi_{1_\star}$. Then, the second row implies

$$\frac{\sin(\xi_1 - \Pi_4(\xi))}{\Pi_3(\xi)} = P + \beta M \sin \tilde{\xi}_1. \tag{6.22}$$

Then from (6.19) and (6.22) together we get

$$\Pi_4(\xi_1) = \arcsin\left(\frac{P - P_L + \beta M \sin \tilde{\xi}_1}{b}\right). \tag{6.23}$$

Notice that $\Pi_4$ is a function of $\xi_1$ only. We make the following assumption:

**Assumption 6.3.3** $\beta < \frac{b-|(P-P_L)|}{M}$
to ensure existence of $\Pi_4(\xi_1)$, where $|\cdot|$ denotes the absolute value.

Next we get $\Pi_3$ from (6.22) and (6.23) as

$$\Pi_3(\xi_1) = \frac{\sin\left(\xi_1 - \arcsin\left(\frac{P-P_L+\beta M \sin\tilde{\xi}_1}{b}\right)\right)}{P + \beta M \sin\tilde{\xi}_1}. \tag{6.24}$$

Notice that $\Pi_3$ is a function of $\xi_1$ only. Here we make the following assumption:

**Assumption 6.3.4** $\beta < \frac{P}{M}$
to ensure boundedness of $\Pi_3(\xi_1)$ for all $\xi_1 \in S^1$. Finally, from (6.24) and the third row of (6.21) we get,

$$\begin{aligned} c(\Pi(\xi)) =& -x_{3_\star} + \Pi_3(\xi_1) + T_{\text{CSC}}\frac{\partial \Pi_3(\xi_1)}{\partial \xi_1}\xi_2, \\ =& -x_{3_\star} + \frac{\sin(\xi_1 - \Pi_4(\xi_1))}{P + \beta M \sin\tilde{\xi}_1} \\ &+ \frac{T_{\text{CSC}}\xi_2 \cos(\xi_1 - \Pi_4(\xi_1))}{P + \beta M \sin\tilde{\xi}_1}\left(1 - \frac{\beta M \cos\tilde{\xi}_1}{\sqrt{1 - \left(\frac{P-P_L+\beta M \sin\tilde{\xi}_1}{b}\right)^2}}\right) \\ &- \frac{T_{\text{CSC}}\xi_2 \beta M \sin(\xi_1 - \Pi_4(\xi_1))\cos\tilde{\xi}_1}{\left(P + \beta M \sin\tilde{\xi}_1\right)^2}. \end{aligned} \tag{6.25}$$

This input $u = c(\Pi(\xi))$ given by (6.25) makes the manifold $\mathcal{M}$ invariant.

Next, we design a control law $u = \psi(\cdot)$ which ensures that the trajectories of the closed-loop system are bounded and converge to the manifold $\mathcal{M}$. It can be verified that an implicit description for the manifold $\mathcal{M}$ in (6.20) can be given by

$$\mathcal{M} = \{(x, y) \in \mathcal{S} \mid \phi(x) = 0\} \tag{6.26}$$

where

$$\begin{aligned} \phi(x) &= x_3 - \Pi_3(x_1) \\ &= x_3 - \frac{\sin\left(x_1 - \hat{y}_1\right)}{P + \beta M \sin\tilde{x}_1} \end{aligned} \tag{6.27}$$

with (6.14d) to be satisfied, where $\tilde{x}_1 := x_1 - x_{1_\star}$ and $\hat{y}_1 := \arcsin\left(\frac{P-P_L+\beta M \sin\tilde{x}_1}{b}\right)$.

Let $z = \phi(x)$ denote the off-the-manifold coordinate. Then, we have

$$\begin{aligned}\dot{z} =& \dot{x}_3 - \dot{\Pi}_3(x_1) \\ =& \frac{1}{T_{\text{CSC}}}\left(-x_3 + x_{3_\star} + \psi\left(x, y, z\right)\right) - \frac{\partial \Pi_3(x_1)}{\partial x_1} x_2\end{aligned} \tag{6.28}$$

where we substitute for $\dot{x}_1$ and $\dot{x}_3$ from (6.14).

To ensure the boundedness of the trajectories of the off-the-manifold coordinate $z$ and also that $\lim_{t\to\infty} z(t) = 0$ we take

$$\dot{z} = -\gamma z, \quad \gamma > 0. \tag{6.29}$$

Then, from (6.28) and (6.29) we can write

$$\psi(x, y, z) = x_3 - x_{3_\star} + T_{\text{CSC}}\left(-\gamma\left(x_3 - \Pi_3(x_1)\right) + \frac{\partial \Pi_3(x_1)}{\partial x_1} x_2\right) \tag{6.30}$$

Next, we compute the control law using the IIDAS methodology as,

$$\begin{aligned}u(x) &= \psi(x, y, \phi(x)) \\ &= x_3 - x_{3_\star} - \gamma T_{\text{CSC}}\left(x_3 - \frac{\sin\left(x_1 - \hat{y}_1\right)}{P + \beta M \sin\tilde{x}_1}\right) + \\ &\quad \frac{T_{\text{CSC}} x_2 \cos(x_1 - \hat{y}_1)}{P + \beta M \sin\tilde{x}_1}\left(1 - \frac{\beta M \cos\tilde{x}_1}{\sqrt{1 - \left(\frac{P - P_L + \beta M \sin\tilde{x}_1}{b}\right)^2}}\right) \\ &\quad - \frac{T_{\text{CSC}} x_2 \beta M \sin(x_1 - \hat{y}_1)\cos\tilde{x}_1}{(P + \beta M \sin\tilde{x}_1)^2}.\end{aligned} \tag{6.31}$$

Finally, we establish boundedness of the trajectories of the closed-loop system (6.14) with the control law (6.31) and the off-the-manifold coordinate $z$

$$\dot{x}_1 = x_2 \tag{6.32a}$$

$$\dot{x}_2 = \frac{1}{M}\left(P - D x_2 - \frac{\sin(x_1 - y_1)}{x_3}\right) \tag{6.32b}$$

$$\dot{x}_3 = \frac{1}{T_{\text{CSC}}}\left(-x_3 + x_{3_\star} + u\right) \tag{6.32c}$$

$$0 = \frac{\sin(x_1 - y_1)}{x_3} - b \sin y_1 - P_L \tag{6.32d}$$

$$\dot{z} = -\gamma z. \tag{6.32e}$$

Here $x_1 \in S^1$ and $y_1 \in S^1$, and hence we have $x_1, y_1 \in \mathcal{L}_\infty$.

We can rewrite (6.32b) as

$$\dot{x}_2 = -\frac{D}{M}x_2 + \Delta(x_1, x_3, y_1) \tag{6.33}$$

where $\Delta(x_1, x_3, y_1) = \frac{1}{M}\left(P - \frac{\sin(x_1 - y_1)}{x_3}\right)$. From Assumption 6.3.1 we have $x_3 \geq d_2 > 0$ and this implies $\Delta(x_1, x_3, y_1) \in \mathcal{L}_\infty$. As we have $D > 0$ and $M > 0$, (6.33) is an asymptotically stable linear system in $x_2$ with a bounded driving function $\Delta(x_1, x_3, y_1)$. This implies $x_2 \in \mathcal{L}_\infty$.

Next, we have $x_3 = z + \Pi_3(x_1)$. We have, from (6.29), that $z$ is bounded and $\lim_{t\to\infty} z(t) = 0$. Also, from Assumption 6.3.4 we have that $\Pi_3(x_1)$ is bounded for all $x_1 \in S^1$, and hence we can conclude boundedness of $x_3$.

Thus, we have shown that the trajectories of (6.32) are bounded and $\lim_{t\to\infty} z(t) = 0$. The above discussion on the control synthesis can be summarized in the following proposition.

**Proposition 6.3.1** *The closed-loop system* (6.14) *with the control law* (6.31) *is locally asymptotically stable at* $(x_\star, y_\star)$.

*Proof* Based on the arguments given above. □

### *6.3.4 Simulation Results*

We take the following simulation parameters: $M = \frac{8}{100\pi}$, $D = \frac{0.4}{100\pi}$, $P = 1.1$ pu, $P_L = 0.8$ pu, $b = 2.5$ pu, $T_{\text{CSC}} = 0.02$ s, $0.2 \leq x_3 \leq 0.6$ and the operating equilibrium is $(x_\star, y_\star) = (0.5759, 0, 0.4, 0.12)$. The tuning parameters are $\beta$ and $\gamma$. From Assumption 6.3.3 and Assumption 6.3.4 an upper bound on the tuning parameter $\beta$ is $\min\{27.48, 43.19\} = 27.48$.

To assess the performance of the proposed control law we assume that a short circuit fault occurs at the far end of the transmission line at time $t = 1$ s for a duration of 0.1 s.

In Fig. 6.3 the open loop response of the system to the transient is shown by dotted lines. The closed-loop response is shown for two different sets of the tuning parameters. The dash-dot lines show the closed-loop response for the case $\beta = 10$ and $\gamma = 10$. The response shows a slight overshoot at start and then oscillations decay in about 7 s In the other case, the oscillations are damped more effectively, in about 3 s. Figure 6.4 shows the phase plots of the response.

## 6.4 Two Machine Stabilization Using a CSC

In this section we consider a two machine system with a CSC described by a set of differential algebraic equations and synthesize a stabilizing control law based on the IIDAS strategy. The two machine system with a CSC is shown in Fig. 6.5. For generators $G_1$ and $G_2$, bus 1 and 3 are the internal buses and, bus 2 and 4 are the

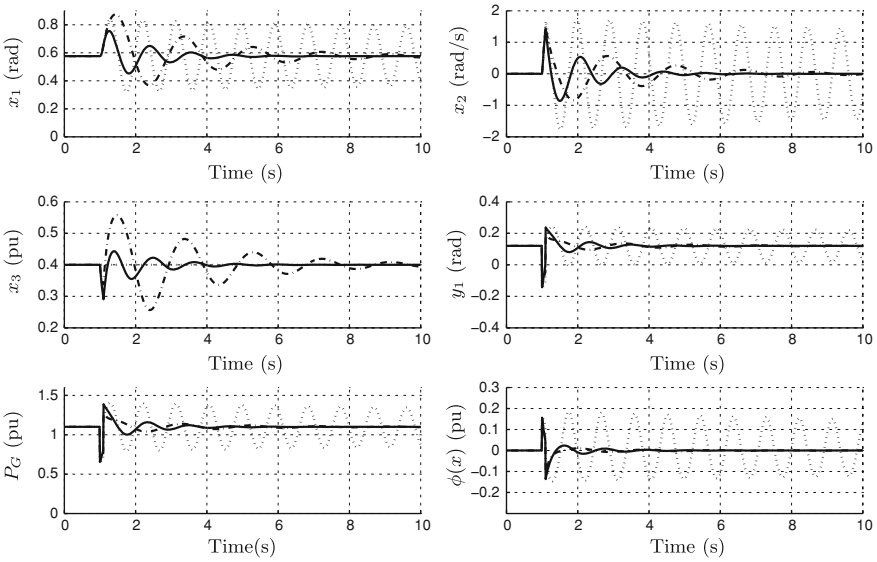


**Fig. 6.3** Response of the SMIB system (6.14) with the I&I control law (6.31): *dotted line* (open loop response), *dash-dot line* (closed-loop response with $\beta = 10$ and $\gamma = 10$), *solid line* (closed-loop response with $\beta = 25$ and $\gamma = 10$)

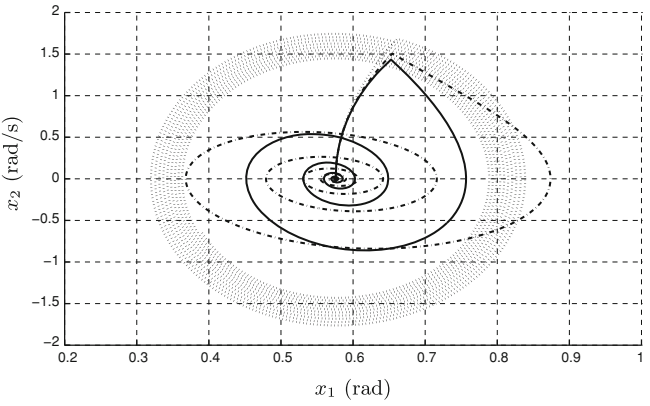


**Fig. 6.4** Phase plots of the SMIB system (6.14) with the I&I control law (6.31): *dotted line* (open loop response), *dash-dot line* (closed-loop response with $\beta = 10$ and $\gamma = 10$), *solid line* (closed-loop response with $\beta = 25$ and $\gamma = 10$)

terminal buses, respectively. For $i = 1, 2$, let $\delta_i$, $\theta_i$ and $\omega_i$ be the rotor angle, the terminal bus voltage angle and rotor angular speed deviation, respectively, for the $i$th generator with respect to a synchronously rotating reference. Let $D_i > 0$, $M_i > 0$, $P_i$ and $P_{Li}$ be the damping constant, moment of inertia constant, the mechanical power input, and the load power of the $i$th generator, respectively. Let $X_i$ be the transient reactance between the internal bus and the terminal bus of the $i$th generator,

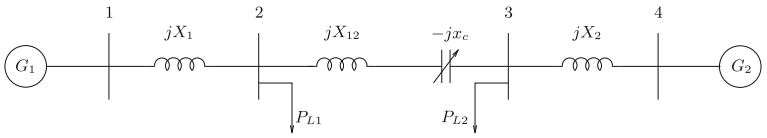


**Fig. 6.5** Two machine system with a CSC

and $X_{12}$ be the reactance of the transmission line connecting the two terminal buses. A CSC, denoted by a capacitive reactance of $x_c$, is connected in series with $X_{12}$, and the effective reactance between the terminal buses is denoted by $x_l$. We assume that the voltages at all the buses are constant and equal to 1 pu. Next, we assume that the rotor is round rotor type, and hence neglect the effect of the saliency of the rotor.

We choose the state variables for the system as $x_1 = \delta_1,\ x_2 = \delta_2,\ x_3 = \omega_1,\ x_4 = \omega_2$, and $x_5 = x_l$. Further, $y_1 = \theta_1$ and $y_2 = \theta_2$ denote the algebraic variables of the system. We denote the state vector of the system by $x = (x_1, x_2, x_3, x_4, x_5) \in S^1 \times S^1 \times I\!R^3$ and the vector of algebraic variables by $y = (y_1, y_2) \in S^1 \times S^1$. Then, the dynamics of the two machine system can be described by the following set of DAEs:

$$\dot{x}_1 = x_3 \tag{6.34a}$$

$$\dot{x}_2 = x_4 \tag{6.34b}$$

$$\dot{x}_3 = \frac{1}{M_1}\left(P_1 - D_1 x_3 - b_1 \sin(x_1 - y_1)\right) \tag{6.34c}$$

$$\dot{x}_4 = \frac{1}{M_2}\left(P_2 - D_2 x_4 - b_2 \sin(x_2 - y_2)\right) \tag{6.34d}$$

$$\dot{x}_5 = \frac{1}{T_{\text{CSC}}}\left(-x_5 + x_{5\star} + u\right) \tag{6.34e}$$

$$b_1 \sin(x_1 - y_1) - \frac{b_{12}\sin(y_1 - y_2)}{x_5} - P_{L1} = 0 \tag{6.35a}$$

$$b_2 \sin(x_2 - y_2) + \frac{b_{12}\sin(y_1 - y_2)}{x_5} - P_{L2} = 0 \tag{6.35b}$$

where $b_1 = \frac{1}{X_1}$, $b_2 = \frac{1}{X_2}$, $b_{12} = 1$, and $x_{5\star}$ is the effective open loop line reactance between bus 3 and 4, at the operating equilibrium.

Equations (6.35) represent the power balance at bus 2 and 3, and are the algebraic constraints of the form (6.1b) on the system dynamics. Thus, the system given by (6.34) is a dynamical system of the form (6.1a) and it evolves on a manifold $\mathcal{S} \subset S^1 \times S^1 \times I\!R^3 \times S^1 \times S^1$ where $\mathcal{S}$ is defined by the algebraic constraints (6.35) as

$$\mathcal{S} := \left\{(x, y) \in S^1 \times S^1 \times I\!R^3 \times S^1 \times S^1 \,|h(x, y) = 0\right\}. \tag{6.36}$$

### 6.4.1 Control Objective

From practical considerations we assume,

**Assumption 6.4.1** The region of operation is

$$\mathcal{D} = \Big\{(x, y) \in S^1 \times S^1 \times I\!R^3 \times S^1 \times S^1 \mid 0 < x_1 - y_1 < \frac{\pi}{2} - d_1, 0 < x_2 - y_2 < \frac{\pi}{2} - d_1, |y_1 - y_2| < \frac{\pi}{2} - d_1, \underline{d_l} < x_5 < \overline{d_l}\Big\},$$

where $d_1 > 0$, $\underline{d_l} > 0$ and $\overline{d_l} > 0$ are small numbers.

*Remark* **6.5** It is to be noted here that, rank $(\text{grad}(h(x, y))) = 2$ in $\mathcal{D}$, and hence $\mathcal{D} \bigcap \mathcal{S}$ is a 5-dimensional immersed submanifold. The bounds $0 < x_i - y_i < \frac{\pi}{2} - d_1$ ensure that the $i$-th machine is operating in generator mode for $i = 1, 2$. The bound $\underline{d_l} < x_5$ implies that the capacitive compensation provided by the CSC is always less than the inductive reactance of the transmission line. That is, the net reactance between the buses 2 and 3 is always inductive. On the other hand, the bound $x_5 < \overline{d_l}$ decides the limit on inductive compensation of the line. Further, we note that in the region $\mathcal{D} \bigcap \mathcal{S}$ we have rank $(\frac{\partial(h(x,y))}{\partial y}) = 2$. This ensures that $y$ is an implicit function of $x$, and the condition in Remark 6.4 is satisfied.

In general, it is difficult to determine the open loop equilibria of a nonlinear system of the form (6.1a), (6.1b). To obtain the open loop equilibria of the system (6.34), (6.35) we equate $\dot{x} = 0$ on the manifold $\mathcal{S}$. An open loop equilibrium of the system is of the form $(\bar{x}, \bar{y}) = (\bar{x}_1, \bar{x}_2, 0, 0, x_{5\star}, \bar{y}_1, \bar{y}_2)$, where $\bar{x}_1, \bar{x}_2, \bar{y}_1$, and $\bar{y}_2$ are the solutions to the simultaneous equations

$$\begin{aligned} P_1 - b_1 \sin(\bar{x}_1 - \bar{y}_1) &= 0 \\ P_2 - b_2 \sin(\bar{x}_2 - \bar{y}_2) &= 0 \\ b_1 \sin(\bar{x}_1 - \bar{y}_1) - \frac{b_{12} \sin(\bar{y}_1 - \bar{y}_2)}{x_{5\star}} - P_{L1} &= 0 \\ b_2 \sin(\bar{x}_2 - \bar{y}_2) + \frac{b_{12} \sin(\bar{y}_1 - \bar{y}_2)}{x_{5\star}} - P_{L2} &= 0. \end{aligned}$$

As mentioned earlier, we denote the operating stable equilibrium in $\mathcal{D} \bigcap \mathcal{S}$ by $(x_\star, y_\star)$. We assume that $(x_\star, y_\star)$ is known to us and state the control objective as,

1. To synthesize a control law $u(x, y)$ in order to make the system given by (6.34)–(6.35) asymptotically stable at $(x_\star, y_\star)$.
2. Synchronous generators generally exhibit poor mechanical damping which results in sustained oscillations. The second control objective is to damp the oscillations effectively, thus improving the transient response.
3. In this direction, the control objective is to choose a suitable lower order target dynamics (6.5) with a desired energy function on a lower dimensional submanifold

$\mathcal{M} \subset \mathcal{S}$ which is defined using a mapping $\Pi$ as in (6.3), map the trajectories of the target dynamics to the (original) higher order manifold using the mapping $\Pi$, and synthesize a control law to asymptotically match the closed-loop system with the mapped target dynamics.

### 6.4.2 Controller Synthesis Using IIDAS

In this section we synthesize an IIDAS based control law to asymptotically stabilize the closed-loop system at the given equilibrium. The first step in the control synthesis is to choose an appropriate target dynamics. The open loop dynamics can be divided into two subsystems- one describing the two machine system, and the other describing the CSC dynamics. We choose the target dynamics depending on the first subsystem as follows: Let $\xi = [\xi_1\ \xi_2\ \xi_3\ \xi_4]^T \in S^1 \times S^1 \times I\!R \times I\!R$ be the state vector and $\eta \in S^1$ be an algebraic variable of the target dynamics. We choose the target dynamics as

$$\dot{\xi}_1 = \xi_3 \tag{6.37a}$$

$$\dot{\xi}_2 = \xi_4 \tag{6.37b}$$

$$\dot{\xi}_3 = -\frac{D_1}{M_1}\xi_3 - \beta_1 \sin(\tilde{\xi}_1 - \eta) \tag{6.37c}$$

$$\dot{\xi}_4 = -\frac{D_2}{M_2}\xi_4 - \beta_2 \sin(\tilde{\xi}_2 - \eta) \tag{6.37d}$$

$$0 = \beta_1 M_1 \sin(\tilde{\xi}_1 - \eta) + \beta_2 M_2 \sin(\tilde{\xi}_2 - \eta) \tag{6.37e}$$

where $\beta_i$ is a positive constant, $\tilde{\xi}_i :\ = \xi_i - \xi_{i\star}$ and $\xi_{i\star}$ is the operating equilibrium of the $i$th generator. We assume that the region of operation for the target dynamics is,

$$\mathcal{D}_T :\ = \left\{(\xi, \eta) \in S^1 \times S^1 \times I\!R \times I\!R \times S^1 \mid \tilde{\xi}_i - \eta \in \left(-\frac{\pi}{2}, \frac{\pi}{2}\right), i = 1, 2\right\}. \tag{6.38}$$

Here, note that (6.37e) defines a smooth constraint manifold $\mathcal{S}_T \subset \mathcal{D}_T$ for the target dynamics (6.37). For (6.37) the set of equilibria is given by

$$E_T :\ = \left\{(a + \xi_{1\star}, a + \xi_{2\star}, 0, 0, a) \in S^1 \times S^1 \times I\!R \times I\!R \times S^1 \mid a \in S^1\right\}. \tag{6.39}$$

Further, in $\mathcal{S}_T$ the algebraic variable $\eta$ can be expressed as a function of $\xi_1$ and $\xi_2$ by expanding (6.37e) and rearranging the terms as

$$\eta(\xi_1, \xi_2) = \tan^{-1}\left(\frac{\beta_1 M_1 \sin\tilde{\xi}_1 + \beta_2 M_2 \sin\tilde{\xi}_2}{\beta_1 M_1 \cos\tilde{\xi}_1 + \beta_2 M_2 \cos\tilde{\xi}_2}\right). \tag{6.40}$$

In a similar way, by differentiating (6.37e) along the trajectories of the target system and rearranging the terms we have,

$$\dot{\eta}(\xi) = \frac{\beta_1 M_1 \cos(\tilde{\xi}_1 - \eta)\xi_3 + \beta_2 M_2 \cos(\tilde{\xi}_2 - \eta)\xi_4}{\beta_1 M_1 \cos(\tilde{\xi}_1 - \eta) + \beta_2 M_2 \cos(\tilde{\xi}_2 - \eta)} \tag{6.41}$$

where, $\eta(\xi_1, \xi_2)$ is given by (6.40).

By differentiating (6.37e) with respect to $\eta$ we have

$$\beta_1 M_1 \cos(\tilde{\xi}_1 - \eta) + \beta_2 M_2 \cos(\tilde{\xi}_2 - \eta) = 0. \tag{6.42}$$

Next, we differentiate (6.37e) with respect to time along the trajectories of the target dynamics,

$$\beta_1 M_1 \cos(\tilde{\xi}_1 - \eta)\left(\dot{\xi}_1 - \dot{\eta}\right) + \beta_2 M_2 \cos(\tilde{\xi}_2 - \eta)\left(\dot{\xi}_2 - \dot{\eta}\right) = 0$$

or

$$\begin{aligned}&\beta_1 M_1 \cos(\tilde{\xi}_1 - \eta)\dot{\xi}_1 + \beta_2 M_2 \cos(\tilde{\xi}_2 - \eta)\dot{\xi}_2 \\ &- \left(\beta_1 M_1 \cos(\tilde{\xi}_1 - \eta) + \beta_2 M_2 \cos(\tilde{\xi}_2 - \eta)\right)\dot{\eta} = 0.\end{aligned}$$

We can rewrite the above equation using (6.42) as,

$$\beta_1 M_1 \cos(\tilde{\xi}_1 - \eta)\dot{\xi}_1 + \beta_2 M_2 \cos(\tilde{\xi}_2 - \eta)\dot{\xi}_2 = 0,$$

that is,

$$\frac{d\xi_1}{d\xi_2} = -\frac{\beta_2 M_2 \cos(\tilde{\xi}_2 - \eta)}{\beta_1 M_1 \cos(\tilde{\xi}_1 - \eta)\dot{x}_1}. \tag{6.43}$$

In the three dimensional space $\mathbb{R}^3$, $E_T$ can be visualized as a straight line joining the point $(1 + \xi_{1\star}, 1 + \xi_{2\star}, 1)$ with the point $(\xi_{1\star}, \xi_{2\star}, 0)$. Then, the projection of $E_T$ (constrained in $\mathcal{D}_T$) in $\xi_1 - \xi_2$ plane is a line with strictly positive slope. On the other hand, from (6.43) we can say that the tangents to the projection of the trajectories (constrained in $\mathcal{D}_T$) in $\xi_1 - \xi_2$ plane have strictly negative slopes. Thus, we can conclude that, for a given initial condition $(\xi_0, \eta_0) \in \mathcal{D}_T$ the trajectory of (6.37), (if at all), intersects $\mathcal{L}$ at a unique point in $\mathcal{D}_T$ which is the equilibrium for that initial condition.

Let the operating equilibrium of (6.37) be denoted by $(\xi_\star, \eta_\star)$. We next show that the target dynamics (6.37) is asymptotically stable at $(\xi_\star, \eta_\star)$ using the energy function

$$H(\xi, \eta) = -\beta_1 \cos(\tilde{\xi}_1 - \eta) - \beta_2 \cos(\tilde{\xi}_2 - \eta) + \frac{1}{2}(\xi_3^2 + \xi_4^2). \tag{6.44}$$

Clearly, the energy function is minimum on $E_T$. The time rate of change of the energy function along the trajectories of the target system is given by

$$\dot{H}(\xi,\eta) = \frac{\partial H(\xi,\eta)}{\partial \xi}\dot{\xi} + \frac{\partial H(\xi,\eta)}{\partial \eta}\dot{\eta}.$$

Note that, from (6.37e) we have $\frac{\partial H(\xi,\eta)}{\partial \eta} = 0$. Then,

$$\begin{aligned}\dot{H}(\xi,\eta) =& \beta_1 \sin(\tilde{\xi}_1 - \eta)\xi_3 + \beta_2 \sin(\tilde{\xi}_2 - \eta)\xi 4 - \frac{D_1}{M_1}\xi_3^2 - \beta_1 \sin(\tilde{\xi}_1 - \eta)\xi_3 \\ & - \frac{D_2}{M_2}\xi_4^2 - \beta_2 \sin(\tilde{\xi}_2 - \eta)\xi 4 \\ =& -\frac{D_1}{M_1}\xi_3^2 - \frac{D_2}{M_2}\xi_4^2.\end{aligned}$$

As $\dot{H}(\xi,\eta)$ is negative semidefinite, we can infer that the target dynamics is stable in the sense of Lyapunov. Using LaSalle's invariance principle we can show that $(\xi_\star, \eta_\star)$ is asymptotically stable. Consider the situation where $\xi_3 \equiv 0$ and $\xi_4 \equiv 0$. In that case, from (6.37) we have $\dot{\xi}_1 = \dot{\xi}_2 = \dot{\xi}_3 = \dot{\xi}_4 \equiv 0$ and hence $\tilde{\xi}_1 \equiv \eta \equiv \tilde{\xi}_2$. Thus, by LaSalle's invariance principle we conclude that the trajectories of the target dynamics asymptotically approach $E_T$. In other words, if the target dynamics is perturbed from the the given initial condition of $(\xi_\star, \eta_\star)$, then $(\xi_\star, \eta_\star)$ itself is the only point which can be assumed by the system.

Consider the mapping $\Pi : \mathcal{S}_T \longrightarrow \mathcal{S}$ defined as

$$\Pi(\xi_1, \xi_2, \xi_3, \xi_4, \eta) \colon = (\xi_1, \xi_2, \xi_3, \xi_4, \Pi_5(\xi,\eta), \Pi_6(\xi,\eta), \Pi_7(\xi,\eta)). \tag{6.45}$$

where $\Pi_5(\xi,\eta)$, $\Pi_6(\xi,\eta)$ and $\Pi_7(\xi,\eta)$ are to be chosen such that,

$$b_1 \sin(\xi_1 - \Pi_6(\xi,\eta)) - \frac{b_{12}\sin(\Pi_6(\xi,\eta) - \Pi_7(\xi,\eta))}{\Pi_5(\xi,\eta)} - P_{L1} = 0 \tag{6.46a}$$

$$b_2 \sin(\xi_2 - \Pi_7(\xi,\eta)) + \frac{b_{12}\sin(\Pi_6(\xi,\eta) - \Pi_7(\xi,\eta))}{\Pi_5(\xi,\eta)} - P_{L2} = 0. \tag{6.46b}$$

Further, consider the manifold $\mathcal{M} \subset \mathcal{S}$ defined as

$$\mathcal{M} \colon = \{(x,y) \in \mathcal{S} \mid \exists (\xi,\eta) \in \mathcal{S}_T \text{such that} (x,y) = \Pi(\xi,\eta)\}. \tag{6.47}$$

We have to choose the mapping $\Pi(\xi,\eta)$ for the target dynamics (6.37) such that the immersion condition (6.6) is satisfied on $\mathcal{M}$, that is,

$$\begin{bmatrix} \xi_3 \\ \xi_4 \\ \frac{1}{M_1}\left[P_1 - D_1\xi_3 - b_1\sin(\xi_1 - \Pi_6(\xi,\eta))\right] \\ \frac{1}{M_2}\left[P_2 - D_2\xi_4 - b_2\sin(\xi_2 - \Pi_7(\xi,\eta))\right] \\ \frac{1}{T_{CSC}}\left[-\Pi_5(\xi,\eta) + x_{5_\star}\right] \end{bmatrix} + \begin{bmatrix} 0 \\ 0 \\ 0 \\ 0 \\ \frac{1}{T_{CSC}} \end{bmatrix} u_i(\Pi(\xi,\eta))$$

$$= \begin{bmatrix} 1 & 0 & 0 & 0 & 0 \\ 0 & 1 & 0 & 0 & 0 \\ 0 & 0 & 1 & 0 & 0 \\ 0 & 0 & 0 & 1 & 0 \\ \frac{\partial\Pi_5(\xi,\eta)}{\partial\xi_1} & \frac{\partial\Pi_5(\xi,\eta)}{\partial\xi_2} & \frac{\partial\Pi_5(\xi,\eta)}{\partial\xi_3} & \frac{\partial\Pi_5(\xi,\eta)}{\partial\xi_4} & \frac{\partial\Pi_5(\xi,\eta)}{\partial\eta} \end{bmatrix} \begin{bmatrix} \xi_3 \\ \xi_4 \\ -\frac{D_1}{M_1}\xi_3 - \beta_1\sin(\tilde{\xi}_1 - \eta) \\ -\frac{D_2}{M_3}\xi_4 - \beta_2\sin(\tilde{\xi}_2 - \eta) \\ \dot{\eta} \end{bmatrix} \tag{6.48}$$

with the constraint (6.46).

The first two rows of (6.48) are trivially satisfied for the mapping (6.45) and the target dynamics (6.37). From the third row we get,

$$\frac{1}{M_1}\left(P_1 - b_1\sin(\xi_1 - \Pi_6(\xi,\eta))\right) = -\beta_1\sin(\tilde{\xi}_1 - \eta)$$

or,

$$\Pi_6(\xi_1,\eta) = \xi_1 - \arcsin\left(\frac{P_1 + \beta_1 M_1\sin(\tilde{\xi}_1 - \eta)}{b_1}\right). \tag{6.49}$$

In a similar way, from the fourth row we get,

$$\Pi_7(\xi_2,\eta) = \xi_2 - \arcsin\left(\frac{P_2 + \beta_2 M_2\sin(\tilde{\xi}_2 - \eta)}{b_2}\right). \tag{6.50}$$

Note that $\Pi_6(\xi_1,\eta)$ is a functions of $\xi_1$ and $\eta$, and $\Pi_7(\xi_2,\eta)$ is a function of $\xi_2$ and $\eta$. Here, we make the following assumptions:

**Assumption 6.4.2** $\beta_1 < \frac{b_1 - P_1}{M_1}$ and $\beta_2 < \frac{b_2 - P_2}{M_2}$
to ensure existence of $\Pi_6(\xi_1,\eta)$ and $\Pi_7(\xi_2,\eta)$, respectively.

Next, we substitute for $\Pi_6(\xi_1,\eta)$ and $\Pi_7(\xi_2,\eta)$ in (6.46). Then, it is clear that we can solve (6.46) for $\Pi_5(\xi,\eta)$ if

$$P_1 + P_2 + \beta_1 M_1\sin(\tilde{\xi}_1 - \eta) + \beta_2 M_2\sin(\tilde{\xi}_2 - \eta) - P_{L1} - P_{L2} = 0, \tag{6.51}$$

that is, if

$$\beta_1 M_1\sin(\tilde{\xi}_1 - \eta) + \beta_2 M_2\sin(\tilde{\xi}_2 - \eta) = 0 \tag{6.52}$$

as, from (6.34) and (6.35) at $(x, y) = (x_\star, y_\star)$ it can be shown that $P_1 + P_2 - P_{L1} - P_{L2} = 0$. Notice that, (6.52) is the same as (6.37e), the constraint defined on the target dynamics. Thus, we can compute $\Pi_5(\xi,\eta)$ as

$$\Pi_5(\xi,\eta) = \frac{2b_{12}\sin(\Pi_6(\xi_1,\eta) - \Pi_7(\xi_2,\eta))}{b_1\sin(\xi_1 - \Pi_6(\xi,\eta)) - b_2\sin(\xi_2 - \Pi_7(\xi,\eta)) - P_{L1} + P_{L2}}$$

or

$$\Pi_5(\xi_1,\xi_2,\eta) = \frac{b_{12}\sin\left(\xi_1 - \xi_2 - \hat{\zeta}_1 + \hat{\zeta}_2\right)}{P_1 - P_{L1} + \beta_1 M_1\sin(\tilde{\xi}_1 - \eta)} \tag{6.53}$$

where we denote $\hat{\zeta}_i := \arcsin\left(\frac{P_i+\beta_i M_i\sin(\tilde{\xi}_i-\eta)}{b_i}\right)$ for $i = 1, 2$. Here we make the following assumption:

**Assumption 6.4.3** $\beta_1 < \frac{|P_1-P_{L1}|}{M_1}$ and $\beta_2 < \frac{|P_2-P_{L2}|}{M_2}$.

This assumption makes $\Pi_5(\xi_1,\xi_2,\eta)$ bounded for all $(\xi_1,\xi_2,\eta) \in S^1 \times S^1 \times S^1$.

Thus we have selected the mapping $\Pi(\xi,\eta)$ which maps the trajectories of the target dynamics from $\mathcal{S}_T$ into the manifold $\mathcal{M} \subset \mathcal{S}$. Here, note that $\Pi_5$ is a function of $\xi_1, \xi_2$ and $\eta$.

Finally, from (6.53) and the last row of (6.48) we get,

$$\begin{aligned} u_i(\Pi(\xi,\eta)) = &- x_{5_\star} + \Pi_5(\xi_1,\xi_2,\eta) \\ &+ T_{\text{CSC}}\left(\frac{\partial\Pi_5(\xi_1,\xi_2,\eta)}{\partial\xi_1}\xi_3 + \frac{\partial\Pi_5(\xi_1,\xi_2,\eta)}{\partial\xi_2}\xi_4 + \frac{\partial\Pi_5(\xi_1,\xi_2,\eta)}{\partial\eta}\dot{\eta}\right), \end{aligned}$$

or

$$\begin{aligned} u_i(\Pi(\xi,\eta)) = &- x_{5_\star} + \frac{b_{12}\sin\left(\xi_1 - \xi_2 - \hat{\zeta}_1 + \hat{\zeta}_2\right)}{P_1 - P_{L1} + \beta_1 M_1\sin(\tilde{\xi}_1 - \eta)} \\ &+ \frac{T_{\text{CSC}} b_{12}\cos\left(\xi_1 - \xi_2 - \hat{\zeta}_1 + \hat{\zeta}_2\right)}{P_1 - P_{L1} + \beta_1 M_1\sin(\tilde{\xi}_1 - \eta)} \\ &\left(\xi_3 - \xi_4 + \frac{\beta_1 M_1\cos(\tilde{\xi}_1 - \eta)(-\xi_3 + \dot{\eta})}{b_1\sqrt{1 - \left(\frac{P_1+\beta_1 M_1\sin(\tilde{\xi}_1-\eta)}{b_1}\right)^2}} + \frac{\beta_2 M_2\cos(\tilde{\xi}_2 - \eta)(\xi_4 - \dot{\eta})}{b_2\sqrt{1 - \left(\frac{P_2+\beta_2 M_2\sin(\tilde{\xi}_2-\eta)}{b_2}\right)^2}}\right) \\ &+ \frac{T_{\text{CSC}} b_{12}\beta_1 M_1\cos(\tilde{\xi}_1 - \eta)\sin\left(\xi_1 - \xi_2 - \hat{\zeta}_1 + \hat{\zeta}_2\right)}{\left(P_1 - P_{L1} + \beta_1 M_1\sin(\tilde{\xi}_1 - \eta)\right)^2}(-\xi_3 + \dot{\eta}) \end{aligned} \tag{6.54}$$

This input $u = u_i(\Pi(\xi,\eta))$ given by (6.54) makes the manifold $\mathcal{M}$ invariant.

Next, we design a control law $u = u_{\text{off}}(\cdot)$ which ensures that the trajectories of the closed-loop system are bounded and converge to the manifold $\mathcal{M}$. Under the mapping $\Pi$ we have that, $\xi_i \mapsto x_i$ for $i = 1, \ldots, 4$. Then, it is clear that $\eta(\xi_1,\xi_2) \mapsto \eta_x := \eta(x_1,x_2)$ and $\dot{\eta}(\xi) \mapsto \dot{\eta}_x := \dot{\eta}(x_1,x_2,x_3,x_4)$. Then, an implicit description of $\mathcal{M}$ can be given as

$$\mathcal{M} := \left\{(x,y) \in \mathcal{S} \mid \tilde{\phi}(x) = 0\right\}. \tag{6.55}$$

where

$$\begin{aligned}\tilde{\phi}(x,\eta_x) &= x_5 - \Pi_5(x_1,x_2,\eta_x)\\ &= x_5 - \frac{\sin\left(x_1 - x_2 - \hat{y}_1 + \hat{y}_2\right)}{P_1 - P_{L1} + \beta_1 M_1 \sin(\tilde{x}_1 - \eta_x)}.\end{aligned} \tag{6.56}$$

with (6.35) to be satisfied, where $\tilde{x}_i := x_i - x_{i_\star}$ and $\hat{y}_i := \arcsin\left(\frac{P_i + \beta_i M_i \sin(\tilde{x}_i - \eta_x)}{b_i}\right)$ for $i = 1, 2$.

Let $z = \tilde{\phi}(x, \eta_x)$ denote the off-the-manifold coordinate. Then, we have

$$\begin{aligned}\dot{z} =& \dot{x}_5 - \dot{\Pi}_5(x_1,x_2,\eta_x)\\ =& \dot{x}_5 - \frac{\partial \Pi_5(x_1,x_2,\eta_x)}{\partial x_1}\dot{x}_1 - \frac{\partial \Pi_5(x_1,x_2,\eta_x)}{\partial x_2}\dot{x}_2 - \frac{\partial \Pi_5(x_1,x_2,\eta_x)}{\partial \eta_x}\dot{\eta}_x\\ =& \frac{1}{T_{\text{CSC}}}\left[-x_5 + x_{5_\star} + u_{\text{off}}(x,y,z)\right] - \frac{\partial \Pi_5(x_1,x_2,\eta_x)}{\partial x_1}x_3 - \frac{\partial \Pi_5(x_1,x_2,\eta_x)}{\partial x_2}x_4\\ & - \frac{\partial \Pi_5(x_1,x_2,\eta_x)}{\partial \eta_x}\dot{\eta}_x\end{aligned} \tag{6.57}$$

where we have substituted for $\dot{x}_1$, $\dot{x}_2$ and $\dot{x}_5$ from (6.35).

To ensure the boundedness of the trajectories of the off-the-manifold coordinate $z$ and also that $\lim_{t\to\infty} z(t) = 0$ we take

$$\dot{z} = -\gamma z, \quad \gamma > 0. \tag{6.58}$$

Then, from (6.57) and (6.58) we can write

$$\begin{aligned}u_{\text{off}}(x,\eta_x,z) =& x_5 - x_{5_\star} - \gamma T_{\text{CSC}}\left(x_5 - \Pi_5(x_1,x_2,\eta_x)\right)\\ & + T_{\text{CSC}}\left(\frac{\partial \Pi_5(x_1,x_2,\eta_x)}{\partial x_1}x_3 + \frac{\partial \Pi_5(x_1,x_2,\eta_x)}{\partial x_2}x_4 + \frac{\partial \Pi_5(x_1,x_2,\eta_x)}{\partial \eta_x}\dot{\eta}_x\right).\end{aligned} \tag{6.59}$$

Thus a stabilizing IIDAS control law is synthesized as

$$\begin{aligned}u(x) =& u_{\text{off}}(x,\eta_x,\tilde{\phi}(x))\\ =& x_5 - x_{5_\star} - \gamma T_{\text{CSC}}\left(x_5 - \frac{b_{12}\sin\left(x_1 - x_2 - \hat{y}_1 + \hat{y}_2\right)}{P_1 - P_{L1} + \beta_1 M_1 \sin(\tilde{x}_1 - \eta_x)}\right)\\ & + \frac{T_{\text{CSC}} b_{12}\cos\left(x_1 - x_2 - \hat{y}_1 + \hat{y}_2\right)}{P_1 - P_{L1} + \beta_1 M_1 \sin(\tilde{x}_1 - \eta_x)}\\ & \left(x_3 - x_4 + \frac{\beta_1 M_1 \cos(\tilde{x}_1 - \eta_x)\left(-x_3 + \dot{\eta_x}\right)}{b_1\sqrt{1 - \left(\frac{P_1 + \beta_1 M_1 \sin(\tilde{x}_1 - \eta_x)}{b_1}\right)^2}} + \frac{\beta_2 M_2 \cos(\tilde{x}_2 - \eta)\left(x_4 - \dot{\eta_x}\right)}{b_2\sqrt{1 - \left(\frac{P_2 + \beta_2 M_2 \sin(\tilde{x}_2 - \eta)}{b_2}\right)^2}}\right)\\ & + \frac{T_{\text{CSC}} b_{12}\sin\left(x_1 - x_2 - \hat{y}_1 + \hat{y}_2\right)\left(\beta_1 M_1 \cos(\tilde{x}_1 - \eta_x)\right)\left(-x_3 + \dot{\eta_x}\right)}{\left(P_1 - P_{L1} + \beta_1 M_1 \sin(\tilde{x}_1 - \eta_x)\right)^2}.\end{aligned} \tag{6.60}$$

Finally, we establish boundedness of the trajectories of the closed-loop system (6.34) with the control law (6.60) and the off-the-manifold coordinate $z$. The closed-loop system is

$$\dot{x}_1 = x_3 \tag{6.61a}$$

$$\dot{x}_2 = x_4 \tag{6.61b}$$

$$\dot{x}_3 = \frac{1}{M_1}\left[P_1 - D_1 x_3 - b_1 \sin(x_1 - y_1)\right] \tag{6.61c}$$

$$\dot{x}_4 = \frac{1}{M_2}\left[P_2 - D_2 x_4 - b_2 \sin(x_2 - y_2)\right] \tag{6.61d}$$

$$\dot{x}_5 = \frac{1}{T_{\text{CSC}}}\left[-x_5 + x_{5_\star} + u\right] \tag{6.61e}$$

$$0 = b_1 \sin(x_1 - y_1) - \frac{b_{12}\sin(y_1 - y_2)}{x_5} - P_{L1} \tag{6.61f}$$

$$0 = b_2 \sin(x_2 - y_2) + \frac{b_{12}\sin(y_1 - y_2)}{x_5} - P_{L2} \tag{6.61g}$$

$$\dot{z} = -\gamma z. \tag{6.61h}$$

Here $x_1, x_2, y_1, y_2 \in S^1$, and hence we have $x_1, x_2, y_1, y_2 \in \mathcal{L}_\infty$.

Next, we can rewrite (6.61c) and (6.61d) as

$$\dot{x}_3 = -\frac{D_1}{M_1}x_3 + \Delta_1(x_1, y_1) \tag{6.62a}$$

$$\dot{x}_4 = -\frac{D_2}{M_2}x_4 + \Delta_2(x_2, y_2) \tag{6.62b}$$

where $\Delta_1(x_1, y_1) = \frac{1}{M_1}[P_1 - b_1 \sin(x_1 - y_1)]$ and $\Delta_2(x_2, y_2) = \frac{1}{M_2}[P_2 - b_2 \sin(x_2 - y_2)]$. Clearly, both $\Delta_1(x_1, y_1) \in \mathcal{L}_\infty$ and $\Delta_2(x_2, y_2) \in \mathcal{L}_\infty$. As we have $D_1 > 0$ and $M_1 > 0$, (6.62a) is an asymptotically stable linear system in $x_3$ with a bounded driving function $\Delta_1(x_1, y_1)$. This implies $x_3 \in \mathcal{L}_\infty$. In a similar way we can show that $x_4 \in \mathcal{L}_\infty$.

Next, we have $x_5 = z + \Pi_5(x_1, x_2)$. We have, from (6.58), that $z$ is bounded and $\lim_{t\to\infty} z(t) = 0$. Also, from Assumption 6.4.3 we have that $\Pi_5(x_1, x_2)$ is bounded for all $(x_1, x_2) \in S^1 \times S^1$, and hence we can conclude boundedness of $x_5$.

Thus, we have shown that the trajectories of (6.61) are bounded and $\lim_{t\to\infty} z(t) = 0$. The above discussion on the control synthesis can be summarized in the following proposition which is an important result in this chapter:

**Proposition 6.4.1** *The closed-loop system* (6.34)–(6.35) *with the control law* (6.60) *is locally asymptotically stable at* $(x_\star, y_\star)$.

*Proof* Based on the arguments given above. □

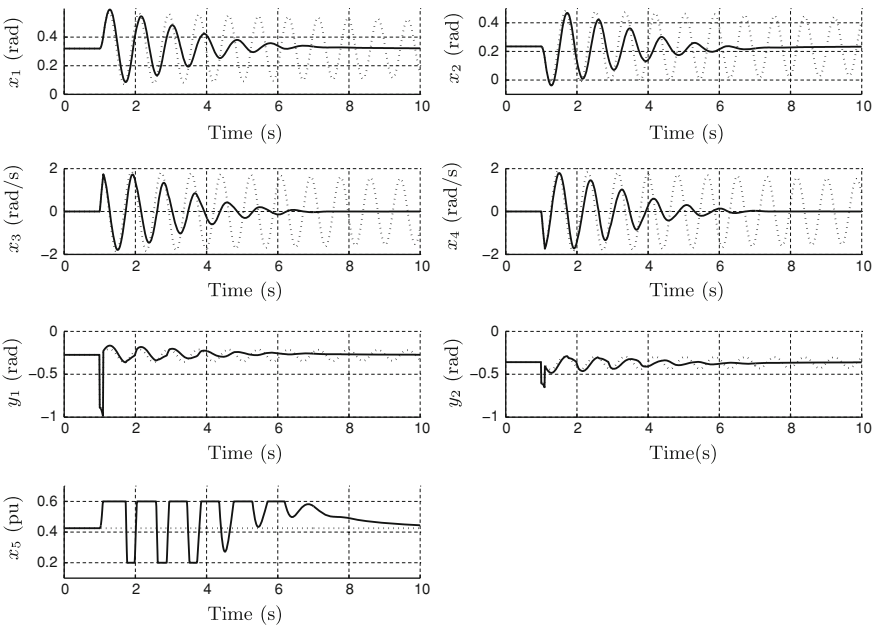


**Fig. 6.6** Response of the two machine system (6.34)–(6.35) with the I&I control law (6.60): *dotted line* (open loop response), *solid line* (closed-loop response with $\beta_1 = 5,\ \beta_2 = 5$ and $\gamma = 5$)

### *6.4.3 Simulation Results for the Two Machine System*

The simulation parameters for the two machine system shown in Fig. 6.5 are assumed as follows: $M_1 = M_2 = \frac{8}{100\pi}$, $D_1 = D_2 = \frac{0.4}{100\pi}$, $P_1 = P_2 = 1.4\,\text{pu}$, $P_{L_1} = 1.2\,\text{pu}$, $P_{L_2} = 1.6\,\text{pu}$, $b_1 = b_2 = 2.5\,\text{pu}$, $b_{12} = 1\,\text{pu}$, $T_{\text{CSC}} = 0.02\,\text{s}$ $0.2 \leq x_5 \leq 0.6$ and the operating equilibrium is $(x_\star, y_\star) = (0.32, 0.2349, 0, 0, 0.4, -0.274, -0.36)$. From Assumption 6.4.2 and Assumption 6.4.3 an upper bound on the tuning parameters $\beta_i, i = 1, 2$ is $\min\{43.19, 7.85\} = 7.85$. We choose $\beta_i = 5, i = 1, 2$.

We assume that a short circuit fault occurs at bus 2 for a duration of 0.1 s at $t = 1$ s. The rotors of both the machines start swinging in response to the transient. Due to poor mechanical damping the oscillations sustain for a long period as shown by dotted plots in Fig. 6.6. The closed-loop response for the tuning parameters $\beta_1 = \beta_2 = 5$ and $\gamma = 5$ is denoted by solid lines. For the closed-loop system the oscillations in both generators die out in about 5 s. The phase portraits for the open loop response and the closed-loop response are shown in Fig. 6.7. The power variations are shown in Fig. 6.8.

Note that, the algebraic equations of the SPM models given by (6.14d) and (6.34) do not correctly describe the algebraic part of a DAE system, since the impact of the reactive power balances are not included. These constraints (reactive power balance)

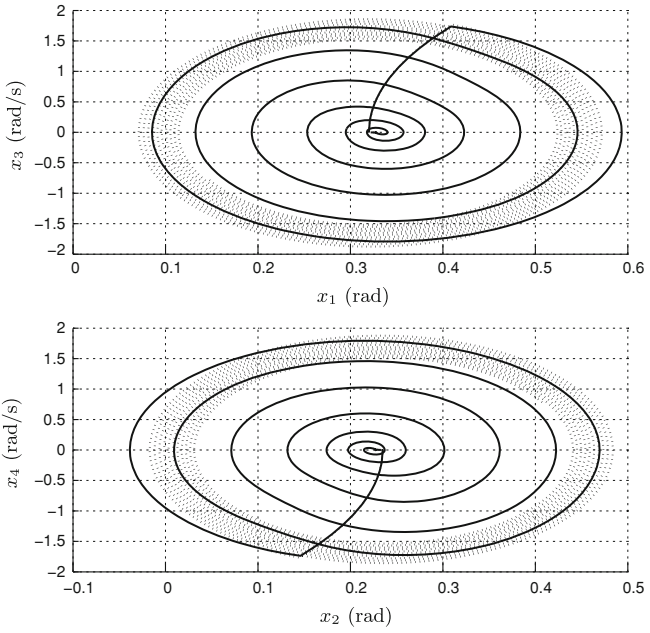


**Fig. 6.7** Phase plots of the two machine system (6.34)–(6.35) with the I&I control law (6.60): *dotted line* (open loop response), *solid line* (closed-loop response with $\beta_1 = 5,\ \beta_2 = 5$ and $\gamma = 5$)

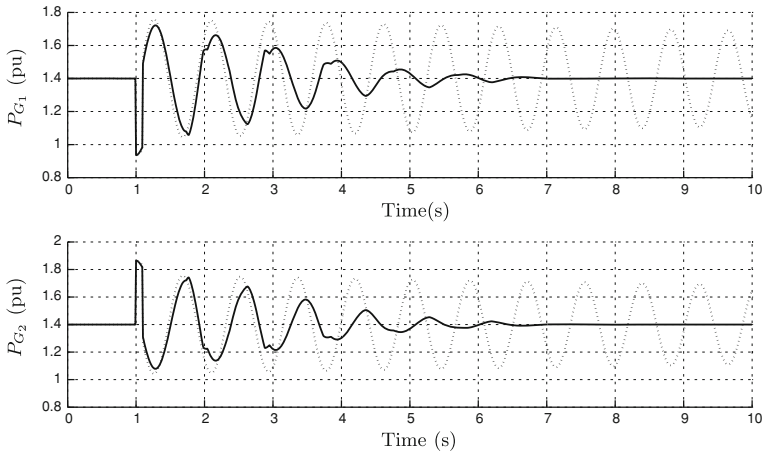


**Fig. 6.8** Power variations of the two machine system (6.34), (6.35) with the I&I control law (6.60): *dotted line* (open loop response), *solid line* (closed-loop response with $\beta_1 = 5,\ \beta_2 = 5$ and $\gamma = 5$)

are indeed quite important and the voltages at the load buses cannot be considered constant.

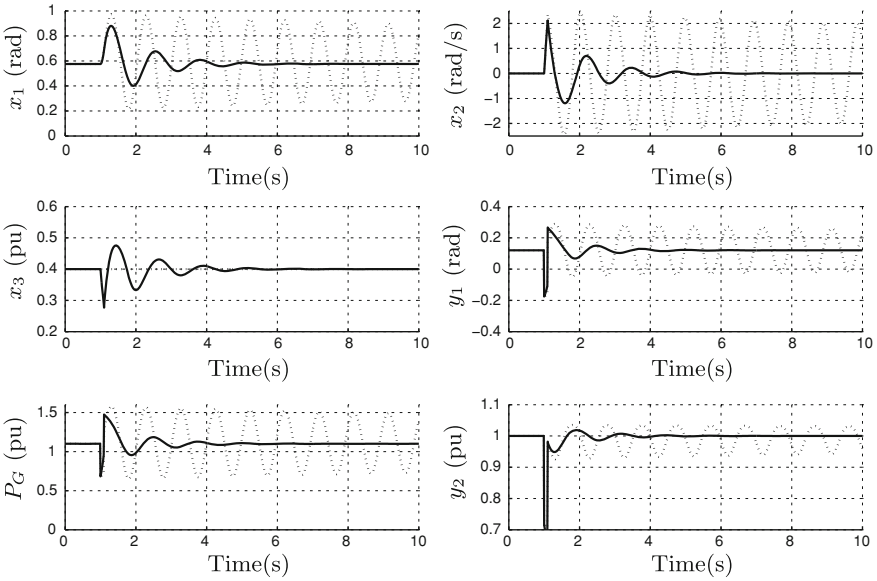


**Fig. 6.9** Response of the detailed model of SMIB system with the I&I control law (6.31): *dotted line* (open loop response), *solid line* (closed-loop response with $\beta = 25$ and $\gamma = 10$)

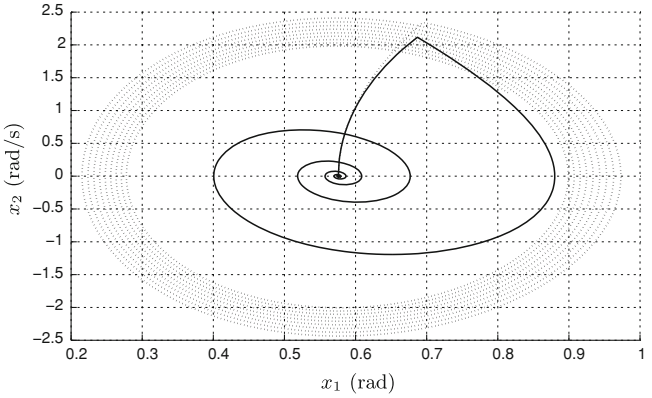


**Fig. 6.10** Phase plots of the detailed model of SMIB system with the I&I control law (6.31): *dotted line* (open loop response), *solid line* (closed-loop response with $\beta = 25$ and $\gamma = 10$)

However, in this attempt to use I&I for synthesizing stabilizing control laws, we have used these somewhat simplified models-(6.14d) and (6.34), similar to the ones given by Bergen and Hill [3] where they assumed frequency dependent load and constant voltage at the buses. In their model all buses in the transmission network are considered as *P*-*V* buses and *Q* at these nodes is not explicitly considered. That is, there is no algebraic equation for reactive power at the buses. As a first step

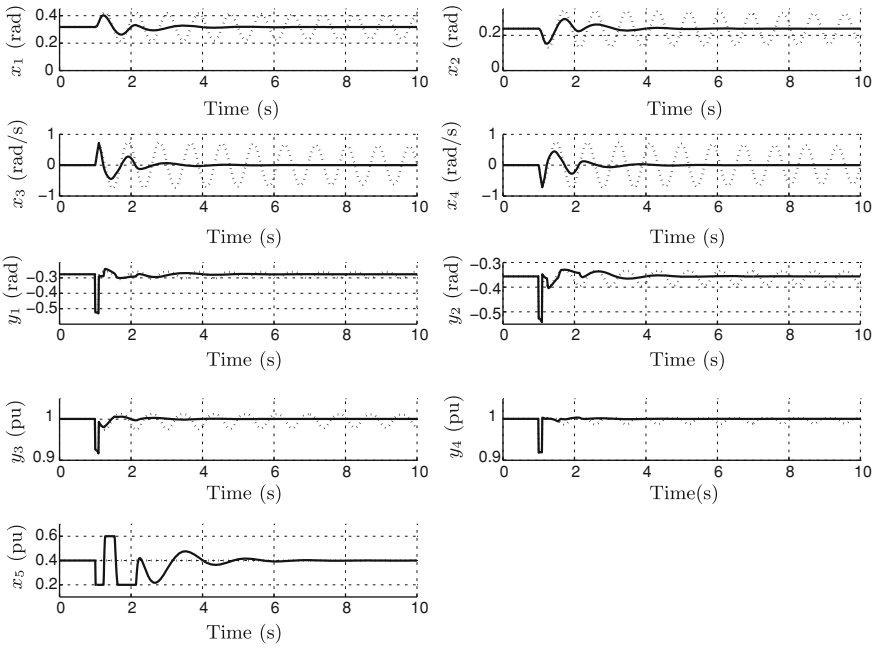


**Fig. 6.11** Response of the detailed model of two machine system with the I&I control law (6.60): *dotted line* (open loop response), *solid line* (closed-loop response with $\beta_1 = 15$, $\beta_2 = 15$ and $\gamma = 5$)

in applying the nonlinear control synthesis technique (I&I) for the power systems with the structure preserving models (SPM) we use a similar modeling approach. This assumption simplifies the control synthesis procedure considerably, as we the number of the algebraic variables as well as the constraints reduce by one each, for every bus to which a load is connected. We agree that, for these control laws to be used in practical scenario we need to include voltage variations in the control synthesis procedure, and the future work has to concentrate on the inclusion of voltage variations and reactive power balance.

Given below are simulation results showing performance of the proposed control law when applied to the more detailed model (with reactive power balance). Figure 6.9 shows the time response and Fig. 6.10 shows the phase plot for the SMIB system. In this case $y_2$ denotes the voltage at the load bus. For the two machine system, the time response is shown in Fig. 6.11 and the phase plot is shown in Fig. 6.12. Here, $y_3$ and $y_4$ denote the voltages at buses 2 and 3, respectively. In both the examples, we have that the control law works satisfactorily to a certain extent.

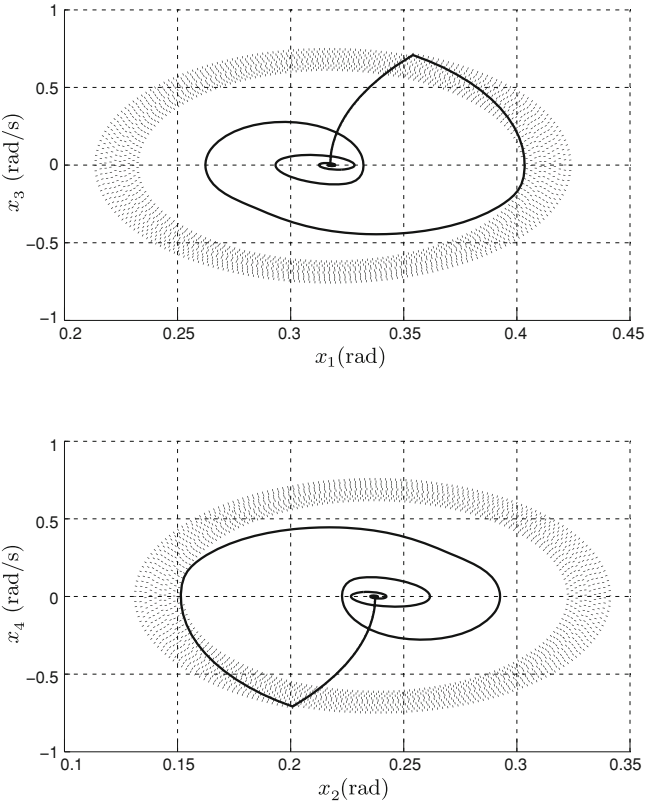


**Fig. 6.12** Phase plots of the detailed model of two machine system with the I&I control law (6.60): *dotted line* (open loop response), *solid line* (closed-loop response with $\beta_1 = 15$, $\beta_2 = 15$ and $\gamma = 20$)

## 6.5 Summary

The I&I methodology available for unconstrained dynamical systems was extended to a class of constrained dynamical systems. The result was then used to synthesize an asymptotically stabilizing control law for an SMIB system and a two machine system with a set of algebraic constraints, using a CSC as an actuator. The power system was modeled using the SPM model, where the rotor dynamics of each machine was described by the swing equation model and the power balance equations at the generator terminal buses were given by the algebraic constraints. The CSC was modeled by a first order system. The simulation results show significant improvement in terms of the magnitude and settling time of the oscillations.

## References

1. J.A. Acosta, R. Ortega, A. Astolfi, I. Sarras, A constructive solution for stabilization via immersion and invariance: the cart and pendulum system. Automatica **44**(9), 2352–2357 (2008)
2. N.S. Manjarekar, R.N. Banavar, R. Ortega, Nonlinear Control Synthesis for Asymptotic Stabilization of the Swing Equation using a Controllable Series Capacitor via Immersion and Invariance. in IEEE Conference on Decision and Control, (Cancun, Mexico, pp. 2493–2498, 2008)
3. A.R. Bergen, D.J. Hill, A structure preserving model for power system stability analysis. IEEE Transaction on Power Apparatus and Systems vol. PAS- 100, pp. 25–35, January 1981

# Chapter 7
# Conclusions and Scope for Future Work

## 7.1 Conclusions

We now summarize the work done in this monograph. We have presented two nonlinear control techniques for power system stabilization at an equilibrium using a CSC. Both the control laws were based on passivity ideas: one involves the notion of interconnection and damping assignment, the other is based on choosing target dynamics on a lower dimensional manifold. The synchronous generator was described using two well known nonlinear models—the second order swing equation and the third order flux-decay model. The actuator, that is the CSC, was modeled using an injection model and a first order model.

So overall, we considered four different cases.

1. In the first case the CSC was modeled by the injection model. This model is based on the assumption that the CSC dynamics is very fast as compared to the SMIB dynamics and hence can be approximated by an algebraic equation. Doing this, we neglect the CSC dynamics and in the open loop system the input vector $g(x)$ takes a complex form—the injection model. Using this injection model and IDA-PBC control methodology we synthesized passivity-based controllers for the two power systems: the SMIB system and a two machine system. For both systems we achieved asymptotically stabilizing control laws. The simulation results show that the control scheme works satisfactorily and improves the transient performance of the power systems. The control effort was smooth with initial sharp spikes.
2. In the second case we included the CSC dynamics as a first order system. We achieved energy shaping control to asymptotically stabilize the closed-loop system for both the models of the SMIB system (the swing equation model and the flux-decay model). The controller performance was found to be effective in the sense that it gave an improved transient response for the closed-loop system. The control effort in these techniques was smooth with just initially sharp transients.
3. In the third case we used a different control methodology, I&I, to synthesize an asymptotically stabilizing control law for the SMIB system with a CSC. Once

N. S. Manjarekar and R. N. Banavar, *Nonlinear Control Synthesis for Electrical Power Systems Using Controllable Series Capacitors*, SpringerBriefs in Applied Sciences and Technology, DOI: 10.1007/978-3-642-27531-9_7, © The Author(s) 2012

again the CSC was described by a first order system. We synthesized a control law to stabilize the swing equation model of the SMIB. The plots show a slow but considerably smooth response to the transients as compared to the IDA-PBC based control law.

4. In the last case we incorporated the power balance algebraic constraint in the load bus to the SMIB swing equation, and extended the I&I to a class of differential algebraic systems and, proposed a stability result. Simulation results showed significant improvement in the transient response. Using the same approach, we presented results for the two-machine case with one CSC.

### *7.1.1 Comparison Between the Two Control Design Strategies*

An important difference between the two control synthesis strategies is as follows. In IDA-PBC, the target dynamics is of the same dimension as that of the open loop system and it is selected by modifying the interconnection and damping structure, and energy of the open loop system. Then, the control synthesis problem becomes one of matching the target system with the closed-loop system exactly. On the other hand, in the I&I strategy a lower dimensional target dynamics is immersed in the original higher dimensional manifold. The control objective is to match the two dynamics on the lower dimensional manifold as also ensuring that the trajectories off-the-manifold reach it asymptotically, that is to say, off-the-manifold the control aim is to match the two models asymptotically. This gives more freedom in choosing the target dynamics in case of the I&I strategy, as compared to IDA-PBC.

In the IDA-PBC strategy, the transient performance of the closed-loop system improves over the open loop response in terms of the magnitude of the oscillations as well as the settling time. In the I&I case as well, the closed-loop response shows similar improvement. Moreover, in the latter case, there are two ways of tuning the response of the system—one is by affecting $\alpha$ (the target dynamics) through elements of the energy function and secondly by changing $\gamma$ which affects how rapidly the system approaches the desired manifold.

For the IDA-PBC control law it is quite straightforward to give estimates of the domain of attraction using the convexity property of the energy functions for the closed-loop systems. For the I&I strategy however, the improvement in the domain of attraction can be shown through simulations.

## 7.2 Future Work

The work proposed here could be extended in the following manner

1. The I&I strategy can be applied to multimachine power systems described by models that are more complex and closer to the actual physical system.
2. Further, a combination of excitation control with the CSC can be investigated from the I&I point of view.